U.PORTO
FACULDADE DE DESPORTO
UNIVERSIDADE DO PORTO

CIAFEL
Centro de Investigação em Atividade Física, Saúde e Lazer

Advancing accelerometer-based mechanical loading assessment: Development and validation of prediction equations and activity classification models

Academic dissertation submitted to obtain a doctoral degree in Physical Activity and Health from the Faculty of Sport of the University of Porto, according to Law 65/2018, from August 16th.

Supervisor: Professor Doctor Hélder Rui Martins Fonseca

Co-supervisor: Professor Doctor José Manuel Fernandes de Oliveira

Lucas de Souza Veras

Porto, 2025

Veras, L. S. (2025). *Advancing accelerometer-based mechanical loading assessment: Development and validation of prediction equations and activity classification models*. Doctoral Thesis in Physical Activity and Health. Faculty of Sports, University of Porto, Porto, Portugal.

Keywords: WEARABLE TECHNOLOGY; GROUND REACTION FORCE; LOADING RATE; MACHINE LEARNING.

Funding Sources

Lucas de Souza Veras was supported by a grant from the Portuguese Foundation for Science and Technology (FCT; grant number UI/BD/150673/2020, doi: 10.54499/UI/BD/150673/2020). The thesis was conducted in the Research Centre in Physical Activity, Health, and Leisure (CIAFEL), a research unit housed in the Faculty of Sport, University of Porto, Porto, Portugal. CIAFEL is funded by the European Regional Development Fund (ERDF) through COMPETE and by FCT (grants UIDB/00617/2020, doi: 10.54499/UIDB/00617/2020 and UIDP/00617/2020, doi: 10.54499/UIDP/00617/2020). CIAFEL is part of the associated Laboratory for Integrative and Translational Research in Population Health (ITR), funded by the FCT (grant LA/P/0064/2020).

To Bernardo, my son.

Everything I have, and everything I am, is yours. Forever.

Acknowledgements

Frst of all, I would like to thank my family, without whom none of this would be possible. To my son, Bernardo, the most precious thing I have. To my wife, Ananda. Thank you for loving me and for being with me no matter what. It wouldn't be the same without you by my side. To my parents, Jussara and Sinval, without your love, caring, and unconditional support throughout all my life, I wouldn't be where I am today.

To all of my friends. To Pedro Rios, my buddy from all those years, I'm finishing my PhD now, then it'll be you, and we'll be able to open our bakery together. To Giorjines, Florêncio and Tiago, who stuck with me since the very beginning. Without you this journey would be harder, and undoubtedly less fun. To all my friends at FADEUP: Leo, Pedro Abdalla, Pedro Oliveira, Daniela, Miguel, Beshoy, Laura, Andrea, Suiane, Ana Flávia, Ariane, and many others. Thank you for your company, your friendship and for all the academic and life advices. I'm going to miss our lunches outside on sunny spring days.

To my supervisors, Professor Hélder Fonseca and Professor José Oliveira, I learned so much from you since my Master's. Thank you for all the contributions, support and patience along the way. To all the other professors in this faculty that help me during my time here, namely Professor José Carlos Ribeiro, director of this doctoral program, Professor Jorge Mota, director of the CIAFEL and Professor Leandro Machado and Professor João Paulo Vilas-Boas, who opened the LABIOMEP doors for me.

Table of Contents

Funding Sources III
Acknowledgements VII
List of Figures XI
List of Tables XVII
List of Equations XXI
Resumo XXIII
Abstract XXV
List of Abbreviations and Symbols XXVII
Chapter 1: General introduction and aims 1
1.1. General Introduction 3
1.2. Aims 8
Chapter 2: Literature review 11
2.1. Bone biology and adaptation 13
2.2. Bone response to mechanical loading 14
2.3. Physical activity and bone health 16
2.4. Mechanical loading assessment 19
2.5. Accelerometry technology 22
2.6. Mechanical loading variables and their prediction using accelerometer data 24
2.6.1. Ground reaction forces and loading rate 24
2.6.2. Ground reaction forces and loading rate prediction using accelerometer data 26
2.6.3. Activity classification and its importance in the context of mechanical loading prediction 28
2.7. Methodological considerations 29
2.8. Clinical applications 32
2.9. Future directions 35
Chapter 3: Original studies 37
3.1. List of publications 39
3.2. Study 1 41

3.3. Study 2 57
3.4. Study 3 79
3.5. Study 4 103
Chapter 4: General discussion 119
4.1. General discussion 121
Chapter 5: Conclusion 133
5.1. General conclusions and future perspectives 135
Chapter 6: References 137
6.1. References 139

List of Figures

Study 1

Figure 1. Distribution of participant's body mass index per speed. Dots represent individual participants 46

Figure 2. Panels A and B show the relationship between variables collected by force plates and accelerometers worn at hip, for the resultant vector. Linear trends for each body mass index category are also depicted. Panel A shows peak magnitudes (pGRF and pACC) while Panel B shows peak rates (pLR and pAR). Panels C and D display Bland-Altman plots demonstrating the agreement between actual and predicted peak ground reaction force (Panel C) and loading rate (Panel D) for the resultant vector from hip-worn accelerometers. Continuous thick lines show bias (average of the differences between actual and predicted values) while dashed lines show the limits of agreement (bias ±1.96 standard deviation). Abbreviations: pACC, peak acceleration; pAR, peak acceleration rate; pGRF, peak ground reaction force; pLR, peak loading rate 47

Supplemental Figure S1. Example of ground reaction force and acceleration signals during the stance phase of walking (left panel) and running (right panel). Signals were mean centered and scaled to units of standard deviation to fit in the same plot window. In this image, the peak of each signal, represented by the start marks, is its maximum magnitude during the stance. The peak acceleration rate and peak loading rate were identified as the steepest part of each curve 53

Supplemental Figure S2. Relationship between peak ground reaction force and acceleration magnitudes. Data from accelerometers worn at ankle (Panels A and D), lower back (Panels B and E) and hip (Panels C and F), for both the resultant vector (Panels A to C) and its vertical component (Panels D to F). Linear trends for each body

mass index category are also depicted. Abbreviations: pACC, peak acceleration; pGRF, peak ground reaction force 54

Supplemental Figure S3. Relationship between peak loading and acceleration rates. Data from accelerometers worn at ankle (Panels A and D), lower back (Panels B and E) and hip (Panels C and F), for both the resultant vector (Panels A to C) and its vertical component (Panels D to F). Linear trends for each body mass index category are also depicted. Abbreviations: pAR, peak acceleration rate; pLR, peak loading rate 54

Supplemental Figure S4. Bland-Altman plots showing agreement between actual and predicted peak ground reaction force for accelerometers worn at ankle (Panels A and D), lower back (Panels B and E) and hip (Panels C and F), for both the resultant vector (Panels A to C) and its vertical component (Panels D to F). Continuous thick lines show bias (average of the differences between actual and predicted values) while dashed lines show the limits of agreement (bias ±1.96 standard deviation). Abbreviations: pGRF, peak ground reaction force 55

Supplemental Figure S5. Bland-Altman plots showing agreement between actual and predicted peak loading rate for accelerometers worn at ankle (Panels A and D), lower back (Panels B and E) and hip (Panels C and F), for both the resultant vector (Panels A to C) and its vertical component (Panels D to F). Continuous thick lines show bias (average of the differences between actual and predicted values) while dashed lines show the limits of agreement (bias ± 1.96 standard deviation). Abbreviations: pLR, peak loading rate 55

Study 2

Figure 1. Overall scheme of the study design and methods employed in the study 61

Figure 2. An example of a participant performing each of the jump types assayed. Panels (A, B) the initial (take-off phase) and final (landing phase) phases of the drop jumps, respectively, while Panels (C, D) show the initial and final phases of the box jumps, respectively, and Panels (E, F) show the initial and final phases of the continuous jumps, respectively 62

Figure 3. Accelerometers' positioning on the body: Details of accelerometer positioning on the ankle, lower back and hip are displayed in Panels (A–C), respectively. Panel (D) shows all accelerometer placements simultaneously 63

Figure 4. Flowchart showing all steps of the data processing 64

Figure 5. Examples of the ground reaction force and acceleration signals for all of the jump types performed. The first column, formed by Panels (A–D), shows the ground reaction force and acceleration signal for accelerometers at the ankle, lower back, and hip for the drop jump from 5 cm height. Panels (E–H) show the same signals, but for the box jumps of 5 cm height, while Panels (I–L) show the signals for the continuous jumps of 5 cm 65

Figure 6. Distribution of the resultant vectors of mechanical loading (peak ground reaction force on Panel (A) and peak loading rate on Panel (B)) and acceleration (peak acceleration on Panel (C) and peak acceleration rate on Panel (D)) variables per jump type and height combination. Abbreviations: BW, body weight; pACC, peak acceleration; pAR, peak acceleration rate; pGRF, peak ground reaction force; pLR, peak loading rate 67

Figure 7. Bland-Altman plots showing agreement between actual and predicted peak ground reaction force (Panel A) and loading rate (Panel B) for the resultant vectors from hip-worn accelerometers. Continuous thick lines show bias (the average of the differences between actual and predicted values), while dashed lines show the limits of agreement (bias ± 1.96 standard deviation). Abbreviations: pGRF, peak ground reaction force; pLR, peak loading rate 69

Supplemental Figure S1. Distribution of the vertical vector of mechanical loading (peak ground reaction force on Panel A and peak loading rate on Panel B) and acceleration (peak acceleration on Panel C and peak acceleration rate on Panel D) variables per jump type and height combination. Abbreviations: BW, body weight; pACC, peak acceleration; pAR, peak acceleration rate; pGRF, peak ground reaction force; pLR, peak loading rate 75

Supplemental Figure S2. Bland-Altman plots showing agreement between actual and predicted peak ground reaction force for accelerometers worn at ankle (Panels A and D), lower back (Panels B and E) and hip (Panels C and F), for both the resultant vector (Panels A to C) and its vertical component (Panels D to F). Continuous thick lines show bias (average of the differences between actual and predicted values) while dashed lines show the limits of agreement (bias ± 1.96 standard deviation). Abbreviations: pGRF, peak ground reaction force 76

Supplemental Figure S3. Bland-Altman plots showing agreement between actual and predicted peak loading rate for accelerometers worn at ankle (Panels A and D), lower back (Panels B and E) and hip (Panels C and F), for both the resultant vector (Panels A to C) and its vertical component (Panels D to F). Continuous thick lines show bias (average of the differences between actual and predicted values) while dashed lines show the limits of agreement (bias ± 1.96 standard deviation). Abbreviations: pLR, peak loading rate 77

Study 3

Figure 1. Bland-Altman plots displaying the level of agreement between actual and predicted pGRF for accelerometers worn at the ankle (panels A, D), lower back (panels B, E), and hip (panels C, F). These plots cover both the resultant vector (panels A-C) and its vertical component (panels D-F). Predictions of pGRF during walking and running were calculated using the equations from Veras et al. (2022)

[20]. The solid lines represent the bias (the mean difference between actual and predicted values), while the dashed lines mark the limits of agreement (bias ± 1.96 standard deviations). Abbreviations: pGRF, peak ground reaction force 87

Figure 2. Bland-Altman plots displaying the level of agreement between actual and predicted pLR for accelerometers worn at the ankle (panels A, D), lower back (panels B, E), and hip (panels C, F). These plots cover both the resultant vector (panels A-C) and its vertical component (panels D-F). Predictions of pLR during walking and running were calculated using the equations from Veras et al. (2022) [20]. The solid lines represent the bias (the mean difference between actual and predicted values), while the dashed lines mark the limits of agreement (bias ± 1.96 standard deviations). Abbreviations: pLR, peak loading rate 87

Figure 3. Bland-Altman plot displaying the level of agreement between actual and predicted pGRF for accelerometers worn at the hip for the vertical vector. Predictions of pGRF during walking and running were calculated using the equation from Neugebauer et al. (2014) [17]. The solid line represents the bias (the mean difference between actual and predicted values), while the dashed lines mark the limits of agreement (bias ± 1.96 standard deviations). Abbreviations: pGRF, peak ground reaction force 88

Figure 4. Bland-Altman plots displaying the level of agreement between actual and predicted pGRF for accelerometers worn at the ankle (panels A, D), lower back (panels B, E), and hip (panels C, F). These plots cover both the resultant vector (panels A-C) and its vertical component (panels D-F). Predictions of pGRF during jumping were calculated using the equations from Veras et al. (2023) [21]. The solid lines represent the bias (the mean difference between actual and predicted values), while the dashed lines mark the limits of agreement (bias ± 1.96 standard deviations). Abbreviations: pGRF, peak ground reaction force 88

Figure 5. Bland-Altman plots displaying the level of agreement between actual and predicted pLR for accelerometers worn at the ankle (panels A, D), lower back (panels B, E), and hip (panels C, F). These plots cover both the resultant vector (panels A-C) and its vertical component (panels D-F). Predictions of pLR during jumping were calculated using the equations from Veras et al. (2023) [21]. The solid lines represent the bias (the mean difference between actual and predicted values), while the dashed lines mark the limits of agreement (bias ± 1.96 standard deviations). Abbreviations: pLR, peak loading rate 89

List of Tables

Study 1

Table 1. Regression equations, R^2 and accuracy indices ……48

Table 2. Accuracy indices of ours and Neugebauer et al. (2014) equation to predict peak vertical ground reaction force with data from hip-worn accelerometers……48

Study 2

Table 1. Regression equations, R^2, and accuracy indices for prediction of pGRF and pLR based on accelerometer-derived data ……68

Study 3

Table 1. Sample characteristics of the Veras et al. (2022) [20], Neugebauer et al. (2014) [17], and Veras et al. (2023) [21] studies ……84

Table 2. Accuracy indices for pGRF and pLR predictions for walking and running based on the Veras et al. (2022) [20] equations. The high prediction errors for pLR reflect challenges in accurately predicting this variable using accelerometers. Factors such as low accelerometer sampling frequency and individual variation in biomechanics likely contribute to the larger discrepancies in pLR compared to pGRF ……..85

Table 3. Accuracy indices for pGRF for walking and running based on the Neugebauer et al. (2014) [17] equation ……..86

Table 4. Accuracy indices for pGRF and pLR prediction for jumping based on the Veras et al., (2023) [21] equations. The pLR predictions for jumping activities show particularly high error rates, with MAPE values exceeding 200%. These errors highlight the difficulty in capturing the rapid, high-magnitude forces involved in jumping, and the difficulty in reflecting measurement sensitivity in pLR predictions ……..86

Table S1. Accuracy indices for pGRF and pLR prediction for different walking and running speeds based on the Veras et al. (2022) [20] equations ……94

Table S2. Accuracy indices for pGRF and pLR prediction for different walking and running speeds based on the Neugebauer et al. (2014) [17] equation ……...96

Table S3. Accuracy indices for pGRF and pLR prediction for different types of jumping based on the Veras et al. (2023) [21] equations ……97

Study 4

Table 1. Accuracy indices of machine learning algorithms for walking, running and jumping activities classification across different accelerometer placements. Cell's background is colored in grayscale, where darker cells represent higher accuracy values ……109

Table 2. Accuracy indices of machine learning algorithms for walking, running and jumping activities classification across different accelerometer placements and activities. Cell's background is colored in grayscale, where darker cells represent higher accuracy values ……...110

Table 3. Confusion matrix for activity classification for each machine learning algorithm. Diagonals represent the correct classification and are highlighted in

bold. All classification scores are equal across all accelerometer placements within the same algorithm ……..111

List of Equations

Study 1

Equation 1. The rates of change were computed through a centred derivative from the beginning of the foot contact to the peak ……..45

Equation 2. The pLR and pAR were defined as the maximum value in the array …45

Study 2

Equation 1. The rates of change were computed through a centered derivative from the beginning of the foot contact to the curve peak ……...64

Equation 2. The pLR and peak acceleration rate (pAR) were defined as the maximum value in the array derived from Equation (1) and represented by $f'_{i_{max}}$ …64

Resumo

Quantificação precisa da carga mecânica relacionada com a atividade física é crucial para compreender como otimizar a saúde óssea através de intervenções de exercício direcionadas. No entanto, o alto custo e a falta de portabilidade associados às placas de força limitam a sua utilidade a ambientes laboratoriais, destacando a relevância do desenvolvimento de estratégias tecnológicas que possam medir com precisão a carga mecânica relacionada com a atividade física. Esta tese teve como objetivo avançar a avaliação da carga mecânica baseada em acelerómetros, desenvolvendo e validando equações de predição para as forças de reação do solo e taxas de carga durante a caminhada, corrida e salto, e modelos de classificação de atividade para diferenciar entre estas atividades. Para isso, uma série de estudos transversais foram realizados explorando a relação entre o sinal obtido por placas de força laboratoriais durante a realização de várias atividades físicas distintas e o sinal obtido por acelerómetros colocados em diferentes localizações anatómicas. Os dois primeiros estudos demonstraram que a força de reação do solo de pico poderia ser prevista com precisão usando dados de acelerómetros do tornozelo, parte inferior das costas e anca, com erros percentuais absolutos médios de cerca de 7% para caminhada e corrida e cerca de 14% para salto. No entanto, as equações de predição da taxa de carga de pico produziram menor precisão, com erros percentuais absolutos médios variando de 17,7% a 24,7%. O terceiro estudo, uma validação externa das equações de predição existentes, revelou uma variabilidade substancial na precisão, com as equações da taxa de carga de pico apresentando os maiores erros. O quarto estudo desenvolveu modelos de aprendizagem automática para classificar atividades de caminhada, corrida e salto, alcançando alta precisão (>90% de concordância) em todas as colocações de acelerómetros. Em conclusão, esta tese avança o campo da avaliação da carga mecânica baseada em acelerómetros, fornecendo equações de predição validadas para forças de reação do solo e taxas de carga durante a caminhada, corrida e salto, bem como modelos precisos de classificação de atividades. Pesquisas futuras devem concentrar-se no refinamento destes modelos, expandindo a sua aplicação e explorando o seu potencial para otimizar a saúde óssea.

Palavras-chave: ACELEROMETRIA; FORÇAS DE REAÇÃO DO SOLO; TAXA DE CARGA; APRENDIZADO DE MÁQUINA.

Abstract

Accurate quantification of physical activity-related mechanical loading is crucial for understanding how to optimize bone health through targeted exercise interventions. However, the high cost and lack of portability associated with force plates limit their utility to laboratory settings, highlighting the relevance of developing technological strategies that accurately measure physical activity-related mechanical loading. This thesis aimed to advance accelerometer-based mechanical loading assessment by developing and validating prediction equations for ground reaction forces and loading rates during walking, running, and jumping, and activity classification models to differentiate between these activities. To accomplish that, a series of cross-sectional studies explored the relationship between the signal obtained by laboratory force plates during the performance of several distinct physical activities and the signal obtained by accelerometers placed on different anatomical locations. The first two studies demonstrated that peak ground reaction force could be accurately predicted using accelerometer data from the ankle, lower back, and hip, with mean absolute percent errors of around 7% for walking and running and around 14% for jumping. However, peak loading rate prediction equations yielded lower accuracy, with mean absolute percent errors ranging from 17.7% to 24.7%. The third study, an external validation of existing prediction equations, revealed substantial variability in accuracy, with peak loading rate equations showing the highest errors. The fourth study developed machine learning models for classifying walking, running, and jumping activities, achieving high accuracy (>90% of agreement) across all accelerometer placements. In conclusion, this thesis advances the field of accelerometer-based mechanical loading assessment by providing validated prediction equations for ground reaction forces and loading rates during walking, running, and jumping, as well as accurate activity classification models. Future research should focus on refining these models, expanding their application, and exploring their potential for informing personalized interventions to optimize bone health.

Keywords: WEARABLE TECHNOLOGY; GROUND REACTION FORCE; LOADING RATE; MACHINE LEARNING.

List of Abbreviations and Symbols

BMI [Body mass index]

FFT [Fast Fourier transform]

KNN [K-nearest neighbors]

MAE [Mean absolute error]

MAPE [Mean absolute percentage error]

pACC [Peak acceleration]

pAR [Peak acceleration rate]

pGRF [Peak ground reaction force]

pLR [Peak loading rate]

R^2 [Coefficient of determination]

RF [Random forest]

RMSE [Root mean square error]

ROC-AUC [Receiver operating characteristic - area under curve]

SD [Standard deviation]

SVM [Support vector machine]

$\bar{X}$	[Mean]
κ	[Kappa coefficient]
BMI	[Body mass index]

Chapter 1: General introduction and aims

1.1. General Introduction

Skeletal tissue can modify its structure and strength in response to the mechanical demands placed upon it [1,2]. This process, known as mechanotransduction, involves the conversion of mechanical stimuli into biochemical signals that influence bone cell activity [3,4]. The basic principles of bone mechanotransduction involve detecting mechanical forces by bone cells, especially osteocytes [5], and other cells such as osteoblasts and lining cells [6], which trigger signaling cascades that regulate bone modeling and remodeling [2,7,8]. Mechanical loading plays a key role in stimulating bone formation and inhibiting bone resorption [1,9], leading to increases in bone mass and favorable adaptations in bone tissue composition and structure that enhance its strength [10–12].

Several key characteristics, including the magnitude, rate, and frequency of the applied forces, influence the osteogenic potential of mechanical loading [9,13]. High-magnitude forces that induce strains above a certain threshold, applied at high rates and frequencies interspersed with resting periods, appear to provide the most potent stimulus for bone adaptation [9,13–15]. Importantly, impact-generating activities like walking, running and jumping impose these types of osteogenic loading profiles and have consistently been shown to promote increases in bone mineral density, cortical thickness and trabecular microarchitecture [16–20]. Therefore, impact exercise is crucial for bone health and widely prescribed for osteoporosis prevention and management [14,15,17].

Accurate quantification of the mechanical loads imposed on the skeleton during physical activity is crucial for understanding how to optimize bone health through targeted exercise interventions [21,22]. The gold standard for directly measuring ground reaction forces is using force plates, which provide precise and reliable data [23]. However, their high cost, technical complexity, and lack of portability limit their utility in laboratory settings, making it challenging to assess mechanical loading during everyday activities, where monitoring would be

particularly useful. This limitation has driven the search for alternative methods capable of estimating mechanical loading in free-living conditions, which could provide valuable insights into the real-world impact of physical activity on bone health.

Some questionnaires have been developed to estimate mechanical loading associated with participation in specific activities [24,25]. These tools gather data on an individual's present physical activity levels and their past engagement in various types of activities over their lifetime. However, questionnaires only provide rough estimates, rely heavily on subjective recall and cannot provide direct, objective measures of the specific mechanical loading characteristics the person was subjected to during these activities [26]. Studies have shown that mechanical loading estimates obtained by questionnaires appear to have a moderate to weak correlation with bone mass, which may be due to the limited capacity of questionnaires to accurately assess the mechanical loading relevant for bone health [27,28]. In contrast, accelerometers have emerged as a valuable tool for mechanical loading assessment in non-laboratory conditions [29–32]. By directly measuring body accelerations that strongly correlate with ground reaction forces [33–35], accelerometers can provide an objective and quantitative means of assessing the mechanical loading experienced by an individual during their daily activities.

Accelerometers offer several advantages for mechanical loading assessment, including low cost, small size, and the ability to record body accelerations across extended time periods continuously [36,37]. They have been widely used for measuring physical activity levels and estimating energy expenditure [37], but their application for bone-relevant loading quantification is still an emerging area. Numerous studies have demonstrated the potential for using accelerometer-derived variables to estimate mechanical loading [29–32,38,39]. These investigations have shown strong correlations between acceleration metrics and ground reaction forces [33–35]. Furthermore, accelerometer-based loading measures have been directly associated with bone health outcomes, such as bone mineral density [21,22,40],

highlighting their relevance in understanding the relationship between mechanical loading and skeletal adaptation.

Several early studies [29–31,38,39] investigated the use of accelerometers to estimate ground reaction forces, laying the groundwork for this field of research. Neugebauer et al. (2012) were one of the first [29] to develop a regression equation to predict peak vertical ground reaction force from hip accelerometer data in youth during walking and running. Then, Wundersitz et al. (2013) [38] assessed the validity of a trunk-mounted accelerometer for measuring forces during running and change of direction tasks, while Fortune et al. (2014) [31] explored the relationship between peak accelerations from various body-mounted accelerometers and ground reaction forces during walking and running. Neugebauer et al. (2014) [30] refined their previous work, developing equations to estimate peak vertical and braking ground reaction forces from hip accelerations in young adults. Meyer et al. (2015) [39] validated using hip-worn accelerometers against force plates for estimating peak vertical ground reaction forces during various locomotor activities in children. Despite the critical contributions of these early studies, they had some limitations that included small sample sizes, low accelerometer sampling frequencies, data processing techniques that did not fully utilize high-resolution data, and a focus primarily on walking and running activities. To expand this field, future studies would need to address these limitations to capture better the complex loading patterns experienced in daily life. Nevertheless, these early studies provided a valuable foundation, demonstrating the feasibility of using accelerometer-based devices to estimate ground reaction forces during locomotion.

Although ground reaction forces are the most studied mechanical loading variable extracted from accelerometer data [41], and arguably the most important in terms of the effect on bone health [10,42], other variables also influence the osteogenic effect of mechanical loading associated with exercise [9,43,44]. Loading rate, for example, influences bone health outcomes [13,43] and has begun to be predicted in accelerometer-based models [31,32,34], but this prediction still needs

improvement. Some studies have investigated the relationship between accelerometer-derived variables and loading rate. Rowlands and Stiles (2012) [35] found that accelerometer counts and raw acceleration output were positively correlated with both peak ground reaction force and loading rate during walking and running. Liikavainio et al. (2007) [34] reported high linear correlations between the maximal loading rate derived from force plate data and the maximal acceleration transient rate derived from skin-mounted accelerometers on the lower limb during walking. Fortune et al. (2014) [31] developed equations to predict peak loading rate from ankle accelerations during walking and running. Still, the accuracy of loading rate predictions was substantially lower compared to peak ground reaction force predictions. More recently, our research group [Veras et al. (2020) [32]] also developed prediction equations for peak loading rate based on accelerometer data and body mass in adults with a wide range of body mass indices. However, it was found that while the prediction accuracy for peak ground reaction force was high (mean absolute percent error < 7%), the accuracy for peak loading rate was only moderate with a mean absolute percent error or around 20%. These studies demonstrate the feasibility of estimating loading rate from accelerometer data but highlight that the prediction accuracy is currently lower than for peak ground reaction forces. Further research is needed to improve the estimation of the loading rate, as this is an important mechanical loading variable for bone health [13,45,46].

The accuracy of accelerometer-based predictive models for estimating mechanical loading variables depends on several technical and methodological factors. Welk (2005) [47] highlighted the importance of using a representative sample population, a diverse set of representative activities, and appropriate statistical methods in calibration studies. Notably, the type of activity performed can significantly influence the accuracy of prediction equations [47], as the relationship between acceleration and ground reaction forces may differ for activities like walking, running, and jumping [30,35]. Therefore, activity-specific prediction equations may be needed to optimize accuracy across a broad range of movements, particularly those commonly prescribed for bone health improvement interventions. The choice

of accelerometer placement is also crucial, with hip and wrist placements being the most common [37]. Other factors such as accelerometer sampling frequency, epoch length, data processing methods, and sample characteristics can influence prediction accuracy. They should be carefully considered when developing and applying these models [37,47,48].

It is essential to note that while these factors are important in developing accurate predictive models, external validation studies are crucial to ensure the robustness and generalizability of these models [49]. External validation involves testing the predictive model on an independent dataset not used in the model's development [50]. This process helps to assess the model's performance in real-world settings and across different populations. Without it, the model's accuracy and applicability may be limited to the specific dataset and conditions used in its development [49]. Therefore, implementing external validation studies is critical in establishing the reliability and validity of existing mechanical load prediction models, enabling their widespread use in research and clinical settings.

However, a significant challenge in free-living mechanical loading assessment is determining which activity-specific prediction model to apply when the activity is unknown. Activity recognition algorithms can be employed to classify accelerometer data [51–53] to address this issue. While extensive research has been conducted on activity recognition, existing methods may not be optimally suited for bone-specific loading quantification, as they cannot differentiate between some of the activities that are more often prescribed for bone health improvement, such as walking, running, and jumping [16,17,54,55]. Accurately distinguishing between activities with distinct osteogenic potential is crucial for applying appropriate prediction models and load-specific thresholds. Therefore, there is a need to develop activity classification models that are specifically optimized for the demands of bone loading assessment. Integrating activity recognition with activity-specific prediction models is an essential step for implementing mechanical loading monitoring outside the laboratory, as it would enable the application of appropriate models based on

the detected activity type, thereby improving the accuracy and validity of free-living mechanical loading estimation.

The ability to estimate mechanical loading during daily life using wearable accelerometers has important implications for exercise physiology in general and bone health research and practice in particular. By enabling the long-term monitoring of osteogenic physical activity, this technology can provide valuable insights into the population-level relationships between mechanical loading and critical bone outcomes, such as bone mineral density, bone quality, and fracture risk [21,40,43,56]. Moreover, quantifying mechanical loading can facilitate the development of personalized exercise prescriptions, ensuring that individuals meet target doses of bone-stimulating activity. In rehabilitation and injury prevention settings, monitoring mechanical loading can help progress impact exercise while minimizing the risk of excessive forces that may lead to stress fractures [57,58]. As the field of accelerometer-based mechanical loading estimation continues to evolve, the integration of activity-specific prediction models and activity recognition algorithms holds great promise for enhancing the accuracy and validity of free-living assessments. These advances can contribute to a better understanding of the complex relationships between physical activity, mechanical loading, and bone health across diverse populations, informing the development of targeted interventions and public health strategies to promote skeletal health and reduce the burden of osteoporosis and fragility fractures.

1.2. Aims

While accelerometer-based prediction equations are a promising method for enabling the assessment of mechanical loading in free-living conditions, further research is needed to: expand their validity to a broader range of activities, optimize data processing techniques, and integrate activity recognition algorithms. Addressing these limitations is crucial for enhancing the accuracy and practical applicability of accelerometer-based mechanical loading monitoring. Therefore, the

main objectives of this thesis were to: i) develop and validate accelerometer-based mechanical loading prediction equations for estimating peak ground reaction forces and peak loading rates during walking, running, and jumping activities; and ii) develop and validate accelerometer-based activity classification algorithms for differentiating between walking, running, and jumping activities using accelerometer data.

To address each of these objectives, a series of original studies was performed with the following specific aims:

- Study 1: develop and validate accelerometer-based peak ground reaction force and peak loading rate prediction equations for walking and running.
- Study 2: develop and validate accelerometer-based peak ground reaction force and peak loading rate prediction equations for high-impact jumping activities.
- Study 3: externally validate existing accelerometer-based mechanical loading prediction equations by applying them to a sample and testing conditions distinct from the original validation studies.
- Study 4: develop and validate activity classification models for differentiating between walking, running and jumping activities based on accelerometer data.

In summary, this thesis aims to advance the field of accelerometer-based mechanical loading assessment. The four original studies provide a comprehensive approach to addressing current limitations and enhancing the accuracy and practical applicability of these methods for monitoring mechanical loading in free-living conditions.

This thesis is organized into six main chapters. Chapter I includes the general introduction, aims, and an overview of the original research articles that form the core of the thesis. Chapter II presents a narrative literature review on the use of

accelerometers for predicting mechanical loading during physical activity, highlighting current knowledge gaps and areas for future research. Chapter III includes the four original studies conducted to address the thesis objectives. Chapter IV offers an integrative discussion of the findings from the original studies, contextualizing them within the broader field of accelerometer-based mechanical loading assessment. Chapter V summarizes the main conclusions drawn from the research, emphasizing the key contributions and practical implications of the work. Finally, Chapter VI provides a complete list of references cited in Chapters I, II, and IV.

Chapter 2: Literature review

2.1. Bone biology and adaptation

Bone is a dynamic tissue that constantly adapts its structure and strength in response to mechanical stimuli. This process, known as mechanotransduction, involves the conversion of mechanical forces into biochemical signals that regulate bone cell activity and remodeling [1,2,59]. Osteocytes, the most abundant cells in bone, play a central role in sensing mechanical loads and orchestrating the adaptive response [7,8]. When subjected to loading, fluid flow within the lacunar-canalicular network generates shear stresses on the osteocyte cell body and dendritic projections, triggering intracellular signaling cascades that modulate the activity of osteoblasts and osteoclasts [4,8]. The mechanotransduction process enables bone tissue to modify its mass, geometry, and microarchitecture to withstand better the loads placed upon it [10,11].

Julius Wolff first described this adaptive process in the late 19th century and is often referred to as Wolff's law [60]. Wolff postulated that bone adapts its mass and architecture in response to the mechanical loads placed upon it, with bone formation occurring in areas of high stress and bone resorption in low-stress areas [61]. Building upon Wolff's law, Harold Frost later proposed the mechanostat theory to explain how bone senses and responds to mechanical loading at the tissue level [62]. According to the mechanostat theory, bone contains a regulatory mechanism (the "mechanostat") that senses mechanical strains and triggers adaptive changes in bone structure to maintain strains within an optimal range [62,63]. When strains exceed the upper threshold of this range, bone formation is stimulated to increase bone strength, while strains below the lower threshold promote bone resorption to remove excess mass [64].

At the tissue level, bone undergoes modeling and remodeling in response to mechanical stimuli [1,2,65,66]. Modeling involves the independent actions of osteoblasts and osteoclasts to shape the growing skeleton. At the same time, remodeling is a coupled process where osteoclasts resorb old or damaged bone and osteoblasts subsequently form new bone [66]. Mechanical loading stimulates

modeling by promoting osteoblast differentiation and activity, leading to periosteal apposition and increased bone size [2]. Loading also influences remodeling by suppressing osteoclast-mediated resorption and stimulating osteoblast-mediated formation, resulting in a positive net bone balance [1,2].

2.2. Bone response to mechanical loading

A set of fundamental variables, such as the magnitude, rate, frequency, and duration of the loading determines the potential of mechanical loading to promote bone formation [9,67]. High-magnitude loads that generate strains above a certain threshold are more effective at stimulating bone formation than low-magnitude loads [59,68]. The strain threshold for initiating an adaptive response varies depending on the skeletal site and loading conditions [9,69]. However, extremely high strains above the yield point can cause micro damage and may have detrimental effects on bone strength [57,70].

Loading rate, which is how quickly the ground reaction force is applied to the body, is another critical factor influencing bone adaptation [13,46]. High loading rates are more osteogenic than low ones, even when the peak loading magnitudes are similar [13,46]. This rate-dependent effect is thought to be mediated by fluid flow-induced shear stresses within the lacunar-canalicular network, which are greater under high-rate loading [71,72]. *In vivo* studies in animal models have demonstrated that dynamic loading at high strain rates is more effective at enhancing bone formation than static or low-rate dynamic loading [13,73].

The frequency and duration of loading also play important roles in bone adaptation [73,74]. Intermittent or cyclic loading is more osteogenic than continuous loading, as bone cells become desensitized to prolonged mechanical stimuli [74,75]. Inserting rest periods between loading cycles allows for resensitization of the mechanosensory apparatus, enhancing the anabolic response [74,76]. Animal studies have shown that dividing a given loading regimen into multiple short bouts

separated by recovery periods is more effective at increasing bone mass and strength than a single continuous prolonged loading bout [75–77].

Seminal animal studies have provided key insights into the effects of specific loading parameters on bone adaptation. Rubin and Lanyon (1984) [68] demonstrated in roosters that as few as 36 loading cycles per day were associated with new bone formation, and that increasing the number of cycles induced no additional benefit. Later, Rubin et al. (2001) [78] showed that very low-magnitude, high-frequency vibration could increase trabecular bone density in sheep, even though these results were not later confirmed in older humans [79]. Turner et al. (1994) [59] demonstrated that bone formation in rat tibiae increased significantly with higher loading frequencies while showing no response at lower frequencies. This suggests that the osteogenic response is closely linked to fluid flow within the bone matrix. This concept was further supported by Hsieh and Turner (2001) [73], who observed that loading with higher frequencies was more effective than lower frequencies in increasing bone formation in rats, leading to the need of lower strain thresholds to effectively stimulate bone formation. In addition to these findings, Robling et al. (2002) [77] also demonstrated that partitioning a loading protocol into multiple short bouts separated by rest periods enhanced the anabolic response compared to a single more prolonged bout, highlighting the importance of rest periods in optimizing bone adaptation.

While most of these foundational studies were conducted in animals, the principles of mechanical loading have also been shown to apply to humans [16,80,81]. High-impact activities like running and jumping and high-intensity resistance training are more effective at increasing bone mineral density and strength than low-impact activities like walking [16,17,80]. The osteogenic response to loading also varies depending on age and sex, with the highest benefits observed during the pre- and early pubertal years [82,83]. After skeletal maturity, the adaptive response to loading is attenuated but still present, which is particularly relevant for postmenopausal women and older adults with osteoporosis and at risk of fragility

fractures [81,84]. Thus, optimizing the manipulation of mechanical loading variables through targeted exercise interventions remains a key strategy for promoting bone health throughout the lifespan [83–85].

2.3. Physical activity and bone health

Physical activity plays a critical role in developing and maintaining bone health. Weight-bearing activities that generate high-impact forces are particularly effective at stimulating bone formation and increasing bone mineral density [16,86]. These activities produce ground reaction forces several times greater than body weight, inducing strains and stresses that exceed the osteogenic threshold [12] . The repetitive nature of these impacts also provides the dynamic loading necessary for optimal bone adaptation [10,67]. Resistance training is another form of physical activity that can promote bone health by imposing mechanical loads on the skeleton [19,80,87]. Resistance exercises engage large muscle groups and involve compound movements that generate high forces and strains, thus stimulating osteogenic adaptation [10,16].

Numerous studies have demonstrated the beneficial effects of impact activities on bone health across the lifespan [83–85]. In children and adolescents, participation in sports that involve jumping, sprinting, and multidirectional movements has been associated with greater bone mass and strength compared to non-impact sports or sedentary behavior [88,89]. A meta-analysis by Behringer et al. (2014) [90] found that weight-bearing exercise interventions significantly increased bone mineral content in children and adolescents. In premenopausal women, high-impact exercise has been shown to enhance bone mineral density at the hip [80,81] and, when combined with resistance training, also at the lumbar spine [80]. Vainionpää et al. (2006) [21] observed that the intensity of exercise, as measured by the magnitude of vertical acceleration peaks, was positively associated with bone mineral density changes in premenopausal women. In postmenopausal women, high-impact training combined with high-intensity resistance training has been found

to significantly increase bone mineral density at the lumbar spine and femoral neck and increase femoral neck cortical thickness [84].

Walking and running are two of the most common forms of weight-bearing exercise, and their effects on bone health have been extensively studied [91–95]. Walking is a low-impact activity that generates ground reaction forces of 1-2 times body weight while running produces forces of 2-3 times the body weight [16]. Regular walking, mainly at brisk paces, has been frequently associated with higher bone mineral density and lower fracture risk in postmenopausal women, suggesting its potential as an effective weight-bearing exercise for maintaining bone health [95,96], even though it is not recommended for patients with high fracture risk [97]. Running has been consistently associated with increased bone mass and improved bone strength, particularly in weight-bearing regions such as the hip and spine, from young adults to older individuals [94,98]. However, high running volumes may have diminishing returns or even detrimental effects on bone health, possibly due to overuse injuries or energy imbalances [99,100].

Jumping is a high-impact activity that imposes substantial mechanical loads on the skeleton, generating ground reaction forces that reach 6-8 times an individual's body weight [16]. These forces produce highly effective strains in stimulating osteogenic responses, making jumping a potent stimulus for bone adaptation [19,101]. The mechanical loadings induced by jumping also result in high strain rates, which are particularly effective at stimulating bone formation [42,102,103]. Exercise interventions based on jumping activities have been shown to significantly increase bone mineral density and strength in children, adolescents, and premenopausal women [81–83]. In postmenopausal women, jumping combined with other high-impact exercises has been found to attenuate bone loss and improve bone structure [84]. Mechanical loading-induced osteogenic effects are site-specific, with the most remarkable adaptations occurring in skeletal regions that experience the highest strains [68,104]. In the case of jumping, the hip and spine are subjected

to the highest loads during landing, resulting in more pronounced benefits at these sites than other skeletal regions [101,105].

Regarding resistance exercise, a meta-analysis by Martyn-St James and Carroll (2006) [87] found that high-intensity resistance training significantly increased lumbar spine bone mineral density in postmenopausal women, while effects on the femoral neck were inconsistent and non-significant. In older men, resistance training has been shown to enhance bone mass, geometry, and strength, mainly when performed at high intensities and with high loading rates [106,107].

Currently, several exercise recommendations exist for bone health across different populations [16,17,54,55]. The American College of Sports Medicine advises adults to engage in moderate- to high-intensity weight-bearing activities, such as walking, jogging, jumping, and stair climbing, 3 to 5 times per week [16]. The ACSM also recommends practicing moderate to high intensity resistance exercises 2 to 3 times per week [16]. Each weight-bearing and resistance exercise session should last 30 to 60 minutes [16]. Exercise and Sports Science Australia (ESSA) encourages adults to perform impact exercises that generate at least 4 times their body weight in loading magnitude 4 to 7 times per week [17]. These impact exercises can include various types of jumping, performed in 3 to 5 sets of 10 to 20 repetitions, with 1 to 2 minutes of rest between sets [17]. The ESSA also recommends participating in high-intensity resistance exercises (80% to 85% of one repetition maximum) twice a week, with 2 to 3 sets of 8 repetitions each [17]. Additionally, balance exercises are recommended to reduce fall risk, which influences fracture risk [17,108]. The National Osteoporosis Foundation advises regularly practicing weight-bearing and muscle-strengthening exercises to maintain or improve bone strength and balance exercises to lower the risk of falls and fractures [54]. A consensus statement from the United Kingdom emphasizes the importance of resistance exercises for all individuals with osteoporosis [55]. It recommends performing these exercises 2 to 3 times per week, focusing on major muscle groups with 2 to 3 sets of 8 to 12 repetitions [55]. Exercises that strengthen back muscles

are also advised to enhance posture and support the spine [55]. The statement also suggests engaging in moderate-impact activities, such as jumping, skipping, hopping, and running, on most days, aiming for around 50 impacts with rest periods in between [55]. Lastly, to reduce the risk of falls, it recommends the practicing exercises like Tai Chi, dance, yoga, and Pilates, at least 2 times per week [55].

2.4. Mechanical loading assessment

Accurate assessment of mechanical loading during physical activity is essential for understanding the dose-response relationship between loading and bone adaptation and for designing effective interventions to promote bone health [2,9,109]. Several methods have been used to measure or estimate mechanical loading, each with its strengths and limitations [23,25,30–32,35,110,111].

In animal studies, mechanical loading is often assessed using electrical resistance strain gauges attached to the surface of bones. This allows researchers to quantify the mechanical strains experienced by bones during various activities [110]. Pioneering work in this area was conducted by Lanyon and Smith [112], who demonstrated that attaching strain gauges to bones could provide detailed insights into the strain environment during locomotion. These studies revealed remarkable uniformity in peak strains across different species and activities, supporting the mechanostat theory of bone adaptation, which advocates that bone structure adjusts in response to mechanical loading [110]. These techniques have also been applied to human subjects [113]. However, they are invasive and challenging to implement in human studies due to ethical considerations and practical limitations.

Given the difficulties associated with directly measuring mechanical loads in humans, researchers often rely on ground reaction forces as a surrogate measure of mechanical loading [23,114]. Ground reaction forces represent the forces exerted by the ground on a body in contact with it and are typically measured using force plates [23,114]. These devices are the gold standard for assessing mechanical loading during weight-bearing activities [23]. They provide precise data on the

magnitude, direction, and timing of forces acting on the body, enabling researchers to accurately calculate joint moments and stresses [23,41,115]. While force plates offer high accuracy, their use is limited to laboratory settings primarily due to their requirement for specialized settings and ancillary equipment [23,114]. This limitation restricts their application in large-scale or long-term studies examining physical activity and bone health.

Pressure insoles are wearable devices that measure the pressure distribution under the foot during weight-bearing activities [111]. They consist of thin, flexible sensors inserted into the shoe and connected to a data logger or wireless transmitter [41,111]. Pressure insoles provide a portable, low-cost alternative to force plates for estimating ground reaction forces outside the laboratory [116,117]. These insoles contain an array of pressure sensors that measure pressure distribution across the foot during weight-bearing activities [111]. The force estimates are calculated indirectly by integrating the pressure data over the contact area and multiplying by the area of sensor location [111]. However, this method has limitations and may be less accurate compared to plates, which directly measure the three-dimensional forces applied to the ground [23,41,111].

Questionnaires are subjective methods that have been used to assess physical activity and estimate mechanical loading [24,25]. These tools require individuals to recall their participation in various activities over a specified period [118,119]. Questionnaires can provide valuable information on the type, frequency, duration, and intensity of activities, which can then be used to estimate the mechanical loads experienced by the body [24,25]. For example, the Bone-specific Physical Activity Questionnaire assigns load ratings to different activities based on ground reaction forces and asks individuals to report their current and past participation in these activities [25,120]. This questionnaire has been shown to predict bone outcomes in various populations, suggesting it captures relevant information about mechanical loading [120,121]. However, questionnaires and diaries have limitations, such as recall bias, social desirability bias, and lack of

precision in quantifying the intensity and frequency of activities [26,122]. As they do not provide direct measures of mechanical loading, their ability to establish dose-response relationships between loading and bone adaptation is limited [27,28].

Accelerometers are wearable technology equipment that have been used to assess mechanical loading during physical activity [29–32,35,38,39]. Accelerometers are small, lightweight devices that measure accelerations in one or more axes, indicating the magnitude and frequency of the forces experienced by the body [36,123]. They have been widely used in physical activity research to quantify the intensity, duration, and movement patterns in free-living conditions [124,125]. Accelerometers have also been applied to the study of bone loading based on the premise that accelerations are proportional to the forces acting on the body [33–35]. Several studies have shown that accelerometer-derived measures, such as peak acceleration, acceleration gradient, and cumulative acceleration, are associated with ground reaction forces and bone outcomes [34,35,44,103].

Accelerometers also have several limitations in estimating mechanical loading. First, they do not directly measure forces but rather accelerations, which are influenced by soft tissue motion and external vibrations [126]. Second, accelerometers have a limited ability to capture certain types of loading, such as skeletal muscle tension and bending moments, which are also important contributors to bone adaptation [127]. Therefore, they are unsuitable for estimating mechanical loadings generated by resistance training, an important and commonly prescribed exercise mode for improving bone health [16,17,54]. Third, the device's specifications, such as sampling frequency, measurement range, and filtering, can affect accelerometer output, making it difficult to compare results across studies [36,37]. Finally, accelerometers require careful calibration, data processing, and interpretation to ensure valid and reliable results [47,128].

2.5. Accelerometry technology

Accelerometers have emerged as a promising tool for assessing mechanical loading during physical activity due to their ability to measure accelerations that are related to the forces experienced by the body [33–35]. These devices are electromechanical sensors that convert physical motion into electrical signals proportional to the acceleration [123]. Accelerometers typically consist of a proof mass attached to a spring or beam, which deflects in response to accelerations, and a transducer that converts the mechanical displacement into an electrical output [129]. The output is then filtered, amplified, and digitized to produce a time series of acceleration data [123].

Various types of accelerometers are available, each with advantages and limitations based on their sensing mechanism and output characteristics. The most common types include piezoelectric, piezoresistive, and capacitive accelerometers [129]. Recent advancements in microelectromechanical systems technology have led to the development of miniaturized, low-power, and low-cost accelerometers well-suited for wearable applications [130]. This kind of accelerometer, which typically use capacitive sensing, has been widely used in consumer electronics and research-grade devices for physical activity and health monitoring [36,129].

To effectively use accelerometers in research settings, several key steps in data collection and processing must be considered [47,48]. First, the accelerometer captures mechanical acceleration and converts it into an electrical signal [129]. This signal is then calibrated to establish the relationship between the signal and the acceleration, typically assumed to be linear with an offset and gain factor [129,131]. After calibration, the raw acceleration signal is filtered to remove noise and artifacts using low-pass, high-pass, and band-pass filters [132]. Feature extraction is then performed to derive variables from the acceleration data, such as average acceleration, peak acceleration, acceleration gradients, coefficient of variation, and frequency-domain characteristics [35,133]. Finally, validation needs to be done to transform these accelerometer-derived variables into valid biologically meaningful

outcomes, such as energy expenditure or mechanical loading, using established prediction equations or machine learning algorithms based on gold standard procedures [47,48,124].

Several signal processing techniques have been employed to analyze accelerometer data to assess mechanical loading [29,32,44,103]. Peak detection is a common technique that involves identifying the maximum acceleration value within a given time window [32]. Peak accelerations have been shown to correlate with ground reaction forces [33–35] and have been used to estimate the intensity and frequency of impacts during various activities [29–32,38,39]. Time-domain analysis is another technique that involves calculating statistical measures of the acceleration signal, such as mean, standard deviation, and root mean square [134]. These measures provide information about the overall magnitude and variability of the accelerations and have been used to classify different types of activities and movements [133]. Frequency-domain analysis techniques, such as Fourier transforms and wavelet analysis, can decompose the acceleration signal into its constituent frequencies and identify specific patterns of movement [134].

The placement of accelerometers on the body is another important consideration for assessing mechanical loading, as the location and orientation of the device can affect the magnitude and direction of the measured accelerations [37,132]. The most common placement sites are the hip, waist, and wrist, associated with different movement and loading patterns [37]. Hip and waist placements, due to their proximity to the body's center of mass, are often used to assess whole-body movements and vertical accelerations, which are related to ground reaction forces and bone loading [30–32,35,44]. Wrist placement is often used to assess upper limb movements and activities of daily living but may not capture the loading experienced by the lower limbs and torso [135]. Other placement sites, such as the ankle, thigh, and lower back, have also been used to assess specific movements and loading patterns [31,32]. Importantly, the optimal placement site will depend on the specific

research question, population, and activities of interest and may require validation against criterion measures [37].

The dynamic range and sampling frequency of accelerometers are important technical considerations when assessing mechanical loading [32,39,41]. The dynamic range refers to the range of accelerations the device can measure accurately, typically expressed in ±*g*, where 1*g* represents the earth's gravitational acceleration (9.807m·s^{-2}). Accelerometers with a higher dynamic range, such as ±8*g* or ±16*g*, are better suited for capturing high-impact activities and fast movements. In contrast, those with lower dynamic ranges may be sufficient for measuring low-impact activities and slower movements. Another essential aspect is the accelerometer sampling frequency, expressed in Hertz (Hz) [37,41]. It determines the temporal resolution of the acceleration data and the ability to capture high-frequency movements. Higher sampling frequencies, such as 100Hz or above, are necessary for accurately measuring rapid movements and impacts [32,41]. Again, the choice of dynamic range and sampling frequency will depend on the specific research question, the characteristics of the study population, and the activities of interest. It is essential to ensure that the accelerometer specifications are appropriate for capturing the desired range and frequency of mechanical loading to be assessed.

2.6. Mechanical loading variables and their prediction using accelerometer data

2.6.1. Ground reaction forces and loading rate

Ground reaction forces are the forces exerted by the ground on the body during contact and are a key determinant of the mechanical loading experienced by the musculoskeletal system [23,136]. These forces arise from the acceleration of the body's center of mass and are equal and opposite to the forces applied by the body to the ground [23,115]. Ground reaction forces comprise three orthogonal components: vertical, anteroposterior, and mediolateral [23,115,136]. The vertical

component of the ground reaction force is the most studied and typically has the highest magnitude among the three components [23]. This component represents the force acting perpendicular to the ground surface [23]. The anteroposterior component represents the force acting parallel to the ground surface in the direction of movement, while. In contrast, the mediolateral component represents the force acting perpendicular to the direction of movement [23]. The magnitude and timing of these components vary depending on the activity type and the movement phase [115].

During walking and running, the vertical ground reaction force typically exhibits a characteristic pattern with two peaks: an impact peak at heel strike and an active peak during push-off [136]. The impact peak is associated with the rapid deceleration of the foot and leg at initial contact. It is influenced by factors such as foot strike pattern, shoe cushioning, and surface stiffness [136,137]. The active peak, on the other hand, is related to the acceleration of the body's center of mass during midstance and push-off and is affected by factors such as running speed, stride length, and muscle activation [137,138]. The magnitude of the vertical ground reaction force increases with locomotion speed and can reach values of 2-3 times body weight during moderate-intensity running [136].

The anteroposterior ground reaction force demonstrates a biphasic pattern during walking and running, with a braking force during the first half of the stance and a propulsive force during the second half [136]. The braking force occurs as the foot strikes the ground and the body's center of mass decelerates. In contrast, the propulsive force is generated during push-off to accelerate the body's center of mass forward [138]. The magnitude of the anteroposterior ground reaction force is typically smaller than the vertical ground reaction force and is usually less than body weight [136]. The mediolateral ground reaction force, being the smallest component, exhibits a variable pattern that depends on the specific activity and the individual's gait characteristics [115].

Another important variable of ground reaction forces is the loading rate, which refers to the rate of change of the force overtime [13,45,103]. The loading rate is typically measured as the slope of the ground reaction force during the initial impact phase and is expressed in units of force per second [13,103]. High loading rates have been associated with positive bone health effects by eliciting high lacuna-canalicular fluid flow. They are particularly effective in stimulating bone remodeling and increasing bone strength [103]. However, excessive loading rates have also been linked to an increased risk of stress fractures and other overuse injuries, as they generate high strain rates that can cause microdamage to the bone tissue [139]. Loading rates are influenced by running speed, stride length, and muscle activation, and can be modified through gait retraining and other interventions [140].

2.6.2. Ground reaction forces and loading rate prediction using accelerometer data

Ground reaction forces can be estimated from accelerometer data using biomechanical models [41]. The basic principle is that the acceleration of the body's center of mass is proportional to the net force acting on the body, according to Newton's second law of motion [32,41]. By measuring the acceleration of a body segment, such as the hip or trunk, and knowing the segment's mass, the GRF can be estimated using inverse dynamics [37]. However, this approach requires accurate segment kinematics and inertial properties measurements, which can be challenging with wearable sensors [41]. Linear regression models have been used to estimate ground reaction forces from accelerometer data establishing a relationship between the acceleration features and the measured ground reaction forces [29–32]. These techniques have shown promising results, with less than 10% errors for the vertical ground reaction forces during walking and running [29,32]. In addition to linear models, machine learning techniques such as artificial neural networks and support vector machines have also been employed to estimate ground reaction forces from accelerometer data [41].

Several studies have developed and validated ground reaction force prediction models for different populations and activities. Fortune and colleagues (2014) [31] developed models to predict ground reaction force using data from accelerometers worn at the ankle, tibia, thigh, and waist. The study was on a sample of adults and used walking as the activity tested. They achieved accuracies ranging from approximately 7% to 13%, with the ankle-worn accelerometer providing the most accurate estimates. Neugebauer et al. (2014) [30] recruited a sample of adults who wore accelerometers on their hips while walking and running. The vertical ground reaction force's prediction accuracy was around 8%. Veras et al. (2020) [32] also recruited a sample of adult with a wide range of body masses (50-150kg approximately). In this study, participants wore accelerometers at their hip and lower back while walking. Prediction accuracies ranged from around 5% to 7%, and the hip-worn accelerometer achieved the best results. These studies demonstrate the feasibility and accuracy of mechanical loading prediction models based on accelerometer data but also highlight the need for further validation and refinement of the models for different populations and activities [30–32].

Loading rates can also be estimated from accelerometer data using approaches similar to those used for ground reaction forces [31,32]. However, the estimation of loading rates is more challenging, as it requires high sampling rates and low noise levels to capture the rapid changes in acceleration during the impact phase. Studies validating accelerometry-based loading rate prediction models have reported varying levels of accuracy. Veras et al. (2020) [32] developed regression equations incorporating peak acceleration transient rate and body mass to predict peak loading rate in participants with a wide body mass index range, achieving errors of approximately 20%. The study demonstrated the potential for accelerometer-derived loading rate predictions in clinical settings despite errors being higher than for ground reaction force prediction. Similarly, Fortune et al. (2014) [31] demonstrated that ankle- and waist-worn accelerometers provided the most accurate estimates of peak vertical loading rates during walking across various speeds, with mean absolute differences of 23-26%. These findings highlight the

feasibility of using accelerometers to estimate loading rates in dynamic activities, although improvements in technology and model refinement are necessary to enhance prediction accuracy further.

2.6.3. Activity classification and its importance in the context of mechanical loading prediction

Activity classification, which involves identifying and categorizing different types of physical activities, plays a crucial role in mechanical loading prediction. Different activities exhibit distinct loading patterns and require specific prediction models [35]. Accurate activity classification can enhance the accuracy and specificity of mechanical loading prediction by selecting the appropriate model for each activity, thereby avoiding the application of unsuitable models for each movement pattern.

Activity classification can be performed using machine learning algorithms, such as decision trees, support vector machines, and artificial neural networks [141]. These algorithms learn the relationship between the sensor data and the activity labels based on a training dataset that includes both the sensor data and the corresponding activity labels [141]. The trained algorithm can then classify new sensor data into different activity categories based on the learned patterns and rules [141].

Several studies have developed and validated activity classification models for different populations and activities. Cleland et al. (2013) [142] developed a support vector machine algorithm to classify six activities (walking, running, sitting, lying, standing, and walking up and down the stairs) based on accelerometer data from the chest, wrist, lower back, hip, thigh, and foot in young adults. The model had an overall accuracy of around 96% and could effectively distinguish between activities with different loading patterns, such as walking and running. Sasaki et al. (2016) [143] developed a support vector machine and random forest algorithms to classify five activity types (sedentary, standing, household, locomotion, recreational) based on hip, wrist, and ankle accelerometer data in free-living older adults. The

algorithms trained on free-living data achieved overall accuracy rates of 58-69%, outperforming lab-trained algorithms. The hip and ankle placements performed slightly better than the wrist in classifying activities. Ellis et al. (2016) [144] developed machine learning algorithms using random forests and hidden Markov models to classify four activity types (sitting, standing, walking/running, and riding in a vehicle) based on hip and wrist accelerometer data in free-living women with overweight or obesity. The hip and wrist accelerometers achieved an overall accuracy of around 87%. While these studies demonstrate the feasibility and accuracy of activity classification models based on accelerometer data, there is a lack of classification methods explicitly designed for the context of bone health-related mechanical loading. Further research is therefore needed to develop and validate activity classification models that can accurately identify and differentiate between activities with distinct osteogenic potential, such as walking, running, and jumping, to improve the assessment of mechanical loading in free-living conditions.

2.7. Methodological considerations

The development and validation of mechanical loading prediction models based on accelerometer data involve several methodological considerations, which can affect the results' accuracy, reliability, and generalizability [37,41,47,48]. These considerations include the study design, sample size, data quality control, statistical approaches, validation methods, and external validity [47,48].

Sample size and data quality control are crucial methodological considerations in mechanical loading research that are closely interconnected [41,47,48]. Smaller sample sizes may limit the reproducibility and external validity of the findings and increase the risk of type II errors. In contrast, larger sample sizes provide more robust and representative results at the cost of increased resource requirements and potentially more complex statistical models [47,48]. To ensure the accuracy and reliability of the data, researchers must implement appropriate data quality control measures, which typically involve three main steps: data cleaning,

filtering, and imputation [37,41,48]. While data quality control is essential for improving the accuracy and reliability of the results, researchers must be aware that it can also introduce bias and reduce data variability.

The selection of appropriate statistical approaches is crucial in determining the type and quality of inferences that can be drawn from the data [48]. Regression-based approaches, such as linear, logistic, and polynomial regression, have been widely used to model the relationship between accelerometer data and mechanical loading variables [30,32]. These approaches offer several advantages, making them particularly useful for estimating associations' magnitude and direction and predicting outcomes based on predictors. Regression-based methods provide high interpretability, allowing researchers to quickly understand the relationship between variables and communicate their findings to a broader audience [41,48,145]. Moreover, these approaches are well-suited for studies with smaller sample sizes and less complex data structures, as they require fewer assumptions and are less computationally intensive compared to more advanced techniques [41,48]. Additionally, regression-based methods can control for confounding variables and assess the relative importance of different predictors, providing a more comprehensive understanding of the factors influencing mechanical loading [146,147]. However, it is essential to note that regression-based approaches assume linear and additive relationships, which may not always capture non-linear and interactive effects [145]. In contrast, machine learning approaches, such as decision trees, support vector machines, and artificial neural networks, can model more complex and non-linear relationships and handle high-dimensional and multicollinear data [148]. Still, they often require large and diverse datasets and may be more challenging to interpret and generalize [148]. Ultimately, the choice of statistical approach should be guided by the research question, data characteristics, and the desired balance between interpretability and generalizability, with regression-based methods remaining a robust and widely applicable choice in many mechanical loading studies.

Validation methods are crucial in determining the accuracy and generalizability of prediction models in mechanical loading research [48]. Cross-validation techniques, such as k-fold cross-validation and leave-one-out cross-validation, have been widely employed to estimate prediction error and optimize model parameters [41,48]. These methods involve partitioning the data into training and testing sets and repeatedly fitting and evaluating the models on different subsets of the data [48]. Compared to single-sample methods, cross-validation approaches provide more robust and unbiased estimates of prediction error. However, cross-validation methods may not fully capture the variability and heterogeneity of the population, potentially leading to an overestimation of model performance in new settings [48]. To address this limitation, external validation methods can be employed to provide more direct evidence of the generalizability and transportability of the models [48,147]. External validation involves testing the models on independent datasets from different populations or settings, offering a more rigorous assessment of their performance in real-world scenarios.

External validity is another critical consideration, as it determines the applicability and relevance of the results to real-world settings [48,149]. Most studies have been conducted ising standardized protocols and equipment [29–32,147].in controlled laboratory settings Laboratory settings can provide more accurate and reliable measurements of the mechanical loading variables, ad can control for confounding factors such as speed, surface, and footwear [150]. However, laboratory settings may not reflect the variability and complexity of real-world environments and may limit the ecological validity of the results. Field-based studies, which involve data collection in free-living conditions, can provide more realistic and representative measurements of the mechanical loading variables, and can capture the context and variability of daily activities. The choice of study setting depends on the research question, the available resources, and the desired level of control and generalizability.

2.8. Clinical applications

Developing accurate and reliable methods for predicting mechanical loading from accelerometer data has important research and clinical applications for bone health assessment, monitoring, and management. Bone health is critical to overall health and quality of life, as it affects the risk of fractures, disability, and mortality [151,152]. Accelerometer-based methods for predicting mechanical loading offer a non-invasive, portable, and scalable approach for quantifying the forces experienced by the musculoskeletal system during physical activity [30–32]. These methods can provide valuable insights into the mechanical stimuli that influence bone health, enabling researchers and clinicians to better understand the relationship between physical activity and bone adaptation. By accurately assessing mechanical loading in various settings and populations, accelerometer-based prediction models can inform the development of targeted interventions and monitoring strategies to optimize bone health outcomes.

A potentially important clinical application of accelerometer-based mechanical loading prediction is exercise monitoring and prescription. Exercise is a key modifiable factor for promoting bone health, as it can stimulate bone formation, reduce bone resorption, and improve bone strength and quality [153]. However, the optimal type, intensity, frequency, and duration of exercise for bone health vary depending on the individual's age, sex, health status, and preferences [16,17,94,154]. Accelerometer-based methods can provide personalized and objective data on the mechanical loading experienced during different types of exercise, which can inform the design and monitoring of exercise programs. For example, accelerometer-based methods can be used for exercise that generate high-impact loading, such as jumping and running, which are more effective for stimulating bone formation. Moreover, accelerometer-based methods can be employed to monitor the progression of loading over time, allowing for the adjustment of exercise programs to maintain an appropriate osteogenic stimulus as the individual adapts to the current regimen. Additionally, these methods can

promote adherence to exercise programs by providing patient feedback and motivation.

Accelerometer-based mechanical loading prediction can also play a valuable role in rehabilitating patients with bone health conditions, such as osteoporosis or osteopenia. These conditions are characterized by low bone mass, compromised bone structure, and increased fracture risk, which can lead to pain, disability, and reduced quality of life [54]. Rehabilitation protocols for these conditions typically involve a multifaceted approach, combining pharmacological, nutritional, and physical therapy interventions to improve bone health, reduce fracture risk, and restore function [16,17,54]. Accelerometer-based methods can be used to monitor the mechanical loading experienced during rehabilitation exercises, and to ensure that the exercises are safe, effective, and progressive. For example, mechanical loading prediction methods can identify the types of exercises that generate low-impact loading that are appropriate for these patients. Accelerometer-based prediction methods can also monitor the patient's activity level and sedentary behavior, which are important for bone health and recovery.

In sports performance and injury prevention, accelerometer-based mechanical loading prediction can optimize training programs and reduce the risk of injuries such as stress fractures [57,58]. These fractures are a common type of overuse injury in athletes, particularly in sports that involve repetitive high-impact loading, such as running, jumping, and pivoting [57]. Stress fractures occur when the bone is repetitively subjected to mechanical loads that exceed its capacity to repair and adapt, leading to microdamage accumulation and fracture development [57]. Accelerometer-based methods can be used to monitor the mechanical loading experienced during training and competition and identify the athletes at risk of developing stress fractures [57,58]. For example, accelerometer-based methods can measure the number and magnitude of high-impact loading cycles associated with increased stress fracture risk [58].

Accelerometer-based mechanical loading prediction can benefit various special populations with unique bone health needs and challenges, such as the elderly, individuals with obesity, high level athletes, clinical populations, and bariatric surgery patients [56,58,155,156]. For instance, the elderly population faces a high risk of osteoporosis and fragility fractures due to age-related declines in bone mass and strength [155]. In this context, mechanical loading prediction models can be used to assess the impact of different exercise interventions on bone health in the older people, accelerometer-based approaches can help identify elderly individuals who may not be engaging in sufficient bone-stimulating activities, prompting healthcare professionals to provide targeted recommendations for increasing mechanical loading through exercise or daily activities to maintain or improve bone health. Similarly, patients with obesity may experience bone health problems due to metabolic and hormonal alterations associated with obesity [156]. These prediction methods can be employed to monitor mechanical loading during weight-bearing activities and estimate the potential impact of weight loss interventions on bone health. Also, bariatric surgery patients experience rapid weight loss [157] and changes in mechanical loading post-surgery [56], which can lead to bone loss [158] and increased fracture risk [159]. Accelerometer-based methods can be instrumental in monitoring mechanical loading before and after surgery, aiding in identifying patients at risk of bone health complications [56].

High-level athletes, frequently exposed to high levels of mechanical loading during training and competition, may also benefit from these prediction techniques to optimize their training programs for performance enhancement and injury prevention, particularly in the context of overuse injuries and stress fractures [57,58]. Furthermore, clinical populations, such as patients with osteoporosis, diabetes, and chronic kidney disease, face bone health challenges due to underlying disease processes and medication side effects. In these cases, mechanical loading prediction can help monitor daily activities and exercise and assess the effectiveness of pharmacological and non-pharmacological interventions for bone health.

2.9. Future directions

The accelerometer-based mechanical loading prediction field is undergoing rapid advancements, with novel technologies, methodologies, and applications continually emerging. To fully harness the potential of this field for bone health research and clinical practice, several key areas must be prioritized for future development. From a technical perspective, ongoing efforts should improve the accuracy, reliability, and versatility of accelerometer-based prediction models across diverse populations and activities. This may involve the development of more sophisticated algorithms, the incorporation of machine learning techniques, and the exploration of new sensor configurations and data fusion approaches.

In terms of research needs, future studies should aim to validate and refine existing prediction models in more extensive and more heterogeneous samples, as well as investigate the long-term associations between accelerometer-derived mechanical loading metrics and bone health outcomes. Moreover, there is a need to establish standardized protocols and best practices for data collection, processing, and analysis to ensure the comparability and reproducibility of findings across studies.

From a clinical implementation standpoint, efforts should be directed toward translating accelerometer-based mechanical loading prediction into practical tools and guidelines that can be readily integrated into routine bone health assessment and management. This may involve the development of user-friendly software platforms, the creation of normative databases, and the provision of training and support for healthcare professionals.

Finally, integrating accelerometer-based mechanical loading prediction with other technologies, such as imaging modalities, biomarkers, and digital health platforms, holds immense promise for advancing personalized bone health interventions. By combining multiple data sources, researchers, clinicians, and exercise physiology practitioners can gain a more comprehensive understanding of

an individual's bone health status, risk factors, and response to therapeutic interventions, ultimately enabling the delivery of targeted and effective healthcare.

Chapter 3: Original studies

3.1. List of publications

1. **Veras L**, Diniz-Souza F, Boppre G, Resende-Coelho A, Moutinho-Ribeiro E, Devezas V, Santos-Sousa H, Preto J, Vilas-Boas JP, Machado L, Oliveira J, Fonseca H. Mechanical loading prediction through accelerometry data during walking and running. *European Journal of Sport Science*. 2023 Aug;23(8):1518-1527. doi: 10.1080/17461391.2022.2102437. Epub 2022 Aug 11.

2. **Veras L**, Diniz-Sousa F, Boppre G, Devezas V, Santos-Sousa H, Preto J, Vilas-Boas JP, Machado L, Oliveira J, Fonseca H. Using raw accelerometer data to predict high-impact mechanical loading. *Sensors*. 2023 Feb 16;23(4):2246. doi: 10.3390/s23042246.

3. **Veras L**, Oliveira D, Diniz-Sousa F, Boppre B, Resende-Coelho A, Oliveira J, Fonseca H. External validation of accelerometry based mechanical loading prediction equations. *Applied Sciences*. 2024 Nov 8; 14(22):10292. doi: 10.3390/app142210292

4. **Veras L**, Diniz-Sousa F, Boppre G, Resende-Coelho A, Oliveira J, Fonseca H. Accelerometer-Based Classification of Walking, Running, and Jumping: A Machine Learning Approach for Mechanical Loading Assessment. *Submitted to: Sensors*

3.2. Study 1

Veras L, Diniz-Souza F, Boppre G, Resende-Coelho A, Moutinho-Ribeiro E, Devezas V, Santos-Sousa H, Preto J, Vilas-Boas JP, Machado L, Oliveira J, Fonseca H. Mechanical loading prediction through accelerometry data during walking and running. *European Journal of Sport Science*. 2023 Aug;23(8):1518-1527. doi: 10.1080/17461391.2022.2102437. Epub 2022 Aug 11.

EUROPEAN JOURNAL OF SPORT SCIENCE
2023, VOL. 23, NO. 8, 1518–1527
https://doi.org/10.1080/17461391.2022.2102437

Routledge
Taylor & Francis Group

Check for updates

Mechanical loading prediction through accelerometry data during walking and running

Lucas Veras [a,b], Florêncio Diniz-Sousa [a,b], Giorjines Boppre [a,b], Ana Resende-Coelho [a,b], Edgar Moutinho-Ribeiro [a,b], Vítor Devezas [c], Hugo Santos-Sousa [c], John Preto[c], João Paulo Vilas-Boas [d,e], Leandro Machado [d,e], José Oliveira [a,b] and Hélder Fonseca [a,b]

[a]Research Center in Physical Activity, Health and Leisure (CIAFEL), Faculty of Sport, University of Porto, Porto, Portugal; [b]Laboratory for Integrative and Translational Research in Population Health (ITR), University of Porto, Porto, Portugal; [c]Obesity Integrated Responsability Unity (CRIO), São João Academic Medical Center, Porto, Portugal; [d]Center of Research, Education, Innovation and Intervention in Sport (CIFI2D), Faculty of Sport, University of Porto, Porto, Portugal; [e]Biomechanics Laboratory (LABIOMEP-UP), University of Porto, Porto, Portugal

ABSTRACT

Currently, there is no way to assess mechanical loading variables such as peak ground reaction forces (pGRF) and peak loading rate (pLR) in clinical settings. The purpose of this study was to develop accelerometry-based equations to predict both pGRF and pLR during walking and running. One hundred and thirty one subjects (79 females; 76.9 ± 19.6 kg) walked and ran at different speeds (2–14 km·h^{-1}) on a force plate–instrumented treadmill while wearing accelerometers at their ankle, lower back and hip. Regression equations were developed to predict pGRF and pLR from accelerometry data. Leave-one-out cross-validation was used to calculate prediction accuracy and Bland–Altman plots. Our pGRF prediction equation was compared with a reference equation previously published. Body mass and peak acceleration were included for pGRF prediction and body mass and peak acceleration rate for pLR prediction. All pGRF equation coefficients of determination were above 0.96, and a good agreement between actual and predicted pGRF was observed, with a mean absolute percent error (MAPE) below 7.3%. Accuracy indices from our equations were better than previously developed equations. All pLR prediction equations presented a lower accuracy compared to those developed to predict pGRF. Walking and running pGRF can be predicted with high accuracy by accelerometry-based equations, representing an easy way to determine mechanical loading in free-living conditions. The pLR prediction equations yielded a somewhat lower prediction accuracy compared with the pGRF equations.

Highlights

- Peak ground reaction forces can be accurately predicted through raw accelerometry data.
- These predictions are valid for a broad range of body masses and for ankle, lower back and hip accelerometer placements.
- Peak loading rate prediction presented lower accuracy compared with peak ground reaction force prediction.
- These findings result in a simple method to predict mechanical loading in clinical practice, which is relevant in some areas of sports medicine such as bone health and injury prevention.

KEYWORDS

Activity monitor; force plates; locomotion; raw acceleration; ground reaction force; loading rate

1. Introduction

Physical activity-related mechanical loading plays a key role in bone health, by promoting favourable adaptations on bone mass, geometry and microarchitecture (Fonseca, Moreira-Goncalves, Coriolano, & Duarte, 2014; Turner & Robling, 2003). However, not all forms of mechanical stimulation are equally osteogenic, and the manipulation of variables such as loading magnitude, rate, frequency and volume can produce different bone responses (Turner, 1998; Turner & Robling, 2003). Therefore, the accurate assessment of mechanical loading is of paramount importance to better understand the bone response to physical stimulus. Nonetheless, a limitation in this context is that mechanical loading evaluation is usually performed only by instruments restrained to laboratory settings.

Force plates are the gold standard instrument for mechanical loading measurement (Medved, 2000). However, their cost, need of expertise to collect and analyze data, of a dedicated indoor space and ongoing

CONTACT Lucas Veras lucasdsveras@gmail.com Faculty of Sport, University of Porto, Rua Dr. Plácido Costa, 91, Porto 4200-450, Portugal
Supplemental data for this article can be accessed online at https://doi.org/10.1080/17461391.2022.2102437.
© 2022 European College of Sport Science

calibration and maintenance hinders its application in free-living conditions. Accelerometers, due to their portability, low-cost and reliability, are widely used to objectively measure physical activity related to cardiometabolic outcomes (Migueles et al., 2017; Troiano, McClain, Brychta, & Chen, 2014), and, recently, have been proposed as adequate devices to predict gravitational loading variables (Fortune, Morrow, & Kaufman, 2014; Neugebauer, Collins, & Hawkins, 2014; Neugebauer, Hawkins, & Beckett, 2012; Neugebauer & LaFiandra, 2018; Veras et al., 2020). Given the need to assess mechanical loading in out-of-laboratory environments to control and monitor exercise prescription for bone health, accurate mechanical loading prediction models need to be developed and validated for the most common physical activities prescribed to induce bone adaptations, such as walking, running, and jumping. These models, apart from being accurate, need to be transparent, allowing reproducibility of the results, and ideally offer a tool to facilitate data processing for those who are not familiar with the employed techniques, such as what is already offered for analyzing cardiometabolic variables (Migueles, Rowlands, Huber, & van, Hees, 2019), and increase their applicability.

Ground reaction force is the most studied mechanical loading variable, and its relationship with bone adaptations to exercise is well established (Rantalainen, Heinonen, Komi, & Linnamo, 2008; Rantalainen, Heinonen, Linnamo, Komi, Takala & Kainulainen, 2009; Turner & Robling, 2003). Due to its importance, some studies have already attempted to develop accelerometry-based peak ground reaction force (pGRF) prediction equations in different populations, such as children (Neugebauer et al., 2012), adults (Fortune et al., 2014; Neugebauer et al., 2014), patients with obesity (Veras et al., 2020) and military (Neugebauer & LaFiandra, 2018). Nevertheless, most studies included only low-impact activities. Besides loading magnitude, loading rate is another variable related to bone health (Rowlands, Schuna Jr., Stiles, & Tudor-Locke, 2014) that could potentially be predicted by accelerometer data, but with apparently lower accuracy compared with pGRF (Fortune et al., 2014; Veras et al., 2020). Furthermore, accelerometry-based peak loading rate (pLR) prediction has only been tested during walking (Fortune et al., 2014; Veras et al., 2020).

Since mechanical loading measurements are usually made only in laboratory settings, there is currently no way to determine the osteogenic potential of exercise in real life conditions. Thus, demonstrating that accelerometers are suitable to measure mechanical loading and developing the methods to do so could have important implications for clinical practice as well as exercise monitoring and prescription, allowing to safely monitor exercise recommendations with the aim of improving bone health and decreasing osteoarticular injury risk. Therefore, given this necessity, this study aimed to develop accelerometry-based pGRF and pLR prediction models during walking and running. Our hypothesis was that accelerometry data can accurately predict mechanical loading during both walking and running.

2. Methods

2.1. Study design

This was a cross-sectional study with a convenience sample.

2.2. Participants

A sample of 131 adults (79 males; 32 ± 11.2 years; 165.1 ± 9.6 cm; 76.9 ± 19.6 kg; 28.5 ± 8.1 kg·m^{-2}) was recruited. The inclusion criteria were age between 18 and 65 years and ability to walk and run on a treadmill. Exclusion criteria were any musculoskeletal, neurological, or other limitation that hindered the ability to walk or run safely on a treadmill. Height and body mass were assessed following standard procedures with a stadiometer (model 213; Seca, Hamburg, Germany) and a digital scale (model 899; Seca, Hamburg, Germany), respectively. All participants were informed about the experiments purpose and protocol before giving written informed consent. The study protocol was approved by the local Ethics Committee (CES 192-14).

2.3. Protocol

Data collection took place at Porto Biomechanics Laboratory (LABIOMEP-UP) on an instrumented front-back split-belt treadmill with built-in force plates (AMTI Corporation, Watertown, USA). Before starting the data collection, participants were given time to familiarize with the treadmill. Protocol consisted of walking and running, from 2 to 14 km·h^{-1} with 1 km·h^{-1} increment and 0° slope. Walking and running speeds ranges were 2–6 km·h^{-1} and 7–14 km·h^{-1}, respectively. Walking speeds lasted 1 min and running 30 s. To ensure single foot contact on each force plate, feedback regarding the location on the treadmill was provided by a researcher. Participants wore their own sports shoes throughout the trials.

During the protocol, participants wore three activity monitors, one at their right hip (along the anterior axillary line, at the level of the iliac crest), another at their

15367290, 2023, 8, Downloaded from https://onlinelibrary.wiley.com/doi/10.1080/17461391.2022.2102437 by CAPES, Wiley Online Library on [13/01/2025]. See the Terms and Conditions (https://onlinelibrary.wiley.com/terms-and-conditions) on Wiley Online Library for rules of use; OA articles are governed by the applicable Creative Commons License

lower back (midpoint between the posterior superior iliac spines) and at their right ankle (immediately superior to the lateral malleolus). Activity monitors at the waist level were secured on the same elastic belt with a clip and the one placed on the ankle was secured by an elastic belt fixed with adhesive tape. In all placements, the accelerometer vertical axis was aligned with the body longitudinal axis. The placements at waist level were chosen as they are closer to the body centre of mass, and, therefore, their recorded acceleration could properly represent the acceleration of the body centre of mass. Also, the ankle placement was tested due to its location closer to the ground contact point.

Activity monitors used were the GT9X Link (±16*g* range; ActiGraph, Pensacola, USA) that incorporates primary and secondary triaxial accelerometers. As a manufacturer proprietary filter is applied on the primary, but not on the secondary accelerometer raw data, only data from the latter was used in this study, reducing filtering bias and enhancing data processing replicability.

Data from force plates were collected at 1000 Hz and from accelerometers at 100 Hz (GT9X Link maximum sampling frequency) and operated through the manufacturer-supplied software (force plates: Netforce, Version 3.5.1; AMTI Corporation, Watertown, USA; accelerometers: ActiLife version 6.13.3; Actigraph, Pensacola, USA). Raw ground reaction force (in N) and acceleration (in gravitational acceleration units; $1g = 9.807\ \mathrm{m{\cdot}s^{-2}}$) from the x, y and z vectors were exported.

2.4. Outcomes

The outcomes for this study were the predicted values of pGRF and pLR. The variables derived from the accelerometers, peak acceleration (pACC) and peak acceleration rate (pAR), were used as predictors in the model. To obtain these variables, force plates and accelerometer data were processed using MATLAB (Version 2019a, Mathworks, Natick, USA), as described elsewhere (Veras et al., 2020). Briefly, both ground reaction force and acceleration signals were filtered using a Butterworth fourth-order low-pass filter (20 Hz cut-off), and their resultant vector calculated ($r_i = \sqrt{x_i^2 + y_i^2 + z_i^2}$). After that, pACC values were defined as minimum height of twice the positive acceleration average, during any given speed, and separated by 0.4 s minimum. The signals were adjusted through the time set by the systems clock, with manual correction based on visual inspection, and synchronized by the maximum cross-correlation coefficient. Then, pGRF was determined as the highest value between 0.4 s before and after each pACC. The rates of change were computed through a centred derivative from the beginning of the foot contact to the peak (Equation (1)). The pLR and pAR were defined as the maximum value in the array (Equation (2)). An example of ground reaction force and acceleration curves during the stance phase of both walking and running can be seen in Supplemental Figure S1.

$$f_i' = \frac{f_{i+1} - f_{i-1}}{t_{i+1} - t_{i-1}} \quad (1)$$

$$f_{i_{\max}}' = \max\left(f_i'\right) \quad (2)$$

Regions of interest for data analysis were manually selected where locomotion patterns were constant, representing approximately 20–45 s periods. Then, pGRF, pACC, pLR and pAR means of the resultant and vertical vectors for each participant at each speed for each accelerometer placement were extracted and used in all remaining analyses. In walking and running trials, 53 ± 19 and 24 ± 9 peaks were used to calculate these means, respectively.

2.5. Statistical analyses

Statistical analyses were conducted using R statistical software (version 4.1.1, R Foundation for Statistical Computing, Vienna, Austria). All statistical analyses were registered in an open platform, where R code utilized can be accessed (https://bit.ly/3A6P3Tx). The statistically significant value was set as $\alpha = 0.05$.

Regression equations to predict pGFR and pLR in each vector for each accelerometer placement were developed by linear mixed models. Body mass (kg), body mass index (BMI; $\mathrm{kg{\cdot}m^{-2}}$), and BMI category were tested as predictors in all models. Additionally, pACC and pAR were tested as predictors in pGRF and pLR models, respectively. All predictors were tested as fixed effects, and body mass, pACC and pAR were shown to be significant predictors. Subject and speed were tested as random effects, and the inclusion of both has showed to improve the models. Final models were chosen according to −2 log-likelihood statistics (Field, Miles, & Field, 2012). Traditional coefficient of determination (R^2) was represented by conditional R^2, which estimates the variance explained by the whole model (Nakagawa & Schielzeth, 2013).

Models were validated using the leave-one-out cross-validation approach (Staudenmayer, Zhu, & Catellier, 2012). For this, each participant's data were separated into a testing dataset (one participant at a time) with the remaining data in the training dataset. New linear mixed models with the same outcomes and predictors

15367290, 2023, 8, Downloaded from https://onlinelibrary.wiley.com/doi/10.1080/17461391.2022.2102437 by CAPES, Wiley Online Library on [13/01/2025]. See the Terms and Conditions (https://onlinelibrary.wiley.com/terms-and-conditions) on Wiley Online Library for rules of use; OA articles are governed by the applicable Creative Commons License

as determined for the entire sample were developed using the training dataset and then used to predict the outcome for the participant in the testing dataset. This process was repeated for all participants (131 times). Data from the testing dataset was used in the remaining statistical analysis.

To assess the models prediction accuracy, mean absolute error (MAE), mean absolute percent error (MAPE) and root mean square error (RMSE) were calculated. Although there is no standard threshold defining an acceptable error for mechanical loading prediction, based on previous studies we considered a MAPE <8% to be an accurate prediction (Ancillao, Tedesco, Barton, & O'Flynn, 2018; Fortune et al., 2014; Neugebauer et al., 2014). Methods agreement was evaluated with Bland–Altman plots by plotting the difference between the actual (force plates-measured) and predicted values against their mean. Bias was computed as the mean of these differences and limits of agreement were obtained using ±1.96 standard deviation of the bias (Bland & Altman, 1986). To test whether there were a consistent over or underestimation of the actual values, one-sample *t*-tests were performed to assess if the difference between actual and predicted values were different than zero. Linear regressions were applied to identify if the magnitude of the mean between actual and predicted values influenced the magnitude of their difference. This was done to ascertain if the prediction accuracy was constant throughout the assayed magnitude range, which is known as proportional bias (Giavarina, 2015). These analyses were conducted separately for data from each accelerometer placement and outcome.

Finally, our pGRF prediction equation was compared with a previously published reference equation (Neugebauer et al., 2014), that was developed using similar methods. This comparison was performed in three ways, using: (i) the whole sample; (ii) a subsample of walking trials; (iii) a subsample of running trials. To assess the prediction accuracy, MAE, MAPE and RMSE were calculated using pGRF values predicted from both equations. No pLR prediction equation developed for both walking and running was found to be compared with ours.

3. Results

The sample presented a broad range of body masses (49.6–152.5 kg), from normal weight to severe obesity (19.0–54.0 $kg{\cdot}m^{-2}$). It was expected that participants with higher BMI, due to their probable lower motor ability and physical capacity, would be able to perform the trials only at the lowest speeds. This was precisely what happened and, as it can be observed in Figure 1, the number of data points corresponding to subjects with BMI > 30 $kg{\cdot}m^{-2}$ greatly decreases in speeds above 6 $km{\cdot}h^{-1}$.

As the main variables collected in this experiment were the peak magnitudes and rates of the ground reaction force and acceleration signals, there was a need to first establish their relationship. During locomotion, pACC increases linearly as pGRF increases. Such relation can be observed in Figure 2, Panel A, for hip-worn

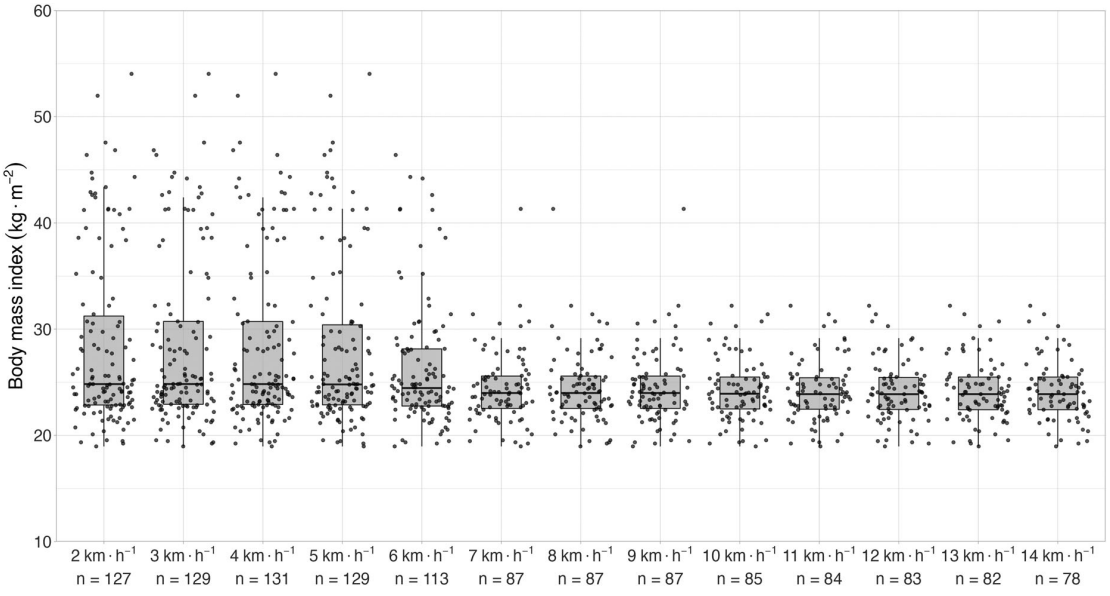


Figure 1. Distribution of participant's body mass index per speed. Dots represent individual participants.

15367290, 2023, 8, Downloaded from https://onlinelibrary.wiley.com/doi/10.1080/17461391.2022.2102437 by CAPES, Wiley Online Library on [13/01/2025]. See the Terms and Conditions (https://onlinelibrary.wiley.com/terms-and-conditions) on Wiley Online Library for rules of use; OA articles are governed by the applicable Creative Commons License

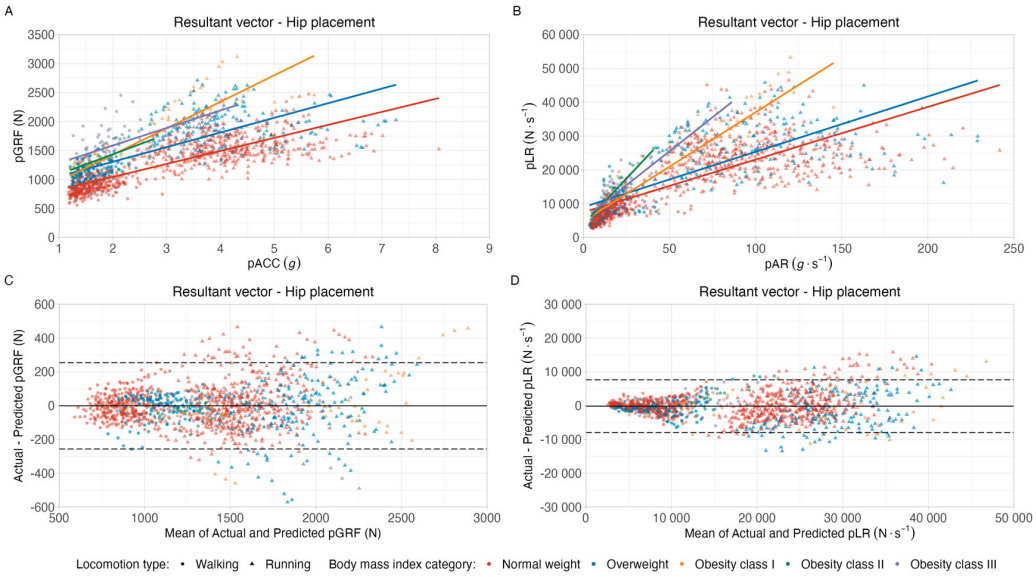


Figure 2. Panels A and B show the relationship between variables collected by force plates and accelerometers worn at hip, for the resultant vector. Linear trends for each body mass index category are also depicted. Panel A shows peak magnitudes (pGRF and pACC) while Panel B shows peak rates (pLR and pAR). Panels C and D display Bland-Altman plots demonstrating the agreement between actual and predicted peak ground reaction force (Panel C) and loading rate (Panel D) for the resultant vector from hip-worn accelerometers. Continuous thick lines show bias (average of the differences between actual and predicted values) while dashed lines show the limits of agreement (bias ±1.96 standard deviation). Abbreviations: pACC, peak acceleration; pAR, peak acceleration rate; pGRF, peak ground reaction force; pLR, peak loading rate.

accelerometers (resultant vector), and in Supplemental Figure S2 for all placements and vectors. Moreover, for the same pACC values, the registered pGRF tended to be higher in subjects with higher BMI. This demonstrates that accelerometer data can adequately discriminate between different BMI categories. However, data from the pAR × pLR relationship show a greater dispersion, especially at higher values, and the different BMI categories cannot be discriminated so well, as can be observed in Figure 2, Panel B, and Supplemental Figure S3.

Regression equations were developed to predict the mechanical loading variables based on accelerometry data. In the pGRF prediction equations, body mass and pACC were significant predictors and, therefore, included in the models. Table 1 shows the regression coefficients, R^2 and accuracy indices from models derived from each accelerometer placement and vector. In the pGRF prediction models, the lowest R^2 was 0.96, showing that the predictor variables can explain variability in the outcome variable to a great extent. Also, MAE and MAPE range were 93.7N–100.7N and 6.7%–7.3%, respectively. RMSE was also computed and ranged between 130.2N and 136.7N. Although all pGRF prediction equations showed very similar results, the one based on the resultant vector from hip-worn accelerometers has shown the best performance, with an R^2 of 0.96, the lowest MAE (93.7N), MAPE (6.7%) and RMSE (130.2N).

Equations to predict pLR were also developed, and included as predictors the pAR and body mass. Regression coefficients, R^2 and accuracy indices for these equations are also shown in Table 1. For these equations, the R^2 ranged between 0.87 and 0.91, which is just slightly lower than the R^2 for the pGRF models. MAE, MAPE and RMSE ranges were 2882N·s^{-1}–3249N·s^{-1}, 17.7%–19.1%, and 3971N·s^{-1}–4619N·s^{-1}, respectively. These results show that the pLR prediction equations were somewhat poorer than those for the pGRF equations. The pLR equation with the lowest error was derived from the resultant vector of hip-worn accelerometers, with an R^2 of 0.90 and a MAE, MAPE and RMSE of 2882N·s^{-1}, 17.7% and 3971N·s^{-1}, respectively.

Bland–Altman plots were built to visualize the agreement between the actual and predicted pGRF and pLR. Bland–Altman plots for the pGRF and pLR resultant vector from hip-worn accelerometers can be seen in Figure 2 (Panels C and D, respectively), and for all accelerometer placements and vectors in the Supplemental Figures S4 and S5. Values for all equations tended to assemble around zero and between the limits of agreement, as shown by, for all models, at least 92% of the data points lie within the limits of agreement. For the

15367290, 2023, 8, Downloaded from https://onlinelibrary.wiley.com/doi/10.1080/17461391.2022.2102437 by CAPES, Wiley Online Library on [13/01/2025]. See the Terms and Conditions (https://onlinelibrary.wiley.com/terms-and-conditions) on Wiley Online Library for rules of use; OA articles are governed by the applicable Creative Commons License

Table 1. Regression equations, R^2 and accuracy indices.

Vector	Accelerometer placement	Regression equations	R^2	MAE	MAPE	RMSE
pGRF prediction equations						
Resultant	Ankle	pGRF (N) = 890.673 − 131.889(pACC) + 7.155(body mass) + 2.027(pACC × body mass)	0.96	95.9	6.8%	130.3
	Lower back	pGRF (N) = 701.358 − 167.229(pACC) + 9.642(body mass) + 2.667(pACC × body mass)	0.96	96.4	6.8%	131.1
	Hip	pGRF (N) = 814.888 − 229.459(pACC) + 7.036(body mass) + 3.934(pACC × body mass)	0.96	93.7	6.7%	130.2
Vertical	Ankle	pGRF (N) = 984.419 − 221.505(pACC) + 6.133(body mass) + 3.201(pACC × body mass)	0.97	99.4	7.3%	134.2
	Lower back	pGRF (N) = 692.456 − 179.912(pACC) + 9.736(body mass) + 2.760(pACC × body mass)	0.96	100.7	7.3%	136.7
	Hip	pGRF (N) = 767.553 − 244.689(pACC) + 7.153(body mass) + 4.258(pACC × body mass)	0.96	96.8	7.1%	133.0
pLR prediction equations						
Resultant	Ankle	pLR ($N{\cdot}s^{-1}$) = 13629.698–94.093(pAR) + 77.299(body mass) + 1.447(pAR × body mass)	0.91	3063	18.9%	4222
	Lower back	pLR ($N{\cdot}s^{-1}$) = 13947.266–129.739(pAR) + 86.996(body mass) + 1.721(pAR × body mass)	0.91	2940	18.3%	4158
	Hip	pLR ($N{\cdot}s^{-1}$) = 13656.930–168.415(pAR) + 60.421(body mass) + 2.776(pAR × body mass)	0.90	2882	17.7%	3971
Vertical	Ankle	pLR ($N{\cdot}s^{-1}$) = 12387.216–68.583(pAR) + 75.546(body mass) + 1.327(pAR × body mass)	0.87	3248	18.6%	4542
	Lower back	pLR ($N{\cdot}s^{-1}$) = 14522.460–112.291(pAR) + 91.448(body mass) + 1.469(pAR × body mass)	0.90	3249	19.1%	4619
	Hip	pLR ($N{\cdot}s^{-1}$) = 13683.896–159.441(pAR) + 63.910(body mass) + 2.752(pAR × body mass)	0.89	3188	18.4%	4432

Abbreviations: MAE, mean absolute error; MAPE, mean absolute percent error; pACC, peak acceleration; pAR, peak acceleration rate; pGRF, peak ground reaction force; pLR, peak loading rate; RMSE, root mean square error.

pGRF equations, a tendency to higher dispersion can be observed for higher magnitudes, which correspond to running trials, especially in values from ankle-worn accelerometers (Supplemental Figure S4, Panels A and D). Prediction equations for pLR showed a more accentuated dispersion, again mainly for higher magnitudes (Supplemental Figure S5). None of the models presented a bias different from zero ($p > 0.05$), demonstrating that they do not consistently over or underestimate the mechanical loading values. Although all equations showed a significant proportional bias ($p < 0.05$), linear regressions presented a low R^2 (highest $R^2 = 0.03$).

Furthermore, we compared the performance of our equations with a reference equation previously published (Neugebauer et al., 2014). As the only comparable equation found was the one to predict pGRF vertical vector using hip-worn accelerometer data developed by Neugebauer et al. (2014), we applied it to our data and computed the MAE, MAPE and RMSE. Then, these indices were compared to the indices for our equation (Table 1). Apart from the overall equations performance, a sub-analysis was done separating walking and running trials. The results of these comparisons can be observed in Table 2. Accuracy indices of our equations were all better compared to the reference equation. Our equation performance was constant between walking and running, indicating that it can be used for both activities without loss of accuracy, which cannot be observed in the reference equation.

Also, to simplify the use of these equations and enhance their applicability, a software package was developed for use in the R statistical software (Veras, 2021). Included in this package are functionalities to read raw accelerometer data, process it and apply the equations to predict both pGRF and pLR. In the package website (https://verasls.github.io/impactr) there are also instructions on how to use it to obtain the predictions, namely in the "Home" and "Get started" sections.

Table 2. Accuracy indices of ours and Neugebauer et al. (2014) equation to predict peak vertical ground reaction force with data from hip-worn accelerometers.

	Our equation			Neugebauer et al. (2014) equation		
Prediction	MAE	MAPE	RMSE	MAE	MAPE	RMSE
Overall	96.8	7.1%	133.0	168.7	13.1%	201.7
Walking	59.0	6.0%	75.6	170.3	16.6%	187.2
Running	132.5	8.1%	170.3	167.1	9.7%	214.6

Abbreviations: MAE, mean absolute error; MAPE, mean absolute percent error; RMSE, root mean square error.

4. Discussion

The purpose of this study was to develop accelerometry-based mechanical loading prediction equations to accurately estimate mechanical loading during walking and running. Predictions were tested with accelerometers placed at different body locations, using both the resultant and vertical vectors, in a set of incremental speeds, ranging from slow walking to running. Our findings demonstrated that accelerometry-based models were a valid and accurate method to estimate pGRF during human locomotion, as all pGRF models presented a MAPE below the 8% threshold. However, accelerometry-based pLR prediction equations resulted in lower accuracy compared to the pGRF.

Comparing our results with previous studies using a similar approach to predict pGRF, our prediction errors are comparable with some studies whose best results are a MAPE approximately 6.0%, but which included only walking in their protocol (Fortune et al., 2014; Neugebauer & LaFiandra, 2018; Veras et al., 2020). Additionally, previous studies that developed pGRF prediction models during both walking and running showed a

17367290, 2023, 8, Downloaded from https://onlinelibrary.wiley.com/doi/10.1080/17461391.2022.2102437 by CAPES, Wiley Online Library on [13/01/2025]. See the Terms and Conditions (https://onlinelibrary.wiley.com/terms-and-conditions) on Wiley Online Library for rules of use; OA articles are governed by the applicable Creative Commons License

MAPE of 8.3% (Neugebauer et al., 2014), which is higher than our results, and 5.2% (Neugebauer et al., 2012) with no model cross-validation, which is similar to our results when no cross-validation is applied (highest value of 5.1% in our models). Nevertheless, models from both studies present a caveat, that is the inclusion of a term in their equations that implies distinguishing between walking and running. This is not easy to be identified from free-living accelerometer data, hindering real-world application of these previous equations. Also, one of these studies included only children and adolescents in their sample (Neugebauer et al., 2012), which present a higher variability in terms of gait pattern compared to adults (Gouelle, Leroux, Bredin, & Mégrot, 2016), making, therefore, this equation unsuitable to use in an adult population. Furthermore, it was observed that the reference equation used (Neugebauer et al., 2014) has a much lower accuracy during walking compared with running (16.6% vs. 9.7%). As this reference equation was not validated in a sample including people with obesity, it performs poorly when applied to data from people with high body mass, as is the case in our sample that performed the walking trials, compared with running trials mostly performed by non-obese people.

To the best of our knowledge, only two studies (Fortune et al., 2014; Veras et al., 2020) have attempted to develop accelerometry-based pLR prediction models, and both studies only included walking. In accordance with our findings, these studies also showed that the prediction error for these models is larger than for the pGRF prediction. One of these studies investigated the use of four different accelerometer placements (ankle, tibia, thigh and waist) to predict pLR and achieved a MAPE ranging between 23.4% and 46.1% (Fortune et al., 2014), while the other obtained a 19.5%–22.4% range using accelerometers at lower back and hip (Veras et al., 2020). It is noteworthy that MAPE results from our pLR models (around 19%) have a better accuracy than these previous investigations. Also, although pLR is an important variable, known for a long time to determine to a great extent bone formation response to mechanical loading (Bassey, Rothwell, Littlewood, & Pye, 1998; Turner, Owan, & Takano, 1995), based on our findings and in previous studies (Fortune et al., 2014; Veras et al., 2020), its prediction through accelerometer data, at the current state of technical accelerometer development, does not seem to yield trustworthy results that can be used in models to predict the bone anabolic response to mechanical loading.

Our findings revealed that ankle, lower back and hip were all valid accelerometer placements to predict pGRF. Despite the similarities, hip was the accelerometer placement with the best prediction accuracy, which reinforces it as the preferable location to collect and analyze accelerometry-measured physical activity. This placement is already well accepted for energy expenditure prediction and physical activity intensity classification (Migueles et al., 2017) and has shown a high mechanical loading prediction ability (Neugebauer et al., 2012; Neugebauer & LaFiandra, 2018; Veras et al., 2020). In addition to testing various accelerometer placements, we also investigated the prediction with both resultant and vertical vectors. Although acceleration and ground reaction force from the vertical vector are the most studied and associated with bone health (Heikkinen, Vihriälä, Vainionpää, Korpelainen, & Jämsä, 2007; Vainionpää et al., 2006), resultant vector of acceleration and ground reaction force during locomotion is greatly determined by the vertical vector. In fact, as can be observed in Supplemental Figure S1, values from both vectors were very similar. Also, mechanical loading prediction based on the resultant acceleration offers the important advantage of not being dependent on the accelerometer correct orientation, which is hard to assure when measuring daily physical activity (Welk, 2005; Wundersitz, Gastin, Robertson, Davey, & Netto, 2015).

Results from our study offer some advantages compared to previous investigations: (i) it includes walking and running, which are among the most usual types of physical activity performed daily; (ii) all models developed, especially for pGRF prediction, presented a similar or better accuracy compared to the results from previous publications; (iii) the accuracy of our models is fairly constant throughout walking and running, notably for the pGRF prediction models, with a MAPE increase from 6% to 8%, showing, therefore, that they can be used adequately for both activities; (iv) in order to apply these models there is no need to manually distinguish the accelerometer data between walking and running, as in previously developed equations (Neugebauer et al., 2014), which facilitates its use with daily living accelerometer data; and (v) along with the creation of these models, a software was developed in the form of an R package to perform all the computations needed to get from the raw accelerometer data to the mechanical loading prediction.

In addition to these technical advantages, our models present some important potential clinical applications. For instance, these models can be used to analyze data from large observational studies and to investigate associations between objectively measured mechanical loading and bone health. Nevertheless, instead of analyzing accelerometer data averaged in epochs as it has

15367290, 2023, 8, Downloaded from https://onlinelibrary.wiley.com/doi/10.1080/17461391.2022.2102437 by CAPES, Wiley Online Library on [13/01/2025]. See the Terms and Conditions (https://onlinelibrary.wiley.com/terms-and-conditions) on Wiley Online Library for rules of use; OA articles are governed by the applicable Creative Commons License

been performed previously (Chastin, Mandrichenko, Helbostadt, & Skelton, 2014; Stiles, Metcalf, Knapp, & Rowlands, 2017), which can have a dilution effect and hinder the detection of higher intensities (Fabre, Lhuisset, Bernal, & Bois, 2020), with our method, raw acceleration can be analyzed at a higher resolution by identifying the pGRF associated with each step taken and establishing, for instance, the number of peaks above a certain magnitude threshold needed to elicit a positive bone adaptation. Another potential application could be the computation of the cumulative mechanical loading by adding up the pGRF of all detected steps (Diniz-Sousa et al., 2021). This information could be used either for the determination of the relationship between mechanical loading accumulated within a certain period (e.g. a day) and the bone response to this loading (Ahola, Korpelainen, Vainionpää, & Jämsä, 2010), or to investigate the causes of bone loss in populations with bone health issues, such as post-bariatric surgery patients (Diniz-Sousa et al., 2021). This approach has already been followed by using equations previously developed by our group (Veras et al., 2020). However, these new equations described in the current study have the advantage of being able to be applied to both types of locomotion (walking and running) and not just walking. Another possible application is in sports training, by monitoring the amount of mechanical loading sustained by athletes and using this information for training loading monitoring and for establishing adequate measures to prevent osteoarticular overload and reduce the risk of osteoarthritis (Vanwanseele, Op De Beéck, Schütte, & Davis, 2020).

Despite the validity of our prediction models, some limitations should be mentioned. First, although the activities included in our protocol (walking and running) are among the most frequently performed motor activities during daily living, our prediction models do not apply to other activities known to influence bone adaptation to mechanical stimuli, such as jumping and direction changing. Second, in the absence of another sample for model validation, the leave-one-out cross-validation method was used, which is the method of choice in these situations (Staudenmayer et al., 2012). Nevertheless, future studies should test the out-of-sample validity of these models. Moreover, the protocol was performed on an instrumented treadmill. The use of a treadmill, although enhancing the study internal validity by the continuously measuring the ground reaction force (Ngoh, Gouwanda, Gopalai, & Chong, 2018) also reduces the external validity due to possible biomechanical changes in the walking and running patterns induced by the treadmill (Kluitenberg, Bredeweg, Zijlstra, Zijlstra, & Buist, 2012). Also, bone adaptation to mechanical stimulation depends not only on external loads, such as ground reaction force, but also on internal loads generated by muscle forces (Robling, 2009). As accelerometers cannot reliably assess muscle force generation, they may have a limited capacity in estimating the bone response to loading in situations where there are no major gravitational loadings involved, such as during resistance training. Lastly, the stance phase in which the pACC and pGRF occur were not coincident, particularly at running speeds. Nevertheless, the prediction method developed in this paper could still accurately predict the active pGRF at both walking and running.

5. Conclusion

Mechanical loading, particularly pGRF, could be accurately predicted by accelerometry-based models. These models are valid for both the resultant and vertical vectors, and for using data from accelerometers placed at ankle, lower back or hip. The prediction models developed in this study have proved to be an efficient method to assess pGRF out of laboratory conditions, with potential applications for monitoring mechanical loading in several contexts and for establishing a relationship between mechanical loading and either beneficial or pathological skeletal and osteoarticular adaptations. Contrary to the pGRF, pLR prediction accuracy was found to be unsatisfactory.

Acknowledgements

The authors thank the participants who took part in this research and all who have collaborated in the research project.

Disclosure statement

No potential conflict of interest was reported by the authors.

Funding

This study was funded by the Foundation for Science and Technology (FCT) [grant number PTDC/DTP-DES/0968/2014] and by the European Regional Development Fund (ERDF) through the Operational Competitiveness Programme (COMPETE) [grant number POCI-01-0145-FEDER-016707]. The study was developed in the Research Centre in Physical Activity, Health and Leisure (CIAFEL) funded by ERDF through the COMPETE and by the FCT [grant number UID/DTP/00617/2020], and Laboratory for Integrative and Translational Research in Population Health (ITR), funded by the FCT [grant number LA/P/0064/2020]. Lucas Veras, Florêncio Diniz-Sousa and Giorjines Boppre are supported by the FCT [grant numbers UI/BD/150673/2020, SFRH/BD/117622/2016 and SFRH/BD/146976/2019].

15367290, 2023, 8, Downloaded from https://onlinelibrary.wiley.com/doi/10.1080/17461391.2022.2102437 by CAPES, Wiley Online Library on [13/01/2025]. See the Terms and Conditions (https://onlinelibrary.wiley.com/terms-and-conditions) on Wiley Online Library for rules of use; OA articles are governed by the applicable Creative Commons License

ORCID

Lucas Veras http://orcid.org/0000-0003-0562-5803
Florêncio Diniz-Sousa http://orcid.org/0000-0001-9042-383X
Giorjines Boppre http://orcid.org/0000-0003-2974-6343
Edgar Moutinho-Ribeiro http://orcid.org/0000-0002-8331-8430
Ana Resende-Coelho http://orcid.org/0000-0003-4017-071X
Vítor Devezas http://orcid.org/0000-0003-1032-4474
Hugo Santos-Sousa http://orcid.org/0000-0001-6176-5654
João Paulo Vilas-Boas http://orcid.org/0000-0002-4109-2939
Leandro Machado http://orcid.org/0000-0001-5332-5974
José Oliveira http://orcid.org/0000-0002-1829-4196
Hélder Fonseca http://orcid.org/0000-0002-9002-8976

References

Ahola, R., Korpelainen, R., Vainionpää, A., & Jämsä, T. (2010). Daily impact score in long-term acceleration measurements of exercise. *Journal of Biomechanics*, *43*(10), 1960–1964.

Ancillao, A., Tedesco, S., Barton, J., & O'Flynn, B. (2018). Indirect measurement of ground reaction forces and moments by means of wearable inertial sensors: A systematic review. *Sensors (Switzerland)*, *18*, 8.

Bassey, E. J., Rothwell, M. C., Littlewood, J. J., & Pye, D. W. (1998). Pre- and postmenopausal women have different bone mineral density responses to the same high-impact exercise. *Journal of Bone and Mineral Research*, *13*(12), 1805–1813.

Bland, J. M., & Altman, D. G. (1986). Statistical methods for assessing agreement between two methods of clinical measurement. *The Lancet*, *1*(8476), 301–310.

Chastin, S. F. M., Mandrichenko, O., Helbostadt, J. L., & Skelton, D. A. (2014). Associations between objectively-measured sedentary behaviour and physical activity with bone mineral density in adults and older adults, the NHANES study. *Bone*, *64*, 254–262.

Diniz-Sousa, F., Veras, L., Boppre, G., Devezas, V., Santos-Souza, H., Preto, J., … Fonseca, H. (2021). The effect of bariatric surgery on gravitational loading and its impact on bone mass. *Bone*, *153*, 116153.

Fabre, N., Lhuisset, L., Bernal, C., & Bois, J. (2020). Effect of epoch length on intensity classification and on accuracy of measurement under controlled conditions on treadmill: Towards a better understanding of accelerometer measurement. *PLoS One*, *15*(1), 1–11.

Field, A., Miles, J., & Field, Z. (2012). *Discovering statistics using R*. London: Sage.

Fonseca, H., Moreira-Goncalves, D., Coriolano, H. J., & Duarte, J. A. (2014). Bone quality: The determinants of bone strength and fragility. *Sports Medicine*, *44*(1), 37–53.

Fortune, E., Morrow, M. M. B., & Kaufman, K. R. (2014). Assessment of gait kinetics using tri-axial accelerometers. *Journal of Applied Biomechanics*, *30*(5), 668–674.

Giavarina, D. (2015). Understanding Bland Altman analysis. *Biochemia Medica*, *25*(2), 141–151.

Gouelle, A., Leroux, J., Bredin, J., & Mégrot, F. (2016). Changes in gait variability from first steps to adulthood: Normative data for the gait variability index. *Journal of Motor Behavior*, *48*(3), 249–255.

Heikkinen, R., Vihriälä, E., Vainionpää, A., Korpelainen, R., & Jämsä, T. (2007). Acceleration slope of exercise-induced impacts is a determinant of changes in bone density. *Journal of Biomechanics*, *40*(13), 2967–2974.

Kluitenberg, B., Bredeweg, S. W., Zijlstra, S., Zijlstra, W., & Buist, I. (2012). Comparison of vertical ground reaction forces during overground and treadmill running. A validation study. *BMC Musculoskeletal Disorders*, *13*(1), 235.

Medved, V. (2000). *Measurement of human locomotion*. Boca Raton: CRC Press.

Migueles, J. H., Cadenas-Sanchez, C., Ekelund, U., Nyström, C. D., Mora-Gonzales, J., Löf, M., … Ortega, F. B. (2017). Accelerometer data collection and processing criteria to assess physical activity and other outcomes: A systematic review and practical considerations. *Sports Medicine*, *47*(9), 1821–1845.

Migueles, J. H., Rowlands, A. V., Huber, F., & van Hees, V. T. (2019). GGIR: A research community–criven open source R package for generating physical activity and sleep outcomes from multi-day raw accelerometer data. *Journal for the Measurement of Physical Behaviour*, *2*(3), 188–196.

Nakagawa, S., & Schielzeth, H. (2013). A general and simple method for obtaining R^2 from generalized linear mixed-effects models. *Methods in Ecology and Evolution*, *4*(2), 133–142.

Neugebauer, J. M., Collins, K. H., & Hawkins, D. A. (2014). Ground reaction force estimates from ActiGraph GT3X+ hip accelerations. *PLoS One*, *9*(6), e99023.

Neugebauer, J. M., Hawkins, D. A., & Beckett, L. (2012). Estimating youth locomotion ground reaction forces using an accelerometer-based activity monitor. *PLoS One*, *7*(10), e48182.

Neugebauer, J. M., & LaFiandra, M. (2018). Predicting ground reaction force from a hip-borne accelerometer during load carriage. *Medicine & Science in Sports & Exercise*, *50*(11), 2369–2374.

Ngoh, K. J., Gouwanda, D., Gopalai, A. A., & Chong, Y. Z. (2018). Estimation of vertical ground reaction force during running using neural network model and uniaxial accelerometer. *Journal of Biomechanics*, *76*, 269–273.

Rantalainen, T., Heinonen, A., Komi, P. V., & Linnamo, V. (2008). Neuromuscular performance and bone structural characteristics in young healthy men and women. *European Journal of Applied Physiology*, *102*(2), 215–222.

Rantalainen, T., Heinonen, A., Linnamo, V., Komi, P. V., Takala, T. E. S., & Kainulainen, H. (2009). Short-term bone biochemical response to a single bout of high-impact exercise. *Journal of Sports Science and Medicine*, *8*(4), 553–559.

Robling, A. G. (2009). Is bone's response to mechanical signals dominated by muscle forces? *Medicine and Science in Sports and Exercise*, *41*(11), 2044–2049.

Rowlands, A. V., Schuna Jr., J. M., Stiles, V. H., & Tudor-Locke, C. (2014). Cadence, peak vertical acceleration, and peak loading rate during ambulatory activities: Implications for activity prescription for bone health. *Journal of Physical Activity & Health*, *11*(7), 1291–1294.

Staudenmayer, J., Zhu, W., & Catellier, D. J. (2012). Statistical considerations in the analysis of accelerometry-based activity monitor data. *Medicine & Science in Sports & Exercise*, *44*(Suppl. 1), S61–S67.

Stiles, V. H., Metcalf, B. S., Knapp, K. M., & Rowlands, A. (2017). A small amount of precisely measured high-intensity habitual physical activity predicts bone heath in pre- and post-menopausal women in UK biobank. *International Journal of Epidemiology*, *46*(6), 1847–1856.

15367290, 2023, 8, Downloaded from https://onlinelibrary.wiley.com/doi/10.1080/17461391.2022.2102437 by CAPES, Wiley Online Library on [13/01/2025]. See the Terms and Conditions (https://onlinelibrary.wiley.com/terms-and-conditions) on Wiley Online Library for rules of use; OA articles are governed by the applicable Creative Commons License

Troiano, R. P., McClain, J. J., Brychta, R. J., & Chen, K. Y. (2014). Evolution of accelerometer methods for physical activity research. *British Journal of Sports Medicine*, *48*(13), 1019–1023.

Turner, C. H. (1998). Three rules for bone adaptation to mechanical stimuli. *Bone*, *23*(5), 399–407.

Turner, C. H., Owan, I., & Takano, Y. (1995). Mechanotransduction in bone: Role of strain rate. *American Journal of Physiology – Endocrinology and Metabolism*, *269*, E438–E442.

Turner, C. H., & Robling, A. G. (2003). Designing exercise regimens to increase bone strength. *Exercise and Sport Sciences Reviews*, *31*(1), 45–50.

Vainionpää, A., Korpelainen, R., Vihriälä, E., Rinta-Paavola, A., Leppäluoto, J., & Jämsä, T. (2006). Intensity of exercise is associated with bone density change in premenopausal women. *Osteoporosis International*, *17*(3), 455–463.

Vanwanseele, B., Op De Beéck, T., Schütte, K., & Davis, J. (2020). Accelerometer based data can provide a better estimate of cumulative load during running compared to GPS based parameters. *Frontiers in Sports and Active Living*, *2*, 1–7.

Veras, L. (2021). impactr: An R package to process raw accelerometer data related to mechanical loading.

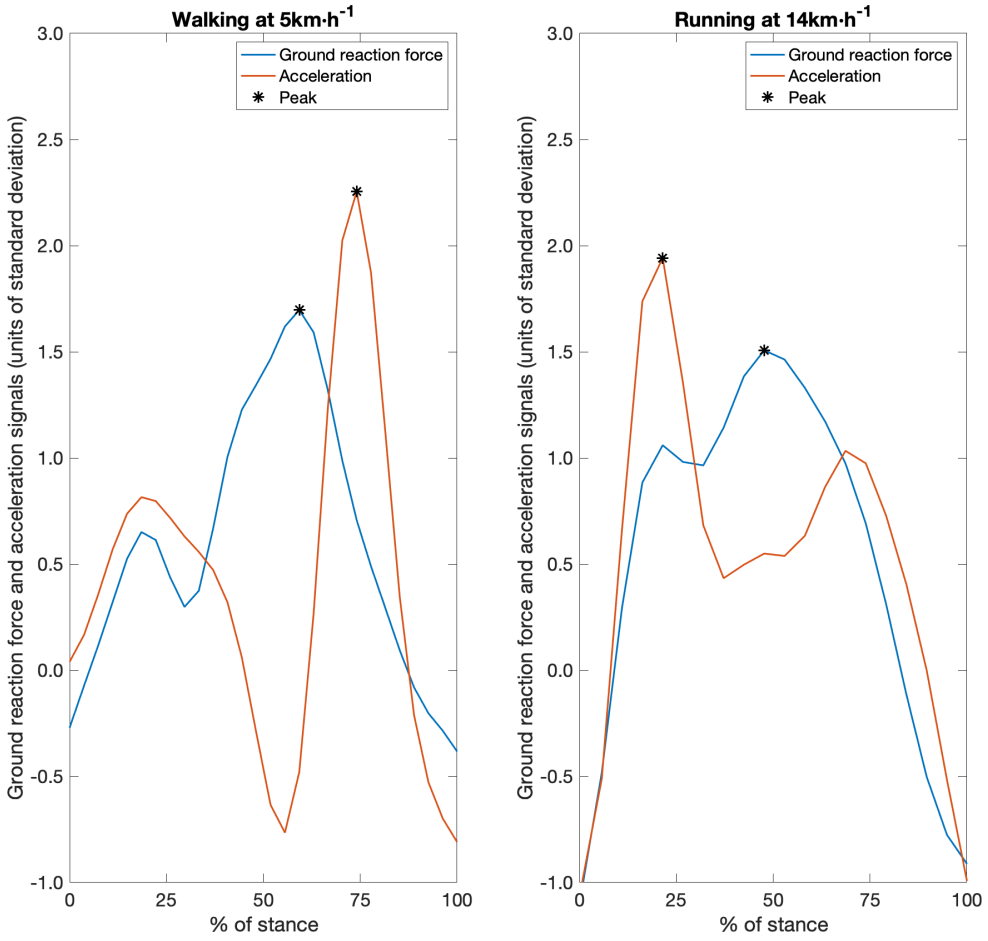
Veras, L., Diniz-Sousa, F., Boppre, G., Devezas, V., Santos-Souza, H., Preto, J., … Fonseca, H. (2020). Accelerometer-based prediction of skeletal mechanical loading during walking in normal weight to severely obese subjects. *Osteoporosis International*, *31*(7), 1239–1250.

Welk, G. J. (2005). Principles of design and analyses for the calibration of accelerometry-based activity monitors. *Medicine & Science in Sports & Exercise*, *37*(Suppl. 11), S501–S511.

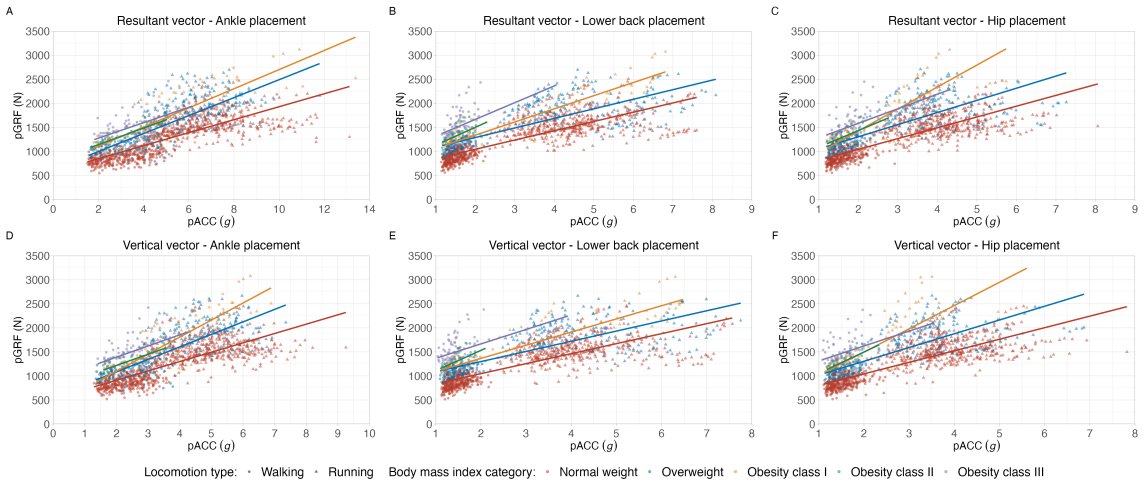
Wundersitz, D. W., Gastin, P. B., Robertson, S., Davey, P. C., & Netto, K. J. (2015). Validation of a trunk-mounted accelerometer to measure peak impacts during team sport movements. *International Journal of Sports Medicine*, *36*(9), 742–746.

15367290, 2023, 8, Downloaded from https://onlinelibrary.wiley.com/doi/10.1080/17461391.2022.2102437 by CAPES, Wiley Online Library on [13/01/2025]. See the Terms and Conditions (https://onlinelibrary.wiley.com/terms-and-conditions) on Wiley Online Library for rules of use; OA articles are governed by the applicable Creative Commons License

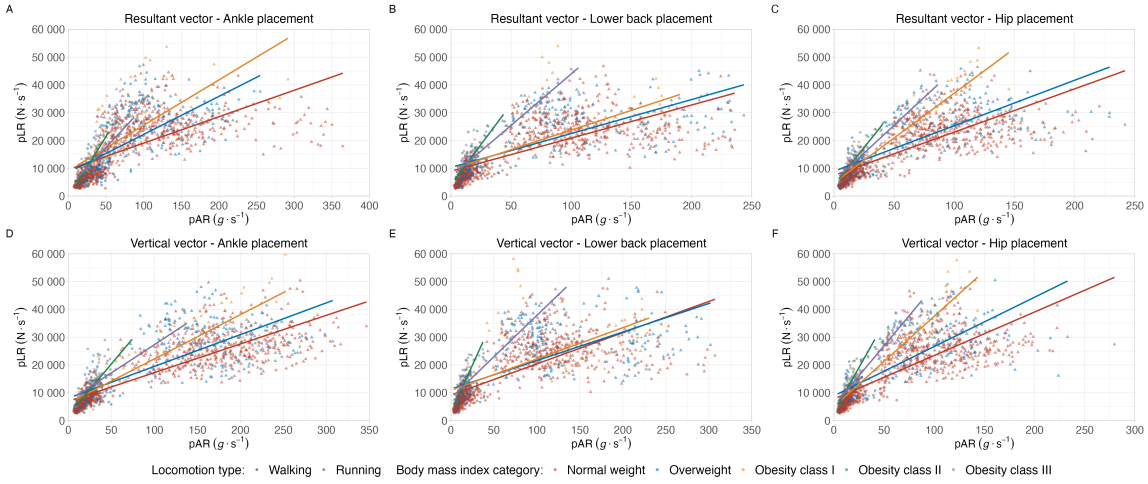
Supplemental Material



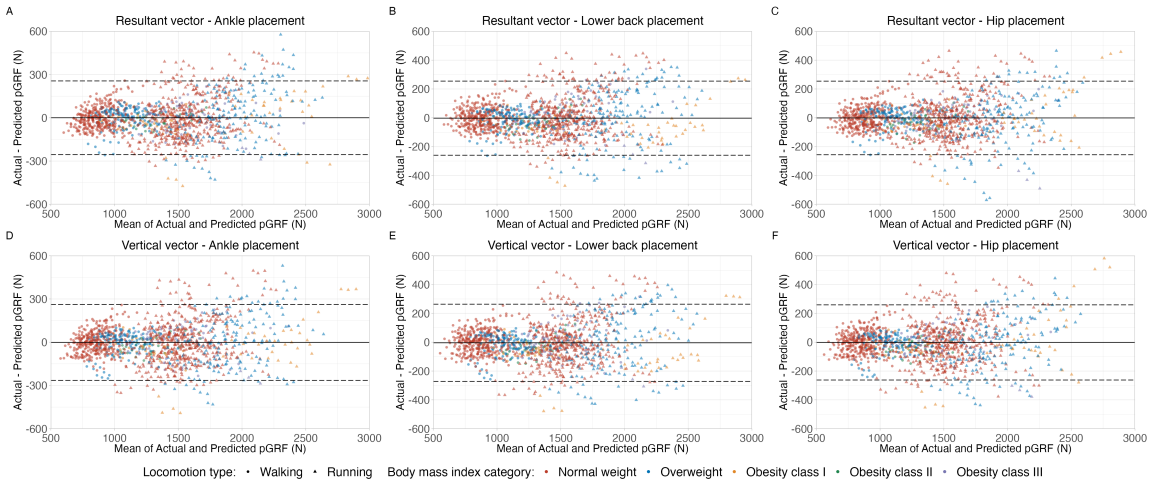
Supplemental Figure S1. Example of ground reaction force and acceleration signals during the stance phase of walking (left panel) and running (right panel). Signals were mean centered and scaled to units of standard deviation to fit in the same plot window. In this image, the peak of each signal, represented by the start marks, is its maximum magnitude during the stance. The peak acceleration rate and peak loading rate were identified as the steepest part of each curve.



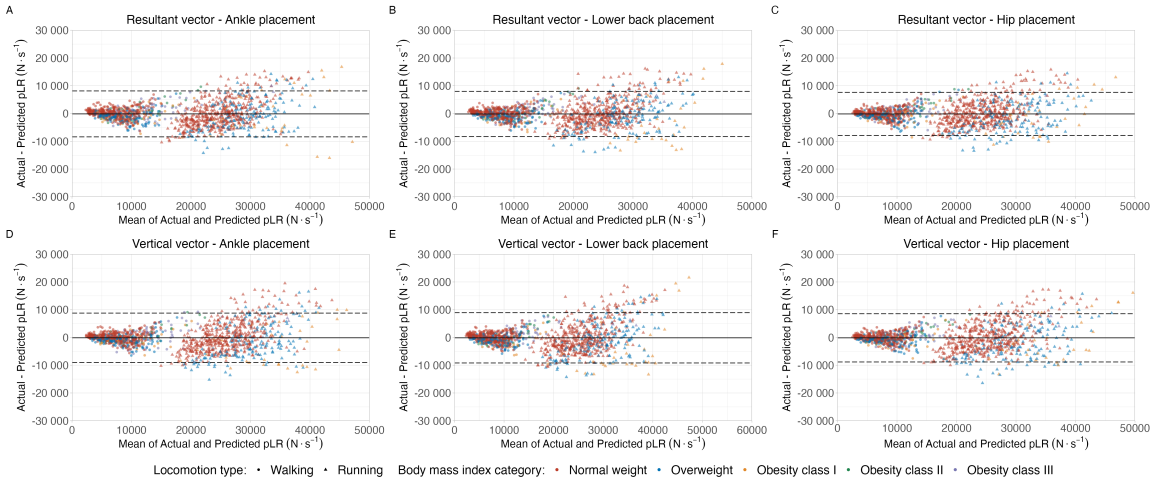
Supplemental Figure S2. Relationship between peak ground reaction force and acceleration magnitudes. Data from accelerometers worn at ankle (Panels A and D), lower back (Panels B and E) and hip (Panels C and F), for both the resultant vector (Panels A to C) and its vertical component (Panels D to F). Linear trends for each body mass index category are also depicted. Abbreviations: pACC, peak acceleration; pGRF, peak ground reaction force.



Supplemental Figure S3. Relationship between peak loading and acceleration rates. Data from accelerometers worn at ankle (Panels A and D), lower back (Panels B and E) and hip (Panels C and F), for both the resultant vector (Panels A to C) and its vertical component (Panels D to F). Linear trends for each body mass index category are also depicted. Abbreviations: pAR, peak acceleration rate; pLR, peak loading rate.



Supplemental Figure S4. Bland-Altman plots showing agreement between actual and predicted peak ground reaction force for accelerometers worn at ankle (Panels A and D), lower back (Panels B and E) and hip (Panels C and F), for both the resultant vector (Panels A to C) and its vertical component (Panels D to F). Continuous thick lines show bias (average of the differences between actual and predicted values) while dashed lines show the limits of agreement (bias ±1.96 standard deviation). Abbreviations: pGRF, peak ground reaction force.



Supplemental Figure S5. Bland-Altman plots showing agreement between actual and predicted peak loading rate for accelerometers worn at ankle (Panels A and D), lower back (Panels B and E) and hip (Panels C and F), for both the resultant vector (Panels A to C) and its vertical component (Panels D to F). Continuous thick lines show bias (average of the differences between actual and predicted values) while dashed lines show the limits of agreement (bias ± 1.96 standard deviation). Abbreviations: pLR, peak loading rate.

3.3. Study 2

Veras L, Diniz-Sousa F, Boppre G, Devezas V, Santos-Sousa H, Preto J, Vilas-Boas JP, Machado L, Oliveira J, Fonseca H. Using raw accelerometer data to predict high-impact mechanical loading. *Sensors*. 2023 Feb 16;23(4):2246. doi: 10.3390/s23042246.

sensors

MDPI

Article

Using Raw Accelerometer Data to Predict High-Impact Mechanical Loading

Lucas Veras [1,2], Florêncio Diniz-Sousa [1,2], Giorjines Boppre [1,2], Vítor Devezas [3], Hugo Santos-Sousa [3], John Preto [3], João Paulo Vilas-Boas [4,5], Leandro Machado [4,5], José Oliveira [1,2] and Hélder Fonseca [1,2,*]

[1] Research Center in Physical Activity, Health and Leisure (CIAFEL), Faculty of Sport, University of Porto, 4200-450 Porto, Portugal
[2] Laboratory for Integrative and Translational Research in Population Health (ITR), University of Porto, 4200-450 Porto, Portugal
[3] Obesity Integrated Responsability Unity (CRIO), São João Academic Medical Center, 4200-319 Porto, Portugal
[4] Center of Research, Education, Innovation and Intervention in Sport (CIFI2D), Faculty of Sport, University of Porto, 4200-450 Porto, Portugal
[5] Biomechanics Laboratory (LABIOMEP-UP), University of Porto, 4200-450 Porto, Portugal
* Correspondence: hfonseca@fade.up.pt; Tel.: +351-220425202; Fax: +351-2255006867

Abstract: The purpose of this study was to develop peak ground reaction force (pGRF) and peak loading rate (pLR) prediction equations for high-impact activities in adult subjects with a broad range of body masses, from normal weight to severe obesity. A total of 78 participants (27 males; 82.4 ± 20.6 kg) completed a series of trials involving jumps of different types and heights on force plates while wearing accelerometers at the ankle, lower back, and hip. Regression equations were developed to predict pGRF and pLR from accelerometry data. Leave-one-out cross-validation was used to calculate prediction accuracy and Bland–Altman plots. Body mass was a predictor in all models, along with peak acceleration in the pGRF models and peak acceleration rate in the pLR models. The equations to predict pGRF had a coefficient of determination (R^2) of at least 0.83, and a mean absolute percentage error (MAPE) below 14.5%, while the R^2 for the pLR prediction equations was at least 0.87 and the highest MAPE was 24.7%. Jumping pGRF can be accurately predicted through accelerometry data, enabling the continuous assessment of mechanical loading in clinical settings. The pLR prediction equations yielded a lower accuracy when compared to the pGRF equations.

Keywords: ground reaction force; loading rate; jumps; validation; biomechanics

check for updates

Citation: Veras, L.; Diniz-Sousa, F.; Boppre, G.; Devezas, V.; Santos-Sousa, H.; Preto, J.; Vilas-Boas, J.P.; Machado, L.; Oliveira, J.; Fonseca, H. Using Raw Accelerometer Data to Predict High-Impact Mechanical Loading. *Sensors* **2023**, *23*, 2246. https://doi.org/10.3390/s23042246

Academic Editor: Mehmet Rasit Yuce

Received: 1 November 2022
Revised: 15 December 2022
Accepted: 15 February 2023
Published: 16 February 2023

Copyright: © 2023 by the authors. Licensee MDPI, Basel, Switzerland. This article is an open access article distributed under the terms and conditions of the Creative Commons Attribution (CC BY) license (https://creativecommons.org/licenses/by/4.0/).

1. Introduction

Bones respond to mechanical loading by altering their properties, such as mass, microarchitecture, and geometry, which ultimately dictate their strength and resistance to fracture [1–3]. Therefore, physical activity is a paramount stimulus to maintain and improve bone health throughout the life course [4]. However, the osteogenic effect of physical activity is highly dependent on the characteristics of mechanical loading [5]. Several studies on experimental animals [1,6,7] have helped to form our understanding of the principles that drive bone tissue's adaptive response to mechanical loading. In general, high-magnitude dynamic impact loading applied at high frequencies and including long rest periods seems to favor increases in bone mass and strength [1]. This seems to corroborate the available evidence from humans. For instance, findings from different types of sports have shown that athletes practicing sports involving high- and/or odd-impact loading (e.g., volleyball and football) have a greater bone mass and estimated bone strength compared to repetitive and low-impact loading sports (e.g., cycling and swimming) [8]. Nevertheless, the precise way in which the manipulation of mechanical loading variables influences bone tissue's

adaptive response in humans is not fully understood, particularly due to the difficulty in accurately assessing bone's mechanical loading and its components in vivo in humans.

Some questionnaires have been developed in an attempt to capture the bone-stimulating characteristics of specific activities [9,10]. However, although the scores generated by such subjective methods seem to be related to bone status, this association appears to be limited and inconsistent across studies [11–13]. A more robust approach to assess mechanical loading is the use of equipment such as force plates—the gold standard for ground reaction force measurement [14]. However, the use of force plates is less applicable in some clinical and research settings, as they are immobile and expensive devices that are limited to assessments in laboratory conditions. In the last few years, objective methods based on wearable devices have been proposed as a solution to overcome these limitations, since acceleration and some mechanical loading variables resulting from body movement have shown to be correlated [15,16]. In fact, several studies using different prediction model approaches (e.g., linear regression, linear mixed models, machine learning) have already shown that, through the use of acceleration data, it is possible to estimate some mechanical loading components that are typically assessed only through force plates, namely, peak ground reaction force (pGRF) [17–25] and peak loading rate (pLR) [19,21,22]. Although accelerometry-based equations have shown high prediction accuracy [21,22], this versatile approach to mechanical loading assessment is not widely used yet, either in clinical practice or research. One of the issues that may contribute to this fact is the lack of validation studies covering a broader spectrum of activities, especially those known to have a greater osteogenic effect, such as high-impact activities.

Until now, studies that have calibrated accelerometers to predict mechanical loading variables have usually employed only simple activities, such as walking [19–21] or walking and running [17,18,22,24], while activities eliciting higher impact loading have not yet been tested. The fact that these accelerometry-based prediction equations are only valid for a limited set of activities hinders their ability to accurately quantify the amount of loading to which a person is subjected daily, as the physical activities performed daily are often composed of other types of activities than just walking and running. Therefore, the validity of these methods should be expanded to other activities that are commonly associated with positive bone adaptations. Jumping exercises, for instance, are frequently used as a strategy to improve bone health in post-menopausal women [26] and elderly men [27]. The direct measurement of the mechanical loading involved in these activities would greatly improve our ability to precisely control the loading regimen elicited by these physical exercises, and to establish a more reliable relationship between mechanical stimulation and the bone's anabolic response and, consequently, to establish a clearer relationship between exercise dose and the extent of the bone's adaptive response [28]. So far, accelerations recorded from body-worn devices have been shown to be correlated with ground reaction forces during jumping [15], and accelerometers have also been successfully used to predict other biomechanical variables during jumping activities [29]. Therefore, the objective of this study was to develop accelerometry-based pGRF and pLR prediction equations for high-impact activities in adult subjects with a broad range of body masses, from normal weight to severe obesity.

2. Methods

An overall scheme of the experimental design and methods employed in this study can be observed in Figure 1.

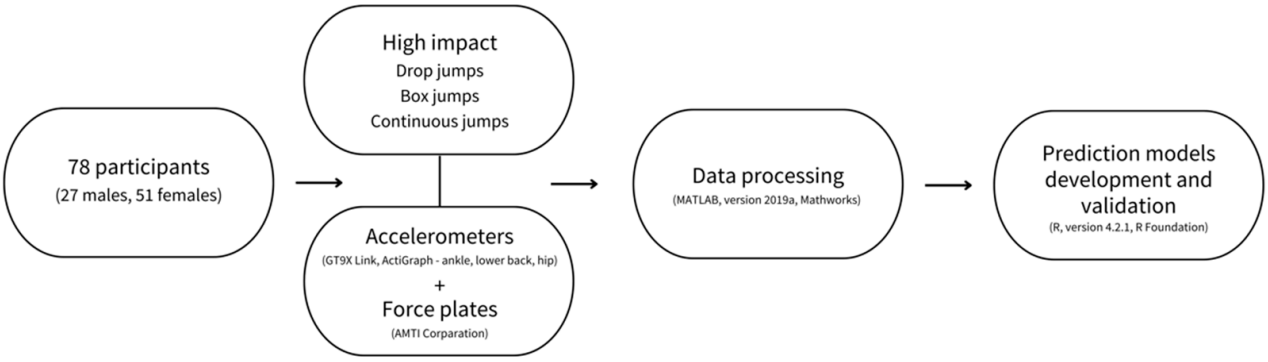


Figure 1. Overall scheme of the study design and methods employed in the study.

2.1. Participants

A total of 78 adults participated in the study (27 males: 34.0 ± 12.3 years, 173.2 ± 6.3 cm, 83.2 ± 14.9 kg, 27.9 ± 5.6 kg·m^{-2}; 51 females: 36.5 ± 11.2 years, 158.1 ± 6.8 cm, 82.0 ± 23.2 kg, 33.0 ± 9.6 kg·m^{-2}; $\overline{X}$ ± SD). The protocol was approved by the local ethics committee (CES 192-14), and all participants were informed about the experiments' purpose and protocol before giving their written informed consent. The inclusion criteria were as follows: age between 18 and 65 years, and the ability to perform the jumps included in the trials. The exclusion criterion was the presence of any acute injury or chronic limitation precluding any of the experimental exercises. The measurement of height (stadiometer model 213; Seca, Hamburg, Germany) and body mass (digital scale model 899; Seca, Hamburg, Germany) was carried out according to standard procedures [30].

2.2. Protocol

The participants completed a series of trials involving jumps of different types and from different heights. First, drop jumps were executed from steps varying from 5 cm to 40 cm high, with 5 cm increments. Then, box jumps were performed starting from the floor up to 5 cm, 15 cm, and 30 cm high boxes. Finally, continuous jumps were carried out at two different heights: 5 cm and 15 cm. Drop and box jumps were executed in two sets of four jumps at each height, with a 30 s interval, and the continuous jumps were performed in one set of 20 s at each height. Before starting the data collection, the participants performed a few repetitions of each jump type—always at the lowest height—to familiarize themselves with the protocol. The jumps were always performed in the following order: drop jumps, box jumps, continuous jumps—and from lower to higher heights. The landing phase of the drop jumps, the take-off phase of the box jumps, and both phases of the continuous jumps were recorded on a force plate at a 1000 Hz sampling frequency (AMTI Corporation, Watertown, USA). The participants were instructed to jump with no restrictions regarding their arm movements, to land two-footed, and to remain stationary on the force plate for around five seconds after landing (except for the continuous jumps). To better characterize the types of jumps performed, the initial and final position of each jump can be seen in Figure 2.

Throughout the protocol, three wearable sensors (GT9X Link; 100 Hz; ±16 g range; ActiGraph, Pensacola, FL, USA) were worn by each participant, at the following placements: (i) right hip (along the anterior axillary line, at the level of the iliac crest); (ii) lower back (at the midpoint between the two posterior superior iliac spines); and (iii) right ankle (immediately superior to the lateral malleolus). The sensors worn at the hip and lower back were positioned on the same tightly secured elastic belt with clips, and the ankle-worn sensor was fixed by an elastic belt and adhesive tape. The wearable sensors were always positioned to ensure the alignment of the accelerometer's vertical axis and the standing body's longitudinal axis. The accelerometers' positioning on the body can be seen in Figure 3. The hip and lower back placements were chosen due to their proximity to the

body's center of mass, and the ankle placement was chosen because its location is closer to the ground contact point. The wearable sensors were set to collect data at 100 Hz, which is the device's maximum sampling frequency.

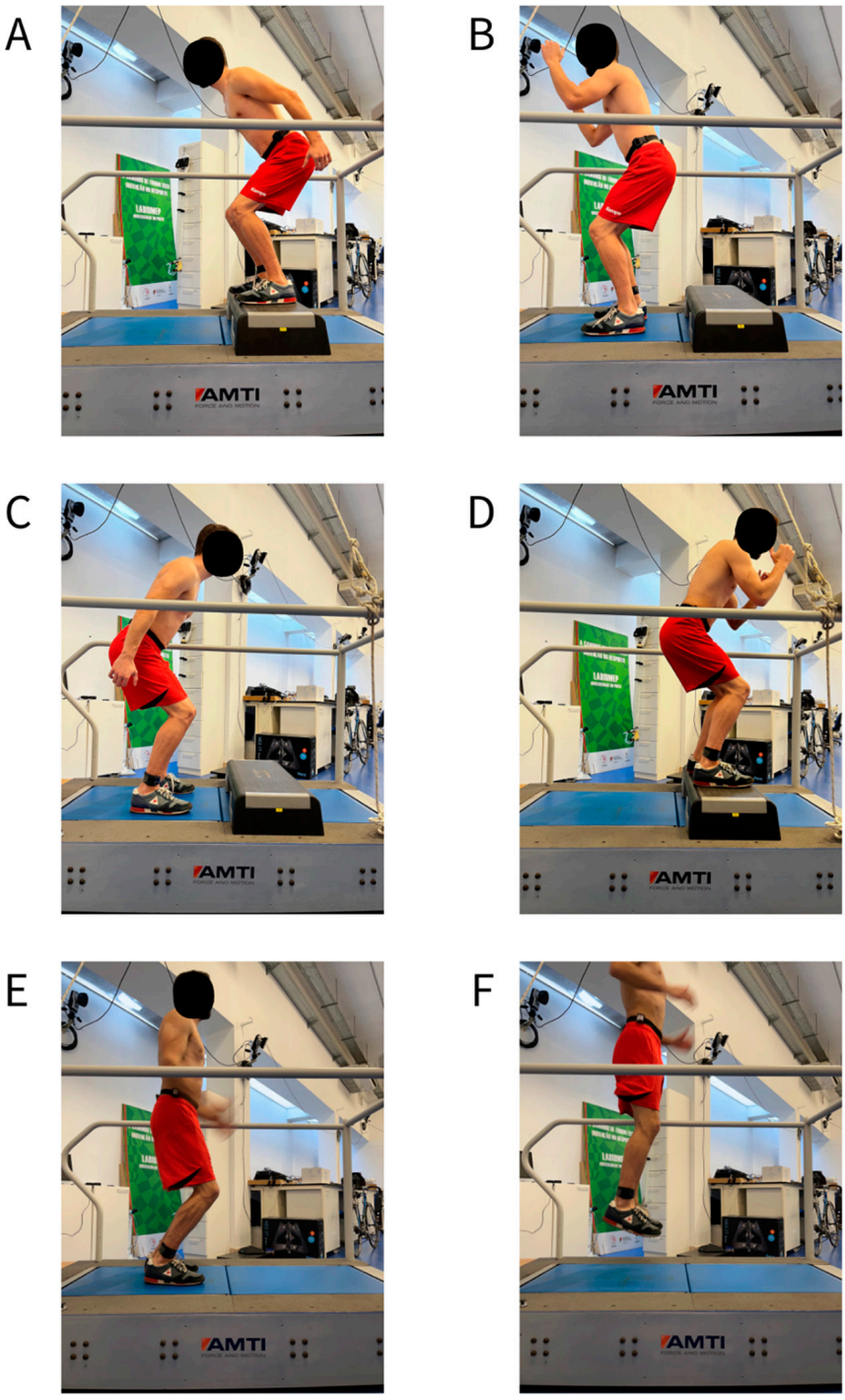


Figure 2. An example of a participant performing each of the jump types assayed. Panels (**A**,**B**) show the initial (take-off phase) and final (landing phase) phases of the drop jumps, respectively, while Panels (**C**,**D**) show the initial and final phases of the box jumps, respectively, and Panels (**E**,**F**) show the initial and final phases of the continuous jumps, respectively.

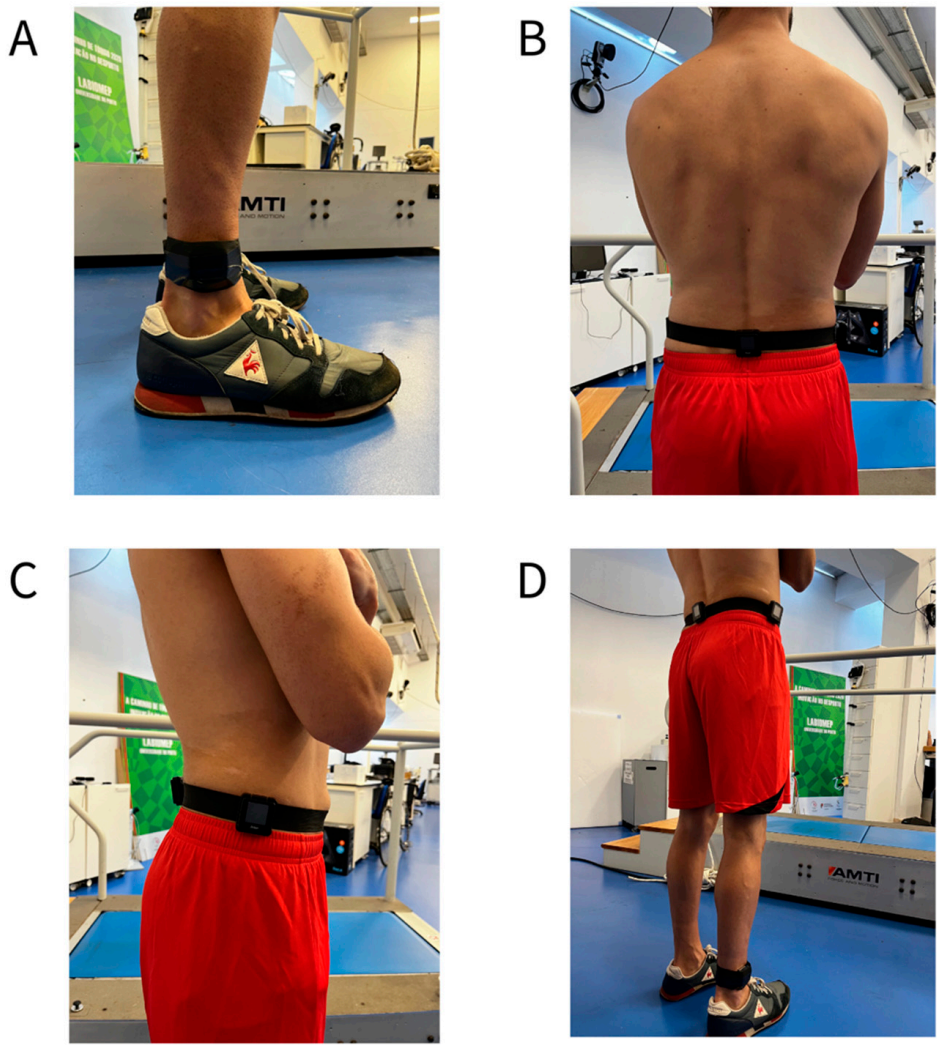


Figure 3. Accelerometers' positioning on the body: Details of accelerometer positioning on the ankle, lower back, and hip are displayed in Panels (**A**–**C**), respectively. Panel (**D**) shows all accelerometer placements simultaneously.

Each wearable sensor used includes a primary and a secondary triaxial accelerometer. As the manufacturer's proprietary filter is not applied to the secondary accelerometer's raw data, only data from this accelerometer were used in this study. This increases the accuracy and replicability of data collection and processing. Data from the force plates (Netforce, Version 3.5.1; AMTI Corporation, Watertown, USA) and accelerometers (ActiLife version 6.13.3; ActiGraph, Pensacola, USA) were operated through the manufacturer-supplied software and exported as raw data from the x, y, and z vectors. The ground reaction force was expressed in newtons (N), and acceleration was expressed in gravitational acceleration units (1 g = 9.807 m·s^{-2}).

2.3. Data Processing

A flowchart showing the steps of the data processing can be seen in Figure 4. MATLAB software (Version 2019a, MathWorks, Natick, MA, USA) was used to process the data from both the force plates and the accelerometers. Data were processed according to the following procedures: First, the ground reaction force signal from the force plate (1000 Hz) was resampled to match the activity monitors' sampling frequency (100 Hz). Then, both the ground reaction force and acceleration signals were filtered using a Butterworth fourth-

order low-pass filter, with a 20 Hz cutoff frequency, to attenuate the noise. This cutoff frequency was selected based on visual inspection of the signals' frequency spectra after a fast Fourier transform (FFT). Afterwards, the ground reaction force and acceleration's resultant vector was calculated ($r_i = \sqrt{x_i^2 + y_i^2 + z_i^2}$). After that, both signals were adjusted using the time set by the system's clock and then synchronized by the maximum cross-correlation coefficient. Then, the ground reaction force and acceleration signals were visually inspected, and whenever their peaks were not in the same hundredth of a second, manual adjustments to the synchronization were performed. An example of the ground reaction force and acceleration signals for each jump type can be observed in Figure 5. Next, the peak acceleration (pACC) was determined by the following criteria: (i) a minimum magnitude of three standard deviations above the mean acceleration value recorded during a trial, and (ii) a separation of at least 0.2 s for continuous jumps and 4 s for the other jumps. Then, pGRF was defined as the highest value within $+/-$ 0.2 (continuous jumps) or $+/-$ 4 (drop and box jumps) seconds of each pACC, according to the jump type. The rates of change were computed through a centered derivative from the beginning of the foot contact to the curve peak (Equation (1)). The pLR and peak acceleration rate (pAR) were defined as the maximum value in the array derived from Equation (1) and represented by $f'_{i_{max}}$ in Equation (2).

$$f'_i = \frac{f_{i+1} - f_{i-1}}{t_{i+1} - t_{i-1}} \quad (1)$$

$$f'_{i_{max}} = max\left(f'_i\right) \quad (2)$$

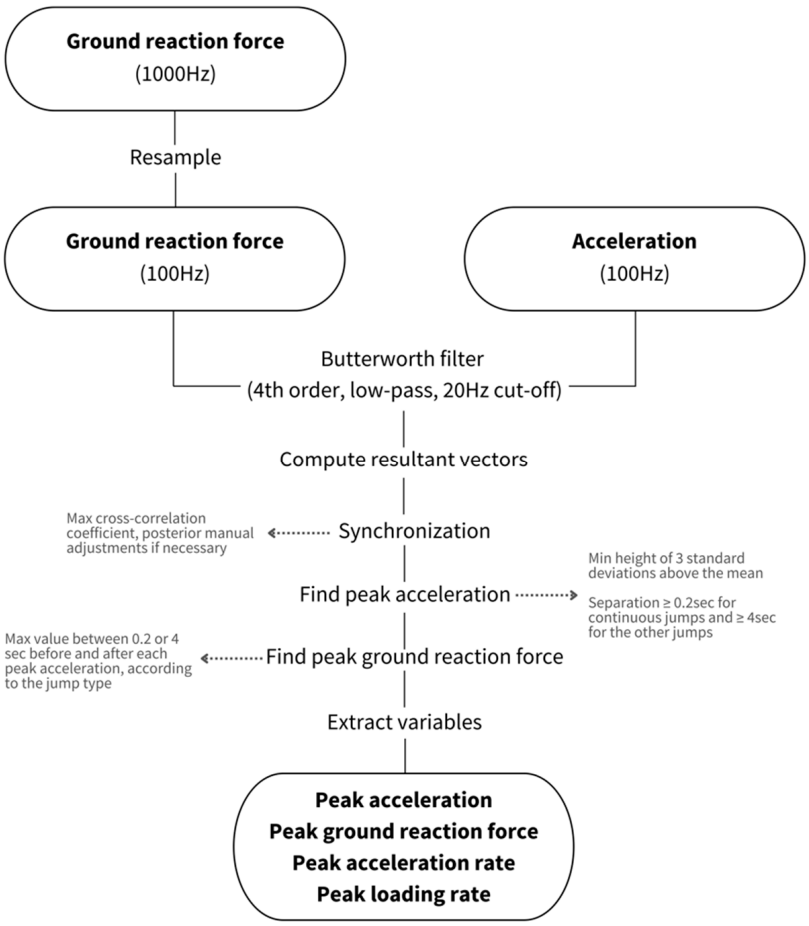


Figure 4. Flowchart showing all steps of the data processing.

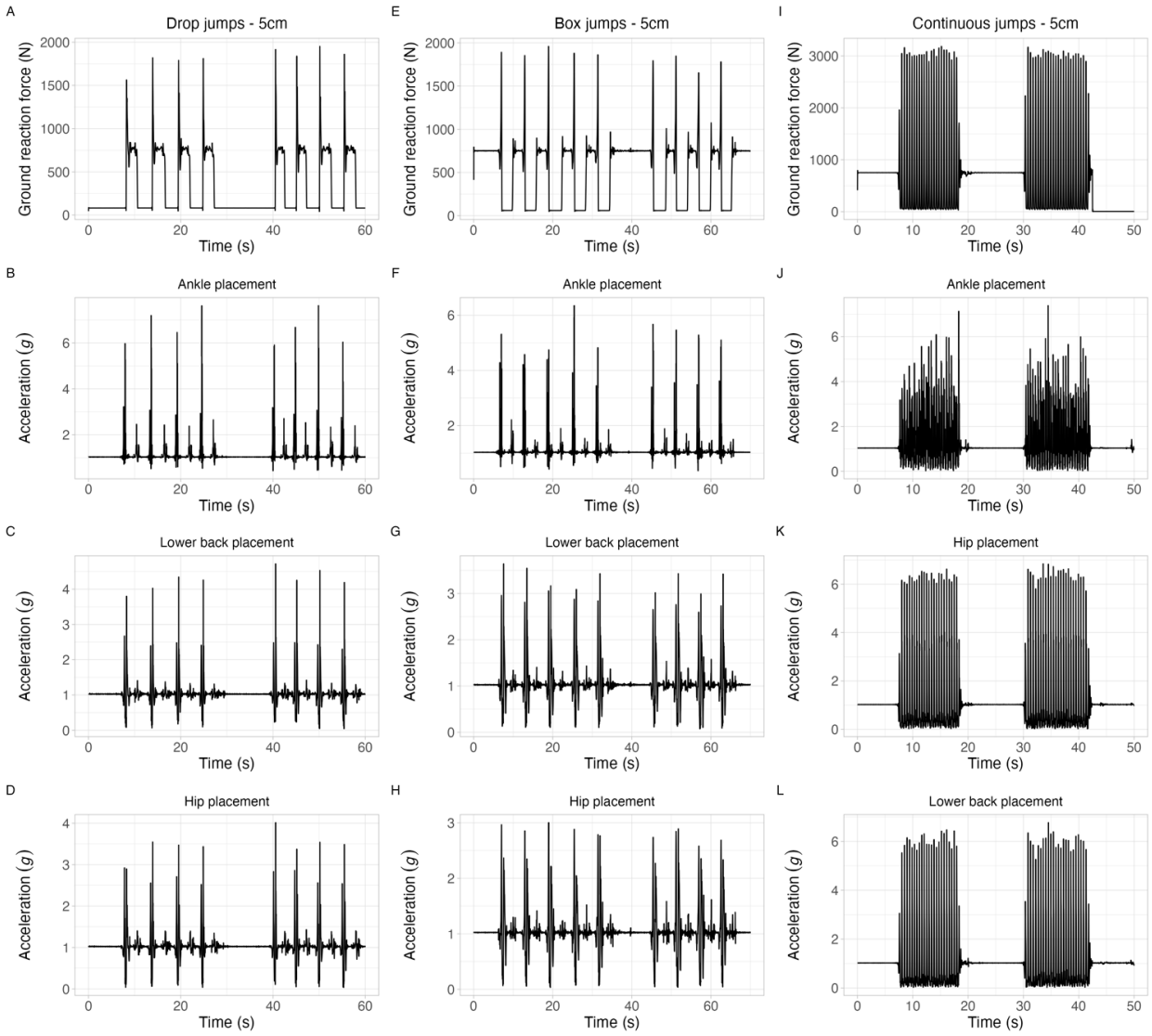


Figure 5. Examples of the ground reaction force and acceleration signals for all of the jump types performed. The first column, formed by Panels (**A**–**D**), shows the ground reaction force and acceleration signal for accelerometers at the ankle, lower back, and hip for the drop jump from 5 cm height. Panels (**E**–**H**) show the same signals, but for the box jumps of 5 cm height, while Panels (**I**–**L**) show the signals for the continuous jumps of 5 cm.

Finally, the mean pGRF, pACC, pLR, and pAR of the resultant vector and its vertical component for each participant at each jump type and height for each accelerometer placement were extracted and used in all subsequent analyses.

2.4. Statistical Analyses

Statistical analyses were performed using R statistical software (version 4.2.1, R Foundation for Statistical Computing, Vienna, Austria). All code used in the data analysis is registered in an open platform (https://bit.ly/3szNSJS, accessed on 31 October 2022). Statistical significance was set as $\alpha = 0.05$.

Linear mixed models were used to develop pGRF and pLR prediction equations for each vector (resultant and vertical) and accelerometer placement (ankle, lower back, and hip). Body mass was tested as a predictor in all models, along with the acceleration magnitude (pACC) in the pGRF models and its rate (pAR) in the pLR models. These

predictors were entered as fixed effects and kept in the model, as all were shown to be significant ($p < 0.05$). The subject and the interaction between jump type and jump height were tested as random effects, and both factors were shown to improve the models. The final models were chosen according to the −2 log-likelihood statistic [31]. The conditional coefficient of determination (R^2), which estimates the variance explained by both fixed and random factors [32], was computed.

Model validation was performed using the leave-one-out cross-validation method [33]. This method consists of separating data from one of the subjects into a testing dataset while keeping the remainder in the training dataset. Then, a new model is developed using the training dataset, with the same parameters that were defined using the entire sample. This new model is then applied to predict the outcome for the subject in the testing dataset. The whole process is repeated once for each participant (78 times). Data from the testing dataset were used in all subsequent analyses.

Model quality was then evaluated both numerically and graphically. The numerical assessment was performed by computing the following accuracy indices: mean absolute error (MAE), mean absolute percentage error (MAPE), and root-mean-square error (RMSE). To visually analyze the agreement between the values predicted by the models and those measured by the force plates, Bland–Altman plots were drawn. These plots are constructed by plotting the mean of the actual and predicted values on the *x*-axis and their difference on the *y*-axis. Then, the bias was calculated as the mean of these differences and plotted as a continuous horizontal line. The limits of agreement were defined as bias ± 1.96 standard deviation and plotted as horizontal dashed lines [34]. To further test whether there was any systematic under- or overestimation of the values by the models, one-sample *t*-tests were performed to check whether the bias were significantly different from zero. Finally, linear regressions were employed to examine whether the difference between the actual and predicted values was affected by their magnitude, thereby verifying whether the prediction was constant throughout the entire magnitude range [35].

3. Results

In our protocol, three distinct jump types were performed, each using several different heights. This variety of jumping trials produced a considerable heterogeneity in the response of both the force-plate- and accelerometer-measured variables. The results obtained for pGRF, pLR, pACC, and pAR, with respect to their resultant vectors, can be observed in Figure 6 (see Supplementary Figure S1 for the vertical vector).

Panels A and B show the force-plate-measured variables normalized by the subject's body mass, and by the pGRF and pLR, respectively. It can be seen that, in the drop jump trials, there is a tendency for the loading magnitude to increase as the jump height increases. This tendency is also observed for the box jumps, but with a lower magnitude. As for the continuous jumps, both assayed heights elicited reasonably similar loading profiles. Panels C and D show the values of the accelerometer-measured variables—pACC and pAR, respectively—for each trial. It can be observed that, for all jump types and heights, data from ankle-worn accelerometers typically record higher values compared to data from the accelerometers placed at the lower back and hip. Moreover, during the drop jumps, there is a constant increase in the values from the ankle accelerometers as the jump height increases, while values from the lower back and hip accelerometers tend to plateau from 30 cm height onwards. As for the box jumps, the pACC values remain reasonably constant throughout the assayed heights, whereas pAR tends to slightly decrease as the jump heights increase. Lastly, for the continuous jumps, both pACC and pAR from the lower-back- and hip-worn accelerometers marginally decrease when comparing the 5 cm to 15 cm jumps. However, the opposite is true for the ankle accelerometers, with their pACC and pAR increasing from 5 cm to 15 cm height.

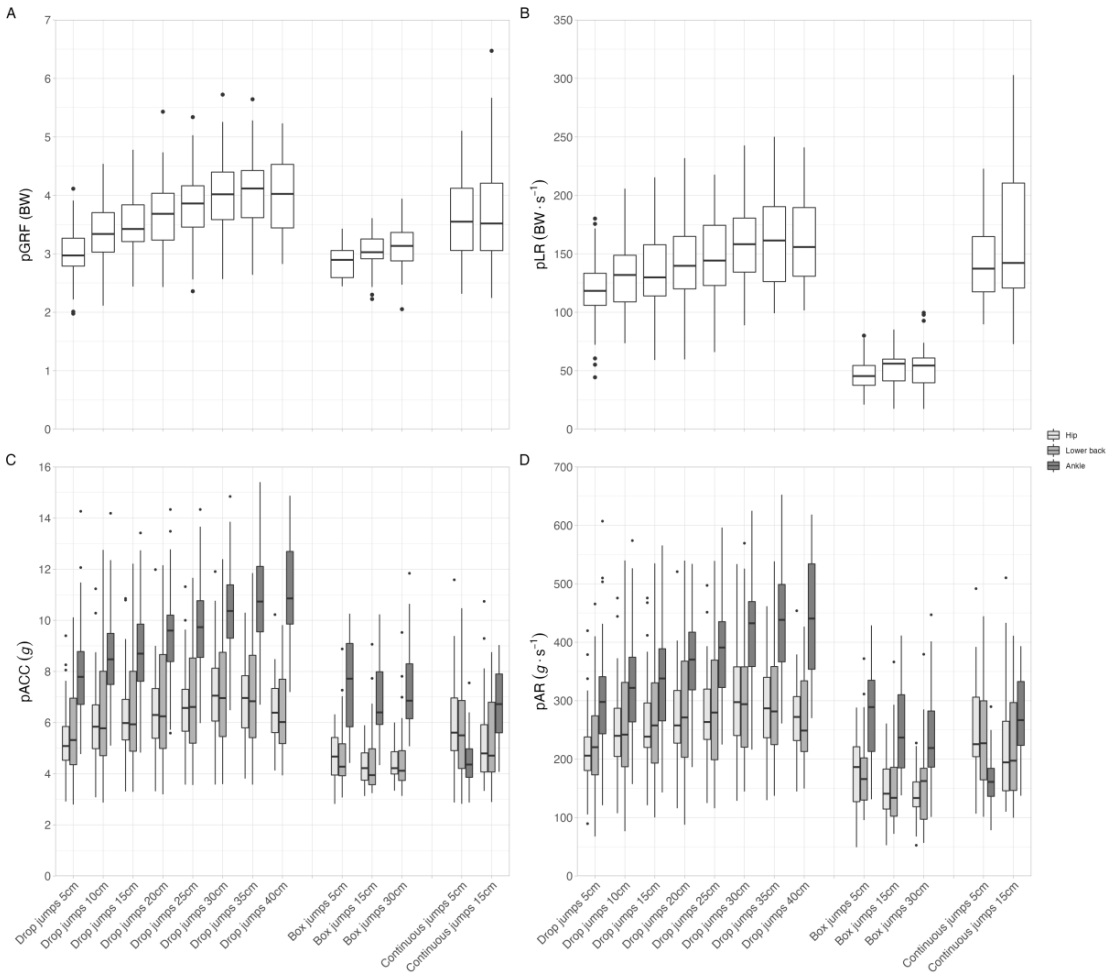


Figure 6. Distribution of the resultant vectors of mechanical loading (peak ground reaction force on Panel (**A**) and peak loading rate on Panel (**B**)) and acceleration (peak acceleration on Panel (**C**) and peak acceleration rate on Panel (**D**)) variables per jump type and height combination. Abbreviations: BW, body weight; pACC, peak acceleration; pAR, peak acceleration rate; pGRF, peak ground reaction force; pLR, peak loading rate.

Accelerometer-based mechanical loading prediction equations were developed based on linear mixed models. The regression coefficients, R^2, and accuracy indices of the models derived from accelerometers worn at the ankle, lower back, and hip, and from the resultant and vertical vectors, are presented in Table 1. The R^2 values for the pGRF models ranged from 0.83 to 0.92, showing that all of the models were able to explain at least 80% of the pGRF variance, and the observed MAPE values were between 12.3% and 14.5%. Despite the similar accuracy results achieved by all equations, the model derived from data from the resultant vector of accelerometers worn at the hip was shown to have the lowest accuracy error, represented by the smallest MAE (302.1 N), MAPE (12.3%), and RMSE (396.6 N).

Table 1. Regression equations, R^2, and accuracy indices for prediction of pGRF and pLR based on accelerometer-derived data.

Vector	Accelerometer Placement	Regression Equations	R^2	MAE	MAPE	RMSE
pGRF prediction equations						
Resultant	Ankle	pGRF (N) = 1551.020 − 132.384(pACC) + 7.927(body mass) + 2.415(pACC × body mass)	0.84	341.2 ± 275.1	13.9% ± 13.4%	438.2 ± 569.4
	Lower back	pGRF (N) = −350.125 + 152.952(pACC) + 22.618(body mass) + 0.654(pACC × body mass)	0.92	376.3 ± 257.9	14.5% ± 10.7%	456.1 ± 508.5
	Hip	pGRF (N) = −493.877 + 188.759(pACC) + 18.008(body mass) + 1.279(pACC × body mass)	0.90	302.1 ± 257.2	12.3% ± 13.4%	396.6 ± 549.2
Vertical	Ankle	pGRF (N) = 1662.525 − 196.301(pACC) + 8.515(body mass) + 3.169(pACC × body mass)	0.83	350.4 ± 282.8	14.4% ± 14.5%	450.1 ± 581.0
	Lower back	pGRF (N) = −287.919 + 131.396(pACC) + 24.338(body mass) + 0.642(pACC × body mass)	0.90	371.0 ± 257.1	14.4% ± 10.9%	451.3 ± 509.8
	Hip	pGRF (N) = −786.169 + 177.403(pACC) + 23.953(body mass) + 1.355(pACC × body mass)	0.88	322.9 ± 273.3	13.3% ± 15.0%	422.9 ± 578.1
pLR prediction equation						
Resultant	Ankle	pLR ($N \cdot s^{-1}$) = 71932.438 − 218.268(pAR) + 74.463(body mass) + 3.474(pAR × body mass)	0.88	18,973 ± 14,494	23.4% ± 26.6%	23,868 ± 29,433
	Lower back	pLR ($N \cdot s^{-1}$) = −1161.976 + 22.804(pAR) + 624.413(body mass) + 2.135(pAR × body mass)	0.89	20,320 ± 14,799	23.9% ± 23.6%	25,132 ± 28,807
	Hip	pLR ($N \cdot s^{-1}$) = 5118.300 + 33.054(pAR) + 346.667(body mass) + 2.835(pAR × body mass)	0.91	16,812 ± 13,485	20.7% ± 24.5%	21,546 ± 27,240
Vertical	Ankle	pLR ($N \cdot s^{-1}$) = 58864.225 − 194.575(pAR) + 142.545(body mass) + 3.733(pAR × body mass)	0.87	18,147 ± 14,387	23.1% ± 28.8%	23,152 ± 29,707
	Lower back	pLR ($N \cdot s^{-1}$) = 8303.550 − 19.708(pAR) + 685.299(body mass) + 1.900(pAR × body mass)	0.88	21,001 ± 14,831	24.7% ± 25.2%	25,704 ± 28,869
	Hip	pLR ($N \cdot s^{-1}$) = −11471.926 + 15.332(pAR) + 691.269(body mass) + 2.670(pAR × body mass)	0.88	18,801 ± 15,478	22.9% ± 27.5%	24,345 ± 30,582

Abbreviations: MAE, mean absolute error; MAPE, mean absolute percentage error; pACC, peak acceleration; pAR, peak acceleration rate; pGRF, peak ground reaction force; pLR, peak loading rate; RMSE, root-mean-square error. Data: mean ± standard deviation.

Compared to the pGRF models, the pLR equations yielded poorer results. Although their R^2 ranged from 0.87 to 0.91, their error measures were high, with MAPE ranging from 20.7% to 24.7%. Nevertheless, similar to the pGRF models developed, the best pLR prediction equation in terms of prediction accuracy was the one from the resultant vector derived from hip-worn accelerometers, even though its error estimates were higher, with an MAE of 16812 N, MAPE of 20.7%, and RMSE of 21545 N.

To visualize the agreement between the pGRF and pLR values measured by the force plates and predicted by the models, a series of Bland–Altman plots were built for both the resultant and vertical vectors and for all accelerometer placements. Figure 7 shows the Bland–Altman plots for the resultant pGRF (panel A) and pLR (panel B) vectors of the hip-worn accelerometers. Both plots show good agreement levels, as at least 94% of the data points are within the limits of agreement and the data tend to cluster around zero. Bland–Altman plots for the other accelerometer placements and vectors also showed the same previously described patterns and can be found in Supplementary Figure S2 for pGRF and in Supplementary Figure S3 for pLR. Moreover, as could be observed from the results of the one-sample *t*-tests, none of the equations presented a bias significantly different from zero ($p > 0.05$). Furthermore, all of the equations showed a proportional bias, i.e., the magnitude of the values influences the prediction error. However, as the linear regressions used to assess the proportional bias presented a very small R^2 (maximum value of 0.10), this effect is negligible.

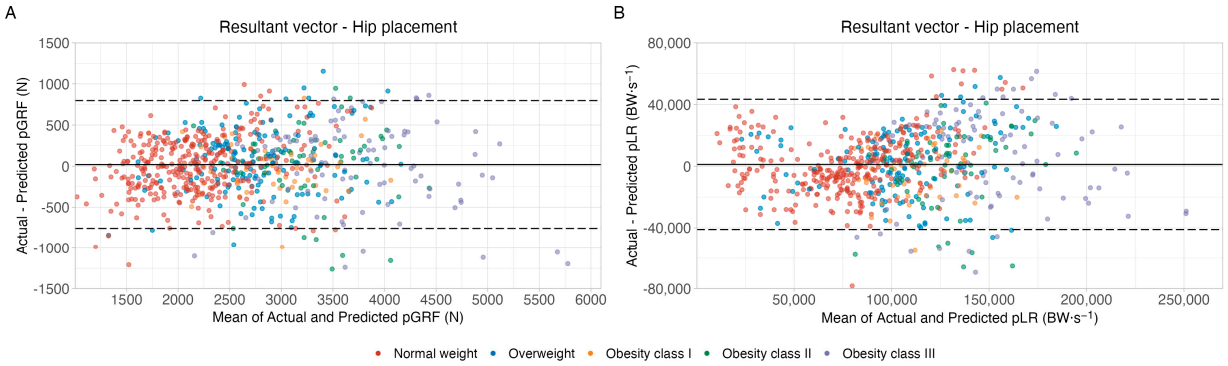


Figure 7. Bland–Altman plots showing agreement between actual and predicted peak ground reaction force (Panel **A**) and loading rate (Panel **B**) for the resultant vectors from hip-worn accelerometers. Continuous thick lines show bias (the average of the differences between actual and predicted values), while dashed lines show the limits of agreement (bias ± standard deviation). Abbreviations: pGRF, peak ground reaction force; pLR, peak loading rate.

Finally, an R package was also developed [36] to simplify the application of all of the necessary data processing steps involved in the implementation of the developed prediction equations. The package website (https://verasls.github.io/impactr, accessed on 31 October 2022) has all of the installation instructions and documentation necessary to apply this method on the user's own data.

4. Discussion

This study aimed to develop accelerometer-based mechanical loading prediction equations for pGRF and pLR, for jumping exercises of different types and heights. We also tested different accelerometer placements and data derived from both the resultant and vertical acceleration vectors. Our results showed that the pGRF prediction models developed for jumping activities based on accelerometry data have an MAPE around 13%. The prediction equations developed for pLR resulted in a lower accuracy, with an MAPE around 22%. These models are the first to be developed specifically for high-impact jumping activities in adults.

When comparing the accuracy indices of the pGRF prediction equations developed in the present study with other equations from past investigations, developed for walking and running, it can be seen that our models have a lower accuracy [17,18,20–22]. This can be explained, at least partially, by the high heterogeneity in the jumping movement patterns, as several combinations of jump types and heights were tested in our study. In addition, subjects with different skill levels were included in the sample, which may have favored heterogeneity. Nevertheless, these MAPE values are similar to the results usually found in accelerometer-based energy expenditure prediction models [37], which have widespread use in research. As for the pLR prediction equations, they presented a lower accuracy compared to the pGRF equations, corroborating previous findings [19,21,22]. This is possibly due to the fact that the loading rate is typically calculated through a derivative of the force signal from the beginning of the foot's contact with the floor to the point where the pGRF is achieved [19,21,22,38]. As this is a small time window—usually less than 0.2 s for the jumps that were performed in our protocol—it requires a fine sampling acquisition that captures small graduations in the force values throughout time, which is difficult to achieve with common accelerometer sampling frequencies, which are usually 100 Hz at maximum. Nevertheless, although our pLR prediction models had worse accuracy compared with the pGRF models, their accuracy was similar or even better than the results from previous studies that developed models to predict pLR during walking only [19,21]. Furthermore, although our prediction equations' error was relatively low, it was accompanied by a high dispersion, as shown by its standard deviation values. This dispersion, however, is somewhat expected, given that our data included several types and heights of jumps, performed with no restriction to arm movements. Nevertheless, we have opted to include this wide range of movement patterns in order to increase the external validity of the equations, conferring them with a greater usability, without, for example, the need for different models for different kinds of jumps, which would hinder the application of the models to real-world data.

Bone increases its mass and optimizes its geometry and microarchitecture in response to adequate mechanical stimulation [1,2], particularly of high magnitude [39,40]. These types of high-intensity impact activities have been shown to be more strongly associated with bone health improvements, even if they are only performed in small volumes throughout the day. In fact, Vainionpää et al. [39] demonstrated that performing a relatively low number (<100) of impacts with pACC above 4.9 g daily is positively associated with increases in bone mineral density. Usually, this acceleration magnitude can be achieved only by specific movements, such as jumps [16,39]. Nevertheless, accelerometry-based mechanical loading regression models have mostly been validated for a set of activities such as walking and running, which elicit relatively low acceleration magnitudes [18,21,22]. The results of our study provide new mechanical loading prediction models for jumping, which is noteworthy because jumping is one of the most popular and effective exercises prescribed for bone health improvement [41], but also one that could increase the risk of fracture in patients with severe osteoporosis and bone fragility. Therefore, it is crucial to develop strategies that can adequately monitor the mechanical loading associated with this activity.

The development of such models was performed with the direct purpose of assessing the loading sustained by the skeletal system during daily physical activity. To date, physical activity monitoring and exercise prescription aiming for bone health promotion have largely been carried out almost blindly or through the use of subjective instruments such as questionnaires. Moreover, the absence of a trustworthy method to monitor daily mechanical loading may preclude the prescription and self-involvement of patients in high-impact activities that may expose them to a higher risk of musculoskeletal injuries. These issues may be overcome with the recent popularization of wearable sensors, such as accelerometers, and their ability to be used as a tool for mechanical loading prediction. This would allow some important clinical applications, as the models developed in this study—when used in combination with other prediction equations for other types of activities [22]—can

be used to fully analyze the mechanical loading spectrum to which people are subjected daily and relate this information with bone health parameters. Therefore, a more complete understanding can be achieved as to how mechanical loading influences bone health by, for instance, identifying the loading volume and magnitude range that are more efficient in inducing bone health benefits. Moreover, the development and distribution of an R package that automates the steps necessary to apply these models enhances their applicability to potential users [16]. This can prove to be an important tool, as the application of these models depends on several laborious steps—such as the application of digital filters to reduce noise from the signal, the detection of the peaks in this signal, and the computation of derivatives to obtain the acceleration rate—necessary for the pRL prediction.

In our protocol, three accelerometer placements (ankle, lower back, and hip) and two vectors (resultant and vertical) were tested. Overall, the prediction models' performance was reasonably consistent among the different placement and vector combinations, allowing some conclusions to be drawn. First, the hip accelerometer placement, which has traditionally been widely employed in research for the direct measurement of physical activity intensity [42], yielded a slightly better accuracy compared to the other placements tested. This is useful considering that previous data collected from hip-worn accelerometers for other purposes can be adequately reanalyzed to obtain mechanical loading predictions. Furthermore, studies that aim to extract mechanical loading together with other variables derived from accelerometry data, and that use the hip as the default accelerometer placement, can reliably use this placement. Second, as the magnitude of the resultant vectors of both pGRF and pLR in the activities that were tested is derived mostly from the vertical vector, and there were no considerable differences in performance between models using both vectors, they can be used interchangeably to predict mechanical loading. In addition, while models using data from the vertical vector allow the use of uniaxial accelerometers, data derived from the resultant vector have the important advantage of not depending on the correct orientation of the accelerometer's axes, which cannot be guaranteed during data collection in free-living conditions [43].

Although the models presented in this study proved to be valid, some limitations ought to be considered. First, the choice of activity to elicit high-impact loading was jumping, and several combinations of jump type and height were tested. Nevertheless, the results presented here cannot be assured for other high-impact activities, or even for other types of jumps that were not tested. Second, no external sample for model validation was recruited. However, the leave-one-out cross-validation method that was used is the recommended strategy in these situations [33]. Third, to apply these models in accelerometer-recorded free-living physical activity data, there would be a need to identify the periods in the acceleration signal in which the activity being performed is jumping. Therefore, other methods for physical activity pattern detection based on accelerometer data, such as the models developed by Wang et al. [44], should be used in combination with these models to allow accurate prediction. Finally, as the jumps were always performed in the same order, the subjects may have experienced fatigue, especially in the last few trials, which could have led to changes in their jumping movement patterns.

In conclusion, accelerometry-based mechanical loading prediction models, especially for pGRF, have proven to be a valid method for determining the mechanical stimulation induced by jumps of various types and heights. These prediction models were validated using data from both the resultant and vertical vectors and with accelerometers placed at the ankle, lower back, and hip. The results from this study will enable the continuous assessment of mechanical loading in clinical settings, providing a means to objectively determine the osteogenic potential of daily physical activity and to better monitor and prescribe exercise aimed to improve bone health. Compared to pGRF, the prediction of pLR showed lower accuracy.

Supplementary Materials: The following supporting information can be downloaded at: https://www.mdpi.com/xxx/s1, Figure S1: Distribution of the vertical vector of mechanical loading (peak ground reaction force on Panel A and peak loading rate on Panel B) and acceleration (peak acceleration on Panel C and peak acceleration rate on Panel D) variables per jump type and height combination. Abbreviations: BW, body weight; pACC, peak acceleration; pAR, peak acceleration rate; pGRF, peak ground reaction force; pLR, peak loading rate; Figure S2: Bland-Altman plots showing agreement between actual and predicted peak ground reaction force for accelerometers worn at ankle (Panels A and D), lower back (Panels B and E) and hip (Panels C and F), for both the resultant vector (Panels A to C) and its vertical component (Panels D to F). Continuous thick lines show bias (average of the differences between actual and predicted values) while dashed lines show the limits of agreement (bias ± 1.96 standard deviation). Abbreviations: pGRF, peak ground reaction force; Figure S3: Bland-Altman plots showing agreement between actual and predicted peak loading rate for accelerometers worn at ankle (Panels A and D), lower back (Panels B and E) and hip (Panels C and F), for both the resultant vector (Panels A to C) and its vertical component (Panels D to F). Continuous thick lines show bias (average of the differences between actual and predicted values) while dashed lines show the limits of agreement (bias ± 1.96 standard deviation). Abbreviations: pLR, peak loading rate.

Author Contributions: Conceptualization: L.V., F.D.-S., G.B., V.D., H.S.-S., J.P., L.M., J.P.V.-B., J.O. and H.F.; Methodology: L.V., F.D.-S., G.B., V.D., H.S.-S., J.P., L.M., J.P.V.-B., J.O. and H.F; Software: L.V. and L.M.; Formal Analysis: L.V. and F.D.-S.; Investigation: L.V., F.D.-S., G.B., V.D., H.S.-S., J.P., L.M., J.P.V.-B., J.O. and H.F.; Writing—Original Draft: L.V., F.D.-S. and H.F.; Writing—Review and Editing: L.V., F.D.-S., G.B., V.D., H.S.-S., J.P., L.M., J.P.V.-B., J.O. and H.F. All authors have read and agreed to the published version of the manuscript.

Funding: This study was funded by the Foundation for Science and Technology (FCT) (grant number PTDC/DTP-DES/0968/2014) and by the European Regional Development Fund (ERDF) through the Operational Competitiveness Programme (COMPETE) (grant number POCI-01-0145-FEDER-016707). The study was developed in the Research Centre in Physical Activity, Health, and Leisure (CIAFEL) funded by the ERDF through the COMPETE and by the FCT (grant number UID/DTP/00617/2020), and in the Laboratory for Integrative and Translational Research in Population Health (ITR), funded by the FCT (grant number LA/P/0064/2020). L.V., F.D.-S., and G.B. are supported by the FCT (grant numbers UI/BD/150673/2020, SFRH/BD/117622/2016, and SFRH/BD/146976/2019).

Institutional Review Board Statement: The study was conducted in accordance with the Declaration of Helsinki, and approved by the Ethics Committee of the Centro Hospitalar Universitário de São João (protocol code CES 192-14, approved on 13 May 2015).

Informed Consent Statement: Informed consent was obtained from all subjects involved in the study.

Data Availability Statement: The data presented in this study are available on request from the corresponding author.

Acknowledgments: The authors thank the participants who took part in this research and all who have collaborated in the research project.

Conflicts of Interest: The authors declare no conflict of interest.

References

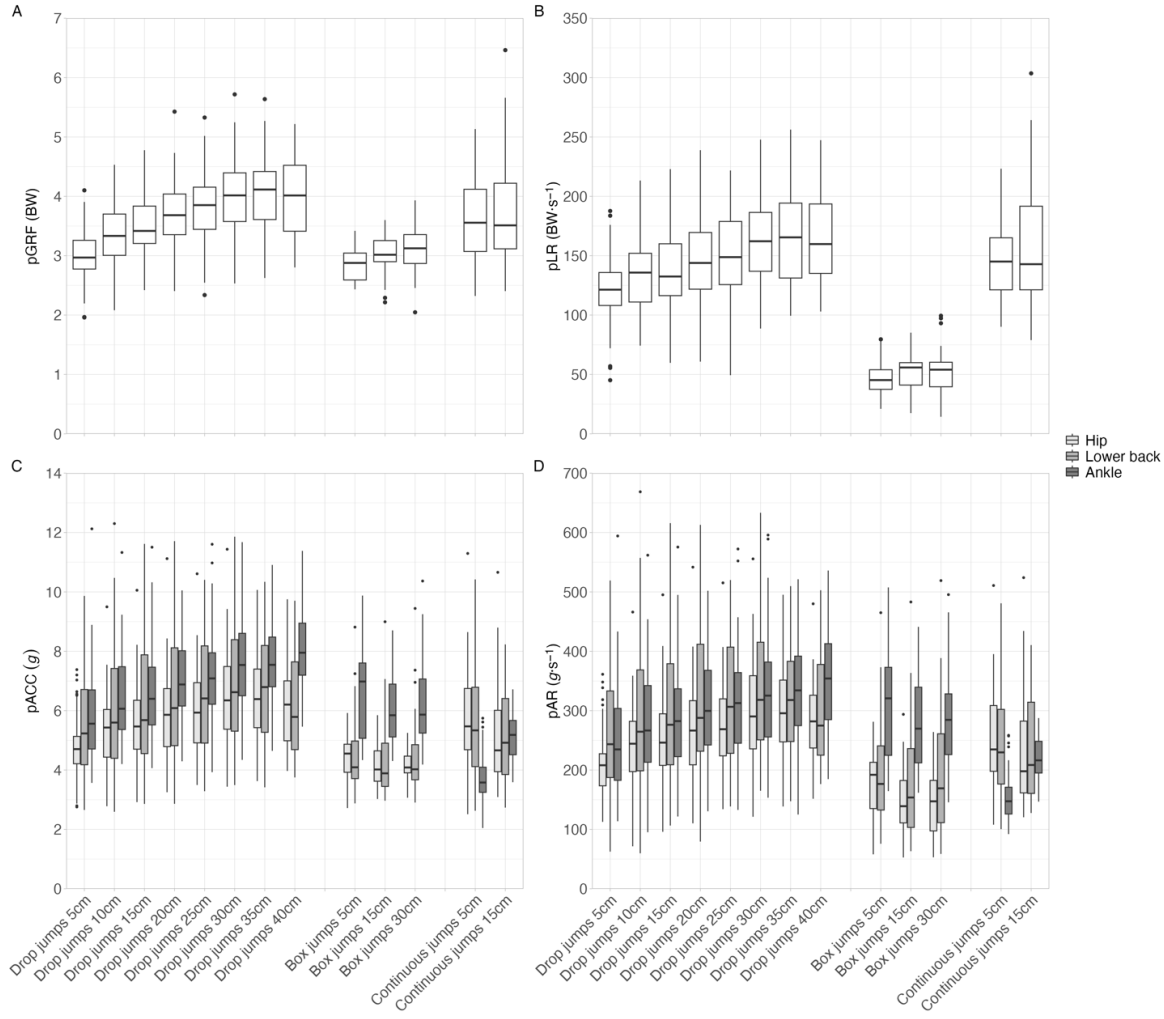
1. Turner, C.H.; Robling, A.G. Designing exercise regimens to increase bone strength. *Exerc. Sport Sci. Rev.* **2003**, *31*, 45–50. [CrossRef]
2. Fonseca, H.; Moreira-Goncalves, D.; Coriolano, H.J.; Duarte, J.A. Bone quality: The determinants of bone strength and fragility. *Sport. Med.* **2014**, *44*, 37–53. [CrossRef]
3. Santos, L.; Elliott-Sale, K.J.; Sale, C. Exercise and bone health across the lifespan. *Biogerontology* **2017**, *18*, 931–946. [CrossRef] [PubMed]
4. Kohrt, W.M.; Bloomfield, S.A.; Little, K.D.; Nelson, M.E.; Yingling, V.R. Physical activity and bone health. *Med. Sci. Sport. Exerc.* **2004**, *36*, 1985–1996. [CrossRef] [PubMed]
5. Burr, D.B.; Robling, A.G.; Turner, C.H. Effects of biomechanical stress on bones in animals. *Bone* **2002**, *30*, 781–786. [CrossRef]
6. Turner, C.H. Three rules for bone adaptation to mechanical stimuli. *Bone* **1998**, *23*, 399–407. [CrossRef]
7. Turner, C.H.; Robling, A.G. Mechanisms by which exercise improves bone strength. *J. Bone Miner. Metab.* **2005**, *23*, 16–22. [CrossRef]

8. Nikander, R.; Kannus, P.; Rantalainen, T.; Uusi-Rasi, K.; Heinonen, A.; Sievänen, H. Cross-sectional geometry of weight-bearing tibia in female athletes subjected to different exercise loadings. *Osteoporos. Int.* **2010**, *21*, 1687–1694. [CrossRef] [PubMed]
9. Groothausen, J.; Siemer, H.; Kemper, H.C.G.; Twisk, J.; Welten, D.C. Influence of peak strain on lumbar bone mineral density: An analysis of 15-year physical activity in young males and females. *Pediatr. Exerc. Sci.* **1997**, *9*, 159–173. [CrossRef]
10. Weeks, B.K.; Beck, B.R. The BPAQ: A bone-specific physical activity assessment instrument. *Osteoporos. Int.* **2008**, *19*, 1567–1577. [CrossRef] [PubMed]
11. Farr, J.N.; Lee, V.R.; Blew, R.M.; Lohman, T.G.; Going, S.B. Quantifying bone-relevant activity and its relation to bone strength in girls. *Med. Sci. Sport. Exerc.* **2011**, *43*, 476–483. [CrossRef]
12. Kim, S.J.; So, W.Y.; Kim, J.; Sung, D.J. Relationship between bone-specific physical activity scores and measures for body composition and bone mineral density in healthy young college women. *PLoS ONE* **2016**, *11*, e0162127. [CrossRef]
13. Kim, S.J.; Baker, B.S.; Sharma-Ghimire, P.; Bemben, D.A.; Bemben, M.G. Association between bone-specific physical activity scores and pQCT-derived measures of bone strength and geometry in healthy young and middle-aged premenopausal women. *Arch. Osteoporos.* **2018**, *13*, 83. [CrossRef]
14. Medved, V. *Measurement of Human Locomotion*; CRC Press: London, UK, 2000.
15. Elvin, N.G.; Elvin, A.A.; Arnoczky, S.P. Correlation between ground reaction force and tibial acceleration in vertical jumping. *J. Appl. Biomech.* **2007**, *30*, 75–81. [CrossRef] [PubMed]
16. Rowlands, A.V.; Stiles, V.H. Acceleration counts and raw acceleration output in relation to mechanical loading. *J. Biomech.* **2012**, *45*, 448–454. [CrossRef] [PubMed]
17. Neugebauer, J.M.; Hawkins, D.A.; Beckett, L. Estimating youth locomotion ground reaction forces using an accelerometer-based activity monitor. *PLoS ONE* **2012**, *7*, e48182. [CrossRef] [PubMed]
18. Neugebauer, J.M.; Collins, K.H.; Hawkins, D.A. Ground reaction force estimates from ActiGraph GT3X+ hip accelerations. *PLoS ONE* **2014**, *9*, e99023. [CrossRef] [PubMed]
19. Fortune, E.; Morrow, M.M.B.; Kaufman, K.R. Assessment of gait kinetics using tri-axial accelerometers. *J. Appl. Biomech.* **2014**, *30*, 668–674. [CrossRef] [PubMed]
20. Neugebauer, J.M.; LaFiandra, M. Predicting ground reaction force from a hip-borne accelerometer during load carriage. *Med. Sci. Sport. Exerc.* **2018**, *50*, 2369–2374. [CrossRef]
21. Veras, L.; Diniz-Sousa, F.; Boppre, G.; Devezas, V.; Santos-Sousa, H.; Preto, J.; Vilas-Boas, J.P.; Machado, L.; Oliveira, J.; Fonseca, H. Accelerometer-based prediction of skeletal mechanical loading during walking in normal weight to severely obese subjects. *Osteoporos. Int.* **2020**, *31*, 1239–1250. [CrossRef]
22. Veras, L.; Diniz-Sousa, F.; Boppre, G.; Resende-Coelho, A.; Moutinho-Ribeiro, E.; Devezas, V.; Santos-Sousa, H.; Preto, J.; Vilas-Boas, J.P.; Machado, L.; et al. Mechanical loading prediction through accelerometry data during walking and running. *Eur. J. Sport Sci.* **2022**. *online ahead of print*. [CrossRef] [PubMed]
23. Komaris, D.; Pérez-Valero, E.; Jordan, L.; Barton, J.; Hennessy, L.; O´Flynn, B.; Machado, G. Predicting three-dimensional ground reaction forces in running by using artificial neural networks and lower body kinematics. *IEEE Access* **2019**, *7*, 156779–156786. [CrossRef]
24. Sharma, D.; Davidson, P.; Müller, P.; Piché, R. Indirect estimation of vertical ground reaction force from a body-mounted INS/GPS using machine learning. *Sensors* **2021**, *21*, 1553. [CrossRef] [PubMed]
25. Alcantara, R.S.; Edwards, W.B.; Millet, G.Y.; Grabowski, A.M. Predicting continuous ground reaction forces from accelerometers during uphill and downhill running: A recurrent neural network solution. *PeerJ* **2022**, *10*, e12752. [CrossRef] [PubMed]
26. Du, J.; Hartley, C.; Brooke-Wavell, K.; Paggiosi, M.A.; Walsh, J.S.; Li, S.; Lin, S. High-impact exercise stimulated localized adaptation of microarchitecture across distal tibia in postmenopausal women. *Osteoporos. Int.* **2021**, *32*, 907–919. [CrossRef] [PubMed]
27. Allison, S.; Poole, K.E.; Treece, G.M.; Gee, A.H.; Tonkin, C.; Rennie, W.J.; Folland, J.P.; Summers, G.D.; Brooke-Wavell, K. The influence of high-impact exercise on cortical and trabecular bone mineral content and 3D distribution across the proximal femur in older men: A randomized controlled unilateral intervention. *J. Bone Miner. Res.* **2015**, *30*, 1709–1716. [CrossRef]
28. Hansford, H.J.; Wewege, M.A.; Cashin, A.G.; Hagstrom, A.D.; Clifford, B.K.; McAuley, J.H.; Ortega, F. If exercise is medicine, why don't we know the dose? An overview of systematic reviews assessing reporting quality of exercise interventions in health and disease. *Br. J. Sport. Med.* **2022**, *56*, 692–700. [CrossRef]
29. White, M.G.E.; Bezodis, N.E.; Neville, J.; Summers, H.; Rees, P. Determining jumping performance from a single body-worn accelerometer using machine learning. *PLoS ONE* **2022**, *17*, e0263846. [CrossRef]
30. National Health and Nutrition Examination Survey. National Health and Nutrition Examination Survey (NHANES) Anthropometry Procedures Manual. Center for Disease Control and Prevention. 2017. Available online: https://wwwn.cdc.gov/nchs/data/nhanes/2017-2018/manuals/2017_Anthropometry_Procedures_Manual.pdf (accessed on 31 October 2022).
31. Field, A.; Miles, J.; Field, Z. *Discovering Statistics Using R*, 1st ed.; SAGE: London, UK, 2012.
32. Nakagawa, S.; Schielzeth, H. A general and simple method for obtaining R2 from generalized linear mixed-effects models. *Methods Ecol. Evol.* **2013**, *4*, 133–142. [CrossRef]
33. Staudenmayer, J.; Zhu, W.; Catellier, D.J. Statistical considerations in the analysis of accelerometry-based activity monitor data. *Med. Sci. Sport. Exerc.* **2012**, *44* (Suppl. 1), S61–S67. [CrossRef]

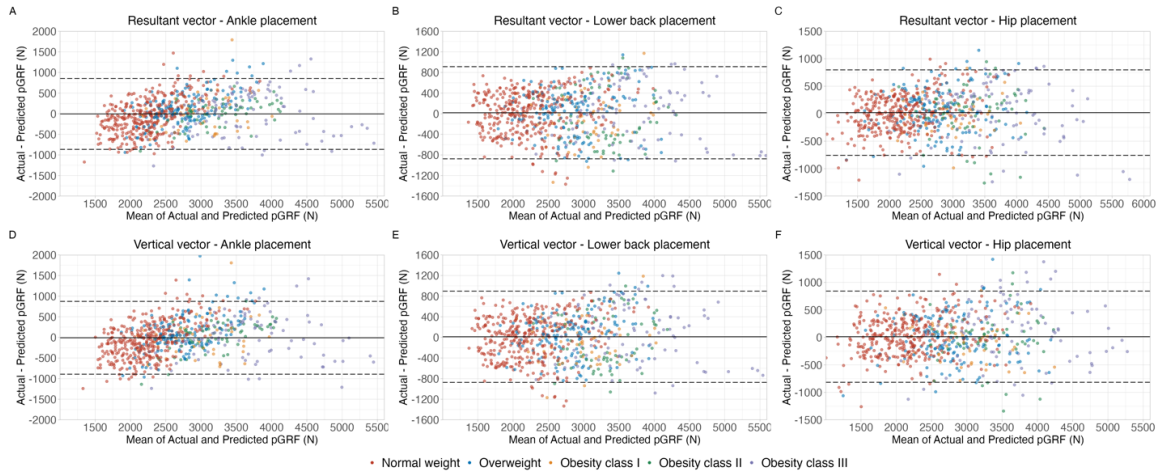
34. Bland, J.M.; Altman, D.G. Statistical methods for assessing agreement between two methods of clinical measurement. *Lancet* **1986**, *327*, 307–310. [CrossRef]
35. Giavarina, D. Understanding Bland Altman analysis. *Biochem. Med.* **2015**, *25*, 141–151. [CrossRef] [PubMed]
36. Veras, L. impactr: An R Package to Process Raw Accelerometer Data Related to Mechanical Loading. 2021. Available online: https://zenodo.org/record/5035523#.Y-ytp3ZBxPY (accessed on 31 October 2022).
37. Diniz-Sousa, F.; Veras, L.; Ribeiro, J.C.; Boppre, G.; Devezas, V.; Santos-Sousa, H.; Preto, J.; Machado, L.; Vilas-Boas, J.P.; Oliveira, J.; et al. Accelerometry calibration in people with class II-III obesity: Energy expenditure prediction and physical activity intensity identification. *Gait Posture* **2020**, *76*, 104–109. [CrossRef] [PubMed]
38. Liikavainio, T.; Bragge, T.; Hakkarainen, M.; Jurvelin, J.S.; Karjalainen, P.A.; Arokoski, J.P. Reproducibility of loading measurements with skin-mounted accelerometers during walking. *Arch. Phys. Med. Rehabil.* **2007**, *88*, 907–915. [CrossRef] [PubMed]
39. Vainionpää, A.; Korpelainen, R.; Vihriälä, E.; Rinta-Paavola, A.; Leppäluoto, J.; Jämsä, T. Intensity of exercise is associated with bone density change in premenopausal women. *Osteoporos. Int.* **2006**, *17*, 455–463. [CrossRef] [PubMed]
40. Stiles, V.H.; Metcalf, B.S.; Knapp, K.M.; Rowlands, A. A small amount of precisely measured high-intensity habitual physical activity predicts bone heath in pre- and post-menopausal women in UK Biobank. *Int. J. Epidemiol.* **2017**, *46*, 1847–1856. [CrossRef] [PubMed]
41. Beck, B.R.; Daly, R.M.; Singh, M.A.F.; Taaffe, D.R. Exercise and sports science australia (ESSA) position statement on exercise prescription for the prevention and management of osteoporosis. *J. Sci. Med. Sport* **2017**, *20*, 438–445. [CrossRef]
42. Migueles, J.H.; Cadenas-Sanchez, C.; Ekelund, U.; Delisle Nyström, C.; Mora-Gonzalez, J.; Löf, M.; Labayen, I.; Ruiz, J.R. Accelerometer data collection and processing criteria to assess physical activity and other outcomes: A systematic review and practical considerations. *Sport. Med.* **2017**, *47*, 1821–1845. [CrossRef]
43. Welk, G.J. Principles of design and analyses for the calibration of accelerometry-based activity monitors. *Med. Sci. Sport. Exerc.* **2005**, *37*, S501–S511. [CrossRef]
44. Wang, J.; Chen, R.; Sun, X.; She, M.F.H.; Wu, Y. Recognizing human daily activities from accelerometer signal. *Procedia Eng.* **2011**, *15*, 1780–1786. [CrossRef]

Disclaimer/Publisher's Note: The statements, opinions and data contained in all publications are solely those of the individual author(s) and contributor(s) and not of MDPI and/or the editor(s). MDPI and/or the editor(s) disclaim responsibility for any injury to people or property resulting from any ideas, methods, instructions or products referred to in the content.

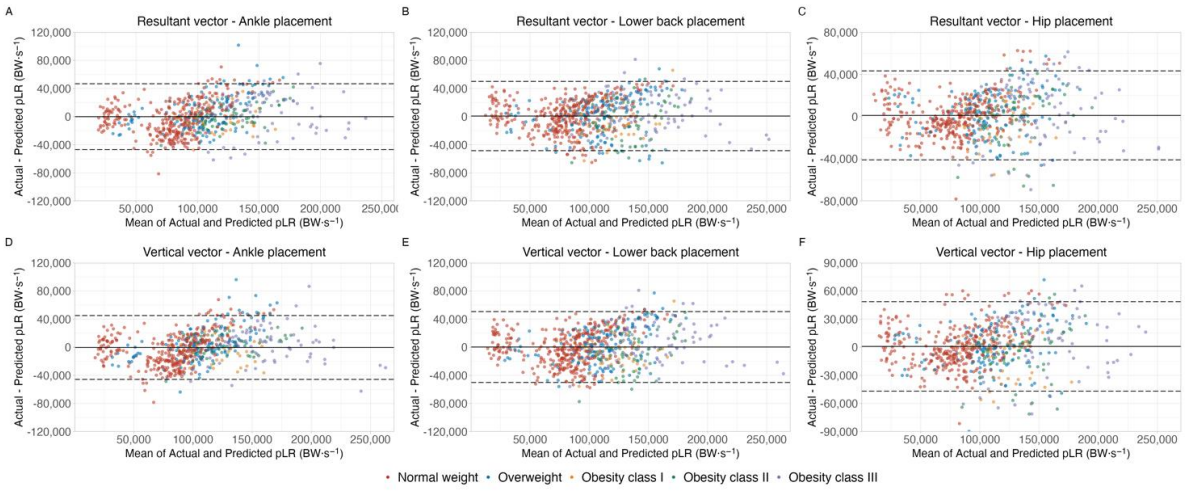
Supplemental Material



Supplemental Figure S1. Distribution of the vertical vector of mechanical loading (peak ground reaction force on Panel A and peak loading rate on Panel B) and acceleration (peak acceleration on Panel C and peak acceleration rate on Panel D) variables per jump type and height combination. Abbreviations: BW, body weight; pACC, peak acceleration; pAR, peak acceleration rate; pGRF, peak ground reaction force; pLR, peak loading rate.



Supplemental Figure S2. Bland-Altman plots showing agreement between actual and predicted peak ground reaction force for accelerometers worn at ankle (Panels A and D), lower back (Panels B and E) and hip (Panels C and F), for both the resultant vector (Panels A to C) and its vertical component (Panels D to F). Continuous thick lines show bias (average of the differences between actual and predicted values) while dashed lines show the limits of agreement (bias ± 1.96 standard deviation). Abbreviations: pGRF, peak ground reaction force.



Supplemental Figure S3. Bland-Altman plots showing agreement between actual and predicted peak loading rate for accelerometers worn at ankle (Panels A and D), lower back (Panels B and E) and hip (Panels C and F), for both the resultant vector (Panels A to C) and its vertical component (Panels D to F). Continuous thick lines show bias (average of the differences between actual and predicted values) while dashed lines show the limits of agreement (bias ± 1.96 standard deviation). Abbreviations: pLR, peak loading rate.

3.4. Study 3

Veras L, Oliveira D, Diniz-Sousa F, Boppre B, Resende-Coelho A, Oliveira J, Fonseca H. External validation of accelerometry based mechanical loading prediction equations. *Applied Sciences*. 2024 Nov 8; 14(22):10292. doi: 10.3390/app142210292

applied sciences

MDPI

Article

External Validation of Accelerometry-Based Mechanical Loading Prediction Equations

Lucas Veras [1,2], Daniela Oliveira [1,2], Florêncio Diniz-Sousa [1,2], Giorjines Boppre [1,2], Ana Resende-Coelho [1,2], José Oliveira [1,2] and Hélder Fonseca [1,2,*]

[1] Research Center in Physical Activity, Health and Leisure (CIAFEL), Faculty of Sport, University of Porto, 4200-450 Porto, Portugal; lucasdsveras@gmail.com (L.V.); ana.dan.oliveira@hotmail.com (D.O.); joseflorenciosousa@gmail.com (F.D.-S.); giorjines_boppre@hotmail.com (G.B.); anccatarina@gmail.com (A.R.-C.); joliveira@fade.up.pt (J.O.)

[2] Laboratory for Integrative and Translational Research in Population Health (ITR), University of Porto, 4200-450 Porto, Portugal

* Correspondence: hfonseca@fade.up.pt

Abstract: Accurately predicting physical activity-associated mechanical loading is crucial for developing and monitoring exercise interventions that improve bone health. While accelerometer-based prediction equations offer a promising solution, their external validity across different populations and activity contexts remains unclear. This study aimed to validate existing mechanical loading prediction equations by applying them to a sample and testing conditions distinct from the original validation studies. A convenience sample of 49 adults performed walking, running, and jumping activities on a force plate while wearing accelerometers at their hip, lower back, and ankle. Peak ground reaction force (pGRF) and peak loading rate (pLR) predictions were assessed for accuracy. Substantial variability in prediction accuracy was found, with pLR showing the highest errors. These findings highlight the need to improve prediction models to account for individual biomechanical differences, sensor placement, and high-impact activities. Such refinements are essential for ensuring the models' reliability in real-world applications, particularly in clinical and biomechanical research contexts, where accurate assessments of mechanical loading are critical for designing rehabilitation programs, injury prevention strategies, and optimizing bone health interventions.

Keywords: ground reaction force; loading rate; accelerometers; validation; biomechanics

check for updates

Citation: Veras, L.; Oliveira, D.; Diniz-Sousa, F.; Boppre, G.; Resende-Coelho, A.; Oliveira, J.; Fonseca, H. External Validation of Accelerometry-Based Mechanical Loading Prediction Equations. *Appl. Sci.* **2024**, *14*, 10292. https://doi.org/10.3390/app142210292

Academic Editor: Ana Martins Amaro

Received: 26 September 2024
Revised: 19 October 2024
Accepted: 7 November 2024
Published: 8 November 2024

Copyright: © 2024 by the authors. Licensee MDPI, Basel, Switzerland. This article is an open access article distributed under the terms and conditions of the Creative Commons Attribution (CC BY) license (https://creativecommons.org/licenses/by/4.0/).

1. Introduction

Physical activity and exercise are among the main factors that induce mechanical loading on bones, which is essential for maintaining and enhancing bone health [1,2]. Engaging in regular weight-bearing activities, such as vigorous walking, running, and jumping [2,3], stimulates bone formation, increases bone mass, and improves bone geometry and microarchitecture [4,5], thereby reducing the risk of osteoporosis and bone fractures [1,6]. These beneficial adaptations occur due mostly to the mechanical forces exerted on bone tissue during physical activity, which are detected by osteocytes and osteoblasts [7] that trigger adaptive signaling responses [8], stimulating bone remodeling and, ultimately, contributing to strengthening bone structure. Accurately measuring these forces is essential for developing effective and safe exercise interventions to enhance bone health and prevent bone loss-related disorders such as osteopenia and osteoporosis [1–3,9], but has been a major challenge to address [10].

Traditionally, mechanical loading has been measured using laboratory-based methods such as force plates, which are considered the gold standard [11]. While these methods provide precise and accurate measurements of ground reaction forces, they are limited by their high cost, the need for specialized equipment and expertise, and their restriction to controlled laboratory environments. More recently, questionnaires have been introduced

to estimate mechanical loading [12], but they are subject to recall bias and cannot provide objective data on the intensity and frequency of physical activities [13–15]. Accelerometer-based prediction equations have emerged as a promising alternative to address these limitations [16–21], offering the advantages of portability, lower cost, and the ability to collect data in free-living conditions [22,23].

Accelerometer-based equations have been developed to predict mechanical loading variables such as peak ground reaction forces (pGRF) and peak loading rate (pLR) from acceleration data [16–21]. These equations have shown potential in various populations and activities, but they are often validated only within the specific contexts of their original studies. Importantly, factors such as sample characteristics, activity type, and testing conditions can exert a major influence on the performance of these models [24]. Individual variability in characteristics such as age [25], gender [25], and BMI [26] can significantly impact the accuracy of these predictions, as these factors influence biomechanical aspects (e.g., gait patterns, center of mass, balance) that can change how the load is borne by the body. Therefore, it is crucial to evaluate the external validation of accelerometer-based equations by testing them on different populations and in diverse activity contexts. Doing so not only uncovers their limitations but also assesses their reliability in real-world scenarios, guiding their refinement and ensuring their effective application in clinical settings to improve bone health interventions. This study aims to validate mechanical loading prediction equations by testing their prediction accuracy against a different sample and testing conditions than those used in the original validation studies, in order to assess their external validation. We tested all previously published equations that could be applied to our data, specifically those using raw accelerometer data from the right hip, lower back, or right ankle, and designed to predict mechanical loading during walking, running, and/or jumping.

2. Materials and Methods

2.1. Participants

A sample of 49 adults, recruited by convenience, participated in this study (26 males; 29.6 ± 9.6 years; 169.1 ± 8.7 cm; 69.6 ± 11.3 kg; 24.3 ± 3.0 kg·m^{-2}; $\overline{X}$ ± SD). Participant recruitment was carried out by means of a University of Porto academic community mailing list with information about the study's objectives, testing protocol, and inclusion and exclusion criteria. Height and body mass were assessed using a stadiometer (model 213; Seca, Hamburg, Germany) and a digital scale (model 899; Seca, Hamburg, Germany), respectively. Inclusion criteria included age between 18 and 65 years and being capable of performing the activities involved in the trials, which included walking, running, and several types of jumping. Exclusion criterion included the presence of any injury or condition that could preclude participation in the experimental exercises, such as musculoskeletal disorders and cardiovascular diseases. All participants were informed about the purpose of the study and activities protocol before giving written informed consent. The study protocol was approved by the local Ethics Committee (CEFADE 15-21).

2.2. Protocol

Data collection was conducted at the Porto Laboratory of Biomechanics (LABIOMEP-UP). Ground reaction force data were collected using five force plates embedded in the floor: three FP4060 (Bertec, Columbus, OH, USA) and two FP6090 (Bertec, Columbus, OH, USA).

During data collection, participants wore three activity monitors (GT9X Link: 100 Hz, ±16 g range; ActiGraph, Pensacola, FL, USA): one placed at the right hip (along the anterior axillary line at the level of the iliac crest), one at the lower back (at the midpoint between the two posterior superior iliac spines), and one at the right ankle (immediately superior to the lateral malleolus). Accelerometer placements at the waist line (right hip and lower back) were selected for their proximity to the body's center of mass, providing a representative measure of overall movement. Right hip placement was chosen due to its widespread use in research involving physical activity measurement with accelerometers. The placement

at the right ankle was selected due to its closeness to the ground contact point, allowing it to capture impact forces during the activities. Hip and lower back accelerometers were securely fastened with clips on an elastic belt, while the ankle accelerometer was held in place with adhesive tape and an elastic belt. The researchers positioned the accelerometers in order to ensure their correct positioning and orientation.

The protocol included data collection during walking, running, and jumping activities. For walking and running, a 10 m path was marked on the laboratory floor, including the force plates in its center. Participants performed normal, slow, and fast walking, followed by slow and fast running, always with a self-selected speed. Three valid attempts were collected for each condition, with a 30 s rest between the walking trials and 1 min between the running trials. Attempts were considered valid if the participant's foot landed entirely on at least one force plate, without stepping on its borders. Participants were not informed about the force plate placement, nor of the necessity to completely step on them during each trial, to avoid altering their natural movement patterns during walking and running.

Participants also completed a series of jumping trials, starting with two types of jumps using a 30 cm high box: (i) drop jumps (from the box to the floor) and (ii) box jumps (from the floor to the box). Then, they performed countermovement jumps with and without arm movements (hands on hips for the latter), horizontal forward jumps (from the floor to the platform and vice versa), side hops (multiple lateral jumps between two force plates, with either both legs together or landing with one foot on each platform), and continuous jumps (starting from a standing position with feet hip-width apart, at two heights: approximately 5 cm for 10–15 repetitions and approximately 15 cm for 5 repetitions). Three valid trials were recorded for drop, box, countermovement, and horizontal forward jumps, while multiple jumps were tested for side hops and continuous jumps. A 1 min rest interval was applied between the jumping trials.

Activity monitors incorporated built-in primary and secondary triaxial accelerometers, with the primary having a dynamic range of ± 8 g and a proprietary filter and the secondary having a dynamic range of ± 16 g with unfiltered data. To avoid filtering bias and increase accuracy and replicability, only data from the secondary accelerometer were used. Data from force plates (Qualysis Track Manager, version QTM 2021.1; Qualysis AB, Gothenburg, Sweden) and accelerometers (ActiLife, version 6.13.3; Actigraph, Pensacola, USA) were processed with the manufacturer's software and exported as raw x, y, and z vector data. Ground reaction forces were reported in Newtons (N), and acceleration in units of gravitational acceleration (1 g = 9.807 $m \cdot s^{-2}$).

2.3. Data Processing

Force plate and accelerometer data were processed using MATLAB (version 2022a; MathWorks, Natick, MA, USA). Due to differing sampling frequencies (1000 Hz for the force plates and 100 Hz for the activity monitor), resampling was necessary. To attenuate noise, data were filtered using a Butterworth fourth-order low-pass filter with a 20 Hz cut-off frequency, determined through Fast Fourier Transform (FFT) and visual examination of the signal's frequency spectrum. The resultant vectors for ground reaction force and acceleration ($r_i = \sqrt{x_i^2 + y_i^2 + z_i^2}$) were calculated. Afterwards, both ground reaction force and acceleration signals were adjusted by their timestamp and synchronized through the maximum cross-correlation coefficient. Then, the signals were visually inspected for confirmation, and the synchronization was manually adjusted, if necessary.

Walking and running peak acceleration were identified based on two criteria: They had to exceed the average acceleration measured in the trial by at least 1 standard deviation (SD), with a minimum gap of 0.2 s between peaks. For drop, box, countermovement, and horizontal forward jumps, peak acceleration was determined as a minimum height of 2 SD above the mean acceleration and a separation of at least 0.4 s. Finally, for the side hops and continuous jumps, peak acceleration was identified by a minimum height of 2 SD above the mean acceleration and by a separation of at least 0.3 s. The peak ground reaction force was defined as the highest ground reaction force value within 0.1 s before and after each peak acceleration.

Rates of change were computed using a centered derivative, and peak loading rate and peak acceleration rate were defined as the maximum values in the array. For each movement type and accelerometer placement, mean values of peak ground reaction force, peak acceleration, peak loading rate, and peak acceleration rate for the resultant vector and its vertical component were obtained and used in all following analyses.

2.4. Statistical Analyses

The statistical analyses were performed using the R software (version 4.3.2; R Foundation for Statistical Computing, Vienna, Austria). The models selected to be tested in this study were as follows: Veras et al., 2022 [20] and Neugebauer et al., 2014 [17] for walking and running, and Veras et al., 2023 [21] for jumping. We predicted all mechanical loading variables from these studies, using the reported model coefficients, on our data. For the studies from Veras et al., 2022 [20] and Veras et al., 2023 [20], pGRF and pLR were predicted using the resultant vector and the vertical component on hip, lower back, and ankle accelerometers. For the study from Neugebauer et al., 2014 [17], only vertical pGRF using the hip accelerometer was predicted, as it was the only equation from their study that could be used with our data. The study from Veras et al., 2022 [20] included walking and running on a force plate-instrumented treadmill, at 13 speeds, ranging from 2 to 14 km·h^{-1} (with 1 km·h^{-1} increments). Neugebauer et al., 2014 [17] tested walking and running on a 15 m straight path that included a force plate, with between 8 and 10 walking and 8 and 10 running self-selected speeds. Veras et al., 2023 [21] tested several heights of drop jumps, box jumps, and continuous jumps.

Accuracy indices, including mean absolute error (MAE), mean absolute percent error (MAPE), and root mean square error (RMSE), were computed. Bland–Altman plots were used to visually analyze agreement between predicted and measured values, with bias and limits of agreement calculated and plotted.

3. Results

Table 1 shows the characteristics of the participants from the studies by Veras et al., 2022 [20], Neugebauer et al., 2014 [17], and Veras et al., 2023 [21]. The studies by Veras et al., 2022 [20] and Veras et al., 2023 [21] involved a larger and older population compared to the study by Neugebauer et al., 2014 [17], which had a younger sample with a lower average body mass index. The diversity in sample characteristics across these studies shows the variability in the populations used to validate mechanical loading prediction equations.

Table 1. Sample characteristics of the Veras et al. (2022) [20], Neugebauer et al. (2014) [17], and Veras et al. (2023) [21] studies.

	Veras et al. (2022) [20]	**Neugebauer et al. (2014) [17]**	**Veras et al. (2023) [21]**
	(52 females, 79 males)	(20 females, 19 males)	(51 females, 27 males)
Age (years)	32.0 ± 11.2	21.2 ± 1.3	35.6 ± 11.6
Height (m)	1.65 ± 0.09	1.73 ± 0.12	1.63 ± 0.09
Mass (kg)	76.9 ± 19.6	67.6 ± 11.5	82.4 ± 20.6
BMI (kg·m^{-2})	28.5 ± 81	22.5 ± 2.3	31.3 ± 8.7

Data presented as mean ± standard deviation. Abbreviations: BMI, body mass index.

3.1. Accuracy of pGRF and pLR Predictions for Walking and Running Using the Veras et al., 2022 [20] Equations

The accuracy of mechanical loading predictions for walking and running using the Veras et al., 2022 [20] equations is summarized in Table 2. The pGRF prediction for walking showed MAE ranging from 557.0 N to 621.7 N across different accelerometer placements, with MAPE values between 74.1% and 83.3%, which can be considered as very large prediction errors. The RMSE values ranged from 567.2 N to 632.5 N, indicating substantial discrepancies between predicted and actual values. For running, the pGRF prediction demonstrated improved accuracy, with MAE values ranging from 189.9 N to 247.5 N,

MAPE between 11.6% and 14.4%, and RMSE from 240.9 N to 314.8 N. The pLR predictions for walking had high MAE values, ranging from 8042.0 $N \cdot s^{-1}$ to 10,328.2 $N \cdot s^{-1}$ and MAPE between 106.5% and 147.6%. In contrast, running pLR predictions showed MAE values from 14,198.7 $N \cdot s^{-1}$ to 22,334.3 $N \cdot s^{-1}$, MAPE between 35.2% and 56.6%, and RMSE from 17,408.8 $N \cdot s^{-1}$ to 26,363.9 $N \cdot s^{-1}$. With these results, particularly MAPE values over 100%, the pLR prediction can be regarded as unacceptable. Supplemental Table S1 describes the pGRF and pLR prediction errors for each separate walking and running speed using the Veras et al., 2022 [20] equation.

Table 2. Accuracy indices for pGRF and pLR predictions for walking and running based on the Veras et al. (2022) [20] equations. The high prediction errors for pLR reflect challenges in accurately predicting this variable using accelerometers. Factors such as low accelerometer sampling frequency and individual variation in biomechanics likely contribute to the larger discrepancies in pLR compared to pGRF.

Vector	Activity	Accelerometer Placement	MAE	MAPE	RMSE
pGRF prediction					
Resultant	Walking	Ankle	606.7	80.0%	617.3
		Lower back	598.7	78.9%	609.9
		Hip	577.4	75.9%	587.7
	Running	Ankle	247.5	14.3%	314.8
		Lower back	218.0	12.9%	271.0
		Hip	189.9	11.6%	240.9
Vertical	Walking	Ankle	621.7	83.3%	632.5
		Lower back	596.8	79.6%	607.3
		Hip	557.0	74.1%	567.2
	Running	Ankle	243.5	14.4%	302.0
		Lower back	239.8	14.1%	295.8
		Hip	199.7	12.1%	248.5
pLR prediction					
Resultant	Walking	Ankle	8847.6	116.0%	9706.2
		Lower back	9460.4	134.0%	10,372.9
		Hip	8713.0	114.8%	9653.9
	Running	Ankle	16,638.6	40.6%	20,459.1
		Lower back	17,539.7	43.1%	21,288.0
		Hip	22,334.3	56.6%	26,363.9
Vertical	Walking	Ankle	8042.0	106.5%	8826.3
		Lower back	10,328.2	147.6%	11,247.3
		Hip	8512.6	113.6%	9334.4
	Running	Ankle	15,729.8	38.9%	19,313.6
		Lower back	16,609.6	40.7%	20,319.9
		Hip	14,198.7	35.2%	17,408.8

Abbreviations: MAE, mean absolute error; MAPE, mean absolute percent error; pGRF, peak ground reaction force; pLR, peak loading rate; RMSE, root mean square error.

3.2. Accuracy of pGRF Predictions for Walking and Running Using the Neugebauer et al., 2014 [17] Equation

The results for walking and running pGRF predictions using the Neugebauer et al., 2014 [17] equation are presented in Table 3. For walking, the pGRF prediction using hip accelerometers had an MAE of 75.0 N, MAPE of 9.7%, and RMSE of 104.9 N. Running predictions showed higher errors, with an MAE of 168.7 N, MAPE of 11.1%, and RMSE of 213.5 N. Compared to Veras et al., 2022 [20], the Neugebauer et al., 2014 [17] equation generally showed a much better accuracy for walking but comparable errors for running. The pGRF prediction errors for each walking and running speed using the Neugebauer 2014 [17] equation are shown in Supplemental Table S2.

Table 3. Accuracy indices for pGRF for walking and running based on the Neugebauer et al. (2014) [17] equation.

Vector	Activity	Accelerometer Placement	MAE	MAPE	RMSE
pGRF Prediction					
Vertical	Walking	Hip	75.0	9.7%	104.9
	Running	Hip	168.7	11.1%	213.5

Abbreviations: MAE, mean absolute error; MAPE, mean absolute percent error; pGRF, peak ground reaction force; RMSE, root mean square error.

3.3. Accuracy of pGRF and pLR Predictions for Jumping Using the Veras et al., 2023 [21] Equations

The accuracy indices for predicting pGRF and pLR during jumping activities using the Veras et al., 2023 [21] equations are displayed in Table 4. MAE values ranged from 378.6 N to 646.2 N and MAPE between 15.2% and 28.1%, which are comparable to the pGRF prediction equations error for running. RMSE values for pGRF predictions during jumping ranged from 499.2 N to 786.2 N. The pLR predictions for jumping were notably less accurate, with MAE values between 25,233.5 $N \cdot s^{-1}$ and 42,578.0 $N \cdot s^{-1}$, and MAPE ranging from 149.0% to 260.3%. Corresponding RMSE values ranged from 28,840.3 $N \cdot s^{-1}$ to 46,675.9 $N \cdot s^{-1}$, indicating unacceptably large prediction errors for loading rate during these high-impact activities. Supplemental Table S3 presents the pGRF and pLR prediction errors for all jumping activities separately, using the Veras et al., 2023 [21] equations.

Table 4. Accuracy indices for pGRF and pLR prediction for jumping based on the Veras et al., (2023) [21] equations. The pLR predictions for jumping activities show particularly high error rates, with MAPE values exceeding 200%. These errors highlight the difficulty in capturing the rapid, high-magnitude forces involved in jumping, and the difficulty in reflecting measurement sensitivity in pLR predictions.

Vector	Accelerometer Placement	MAE	MAPE	RMSE
pGRF prediction				
Resultant	Ankle	646.2	27.2%	786.2
	Lower back	405.3	16.7%	518.9
	Hip	380.6	15.2%	499.2
Vertical	Ankle	633.6	28.1%	762.9
	Lower back	433.1	18.8%	542.0
	Hip	378.6	15.5%	500.8
pLR prediction				
Resultant	Ankle	42,578.0	260.3%	46,675.9
	Lower back	30,446.0	171.4%	33,924.7
	Hip	25,233.5	149.0%	28,840.3
Vertical	Ankle	39,082.2	257.2%	43,130.8
	Lower back	36,628.7	213.6%	39,823.7
	Hip	28,880.9	161.5%	32,443.4

Abbreviations: MAE, mean absolute error; MAPE, mean absolute percent error; pGRF, peak ground reaction force; pLR, peak loading rate; RMSE, root mean square error.

3.4. Bland–Altman Plot Analysis

A Bland–Altman plot of measurements that show high agreement would depict data points scattered randomly around the bias line, with most points falling within the limits of agreement, indicating no systematic bias between the actual and predicted values. In this study, Bland–Altman plots for pGRF prediction using Veras et al., 2022 [20] showed systematic biases for both walking and running activities (Figure 1). The points for walking clustered more tightly around the mean difference line, while running data displayed a larger spread, particularly for higher values of ground reaction force. Similar trends were observed in pLR prediction equations using Veras et al., 2022 [20] (Figure 2), where larger deviations were noted for running compared to walking. Regarding the Bland–Altman plot for walking and running

pGRF prediction using the Neugebauer et al., 2014 [17] equation (Figure 3), the data points are much more evenly distributed around the bias, which is very close to zero, showing no signs of systematic bias. For jumping activities (Figures 4 and 5), Bland–Altman plots indicated substantial biases and wide limits of agreement, especially for pLR prediction (Figure 5).

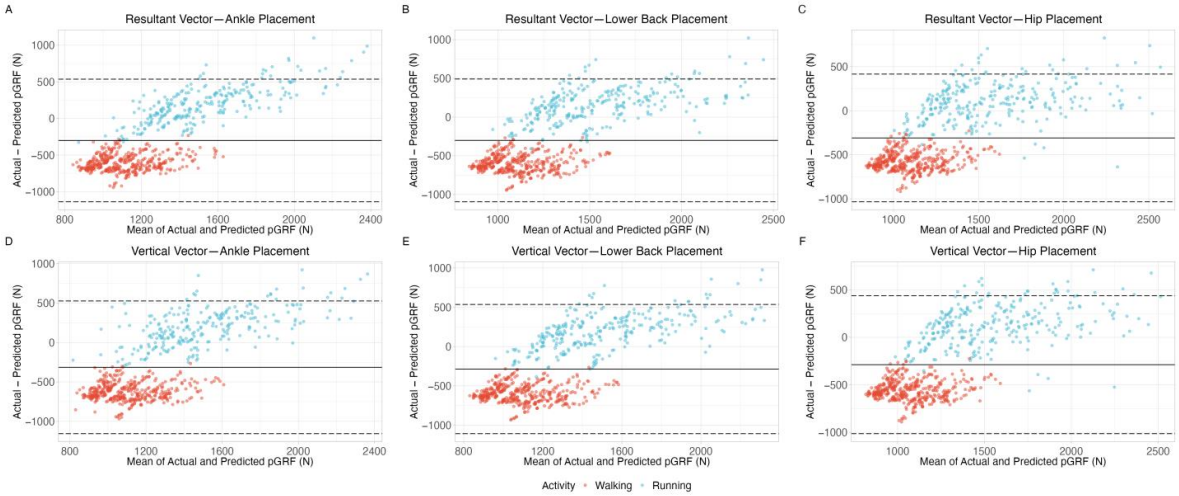


Figure 1. Bland–Altman plots displaying the level of agreement between actual and predicted pGRF for accelerometers worn at the ankle (panels **A**,**D**), lower back (panels **B**,**E**), and hip (panels **C**,**F**). These plots cover both the resultant vector (panels **A**–**C**) and its vertical component (panels **D**–**F**). Predictions of pGRF during walking and running were calculated using the equations from Veras et al. (2022) [20]. The solid lines represent the bias (the mean difference between actual and predicted values), while the dashed lines mark the limits of agreement (bias ±1.96 standard deviations). Abbreviations: pGRF, peak ground reaction force.

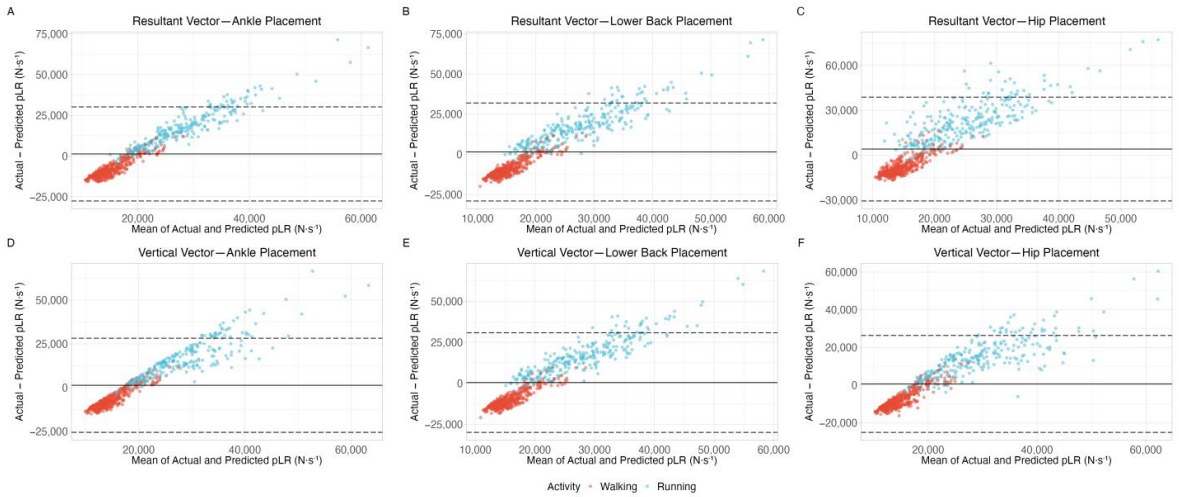


Figure 2. Bland–Altman plots displaying the level of agreement between actual and predicted pL for accelerometers worn at the ankle (panels **A**,**D**), lower back (panels **B**,**E**), and hip (panels **C**,**F**). These plots cover both the resultant vector (panels **A**–**C**) and its vertical component (panels **D**–**F**). Predictions of pLR during walking and running were calculated using the equations from Veras et al. (2022) [20]. The solid lines represent the bias (the mean difference between actual and predicted values), while the dashed lines mark the limits of agreement (bias ±1.96 standard deviations). Abbreviations: pLR, peak loading rate.

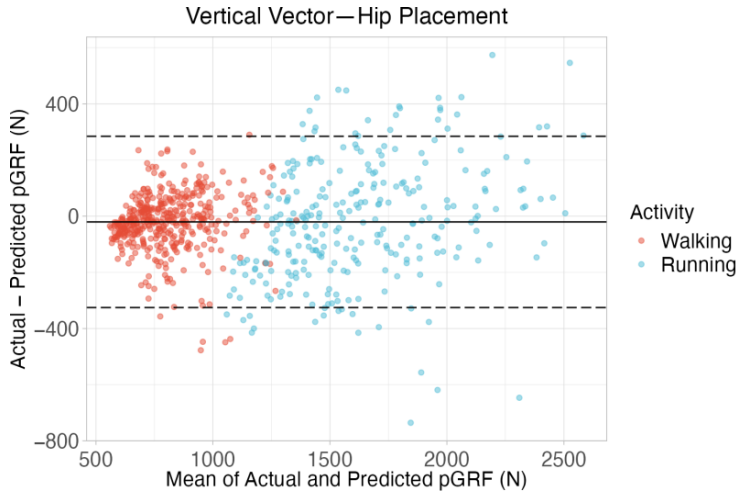


Figure 3. Bland–Altman plot displaying the level agreement between actual and predicted pGRF for accelerometers worn at the hip for the vertical vector. Predictions of pGRF during walking and running were calculated using the equation from Neugebauer et al. (2014) [17]. The solid line represents the bias (the mean difference between actual and predicted values), while the dashed lines mark the limits of agreement (bias ±1.96 standard deviations). Abbreviations: pGRF, peak ground reaction force.

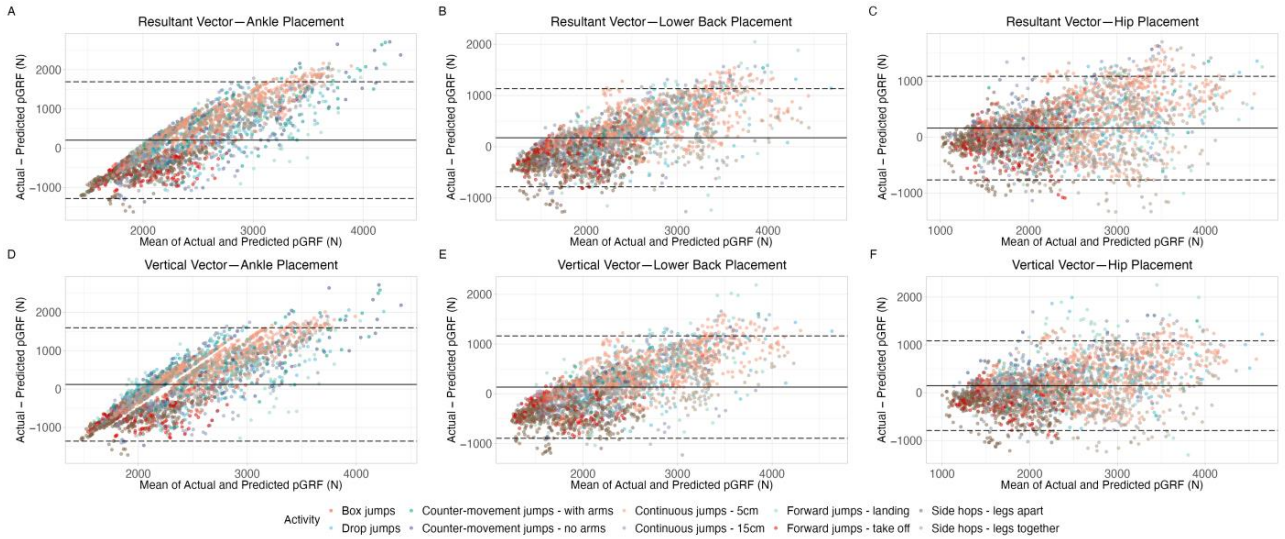


Figure 4. Bland–Altman plots displaying the level of agreement between actual and predicted pGRF for accelerometers worn at the ankle (panels **A**,**D**), lower back (panels **B**,**E**), and hip (panels **C**,**F**). These plots cover both the resultant vector (panels **A**–**C**) and its vertical component (panels **D**–**F**). Predictions of pGRF during jumping were calculated using the equations from Veras et al. (2023) [21]. The solid lines represent the bias (the mean difference between actual and predicted values), while the dashed lines mark the limits of agreement (bias ±1.96 standard deviations). Abbreviations: pGRF, peak ground reaction force.

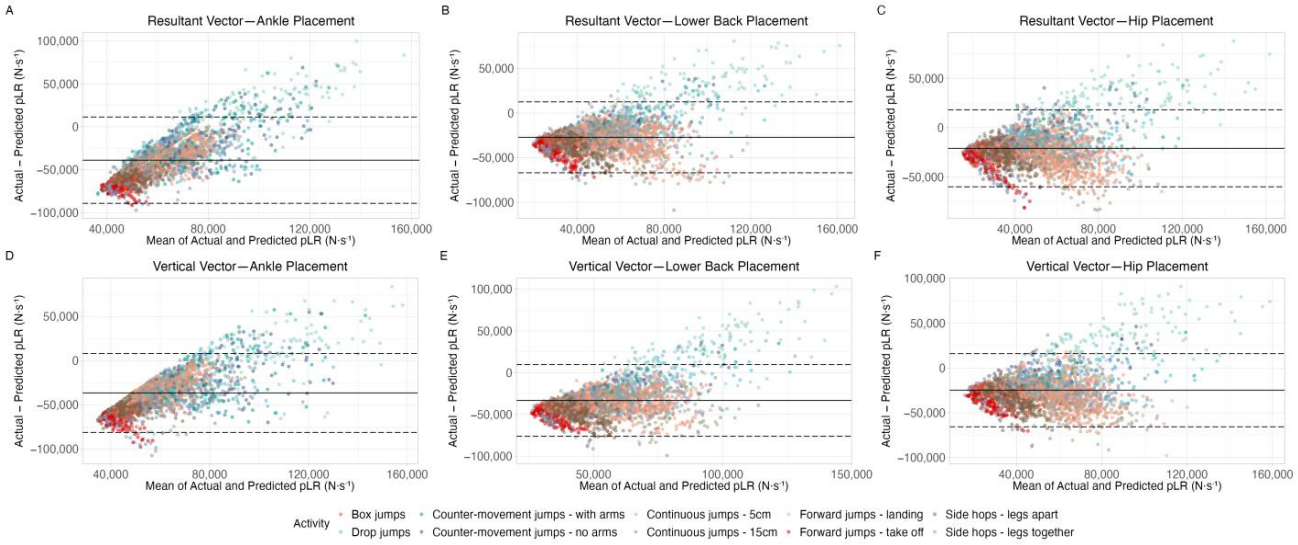


Figure 5. Bland–Altman plots displaying the level of agreement between actual and predicted pL for accelerometers worn at the ankle (panels **A**,**D**), lower back (panels **B**,**E**), and hip (panels **C**,**F**). These plots cover both the resultant vector (panels **A**–**C**) and its vertical component (panels **D**–**F**). Predictions of pLR during jumping were calculated using the equations from Veras et al. (2023) [21]. The solid lines represent the bias (the mean difference between actual and predicted values), while the dashed lines mark the limits of agreement (bias ±1.96 standard deviations). Abbreviations: pLR, peak loading rate.

4. Discussion

The objective of this study was to validate mechanical loading prediction equations previously developed using different sample and testing conditions than the ones used in their original validation studies in order to determine their external validity. This was accomplished by testing the mechanical loading prediction equations developed by Veras et al., 2022 [20], Neugebauer et al., 2014 [17], and Veras et al., 2023 [21] on a new sample performing walking, running, and several jumping activities. The main results indicated varying degrees of prediction accuracy, with discrepancies observed in the prediction errors for different activities and accelerometer placements.

As far as we know, this is the first study to investigate the external validity of mechanical loading prediction equations. External validation is crucial for several reasons [27–29]. Firstly, it ensures that the prediction models are not overfitted to the specific sample and conditions of the original study, thus confirming their robustness and generalizability to other populations and settings. Secondly, this type of validation helps to identify the potential limitations and biases inherent in the original models. For example, models developed with a homogeneous sample may not perform well with a more diverse population, including variations in age, gender, body composition, and physical activity levels, which are all factors that can influence the prediction accuracy [24]. Thirdly, by testing these models in a variety of activity contexts we can better understand their practical applicability in real-world scenarios. This is particularly important for public health and clinical applications [30,31], where accurate and reliable assessments of mechanical loading are needed to prescribe appropriate physical activities, monitor rehabilitation progress, and prevent injury.

When comparing the results of this external validation study with the results of the original studies, some differences emerge. For walking and running, pGRF and pLR predictions using the Veras et al., 2022 [20] equations, the original study reported lower prediction errors, with MAPE ranging from 6.8% to 7.3% for pGRF and 17.7% to 19.1% for pLR. In contrast, our current study found higher MAPE values, especially for walking,

with MAPE exceeding 100% for pLR, indicating less accurate predictions in our external validation sample. Similarly, Neugebauer et al., 2014 [17] reported a MAPE of 8.3% for walking and running pGRF predictions, which is slightly better than the 9.7% and 11.1% MAPE observed in our study. For jumping activities, Veras et al., 2023 [21] reported MAPE values between 12.3% and 14.5% for pGRF and 20.7% to 24.7% for pLR. Our current external validation study found significantly higher errors, particularly for pLR predictions during jumping, with MAPE values reaching up to 260.3%. These greater errors were, to some degree, expected because external validation involves testing the models on different populations and conditions than those used in the original studies, for which the models were optimized. When applied to new, more variable datasets, the models are likely to encounter variations that they were not initially exposed to, which usually leads to higher prediction errors [24,27,28].

The high errors observed in pLR predictions stem from several factors. First, pLR is an inherently volatile variable, reflecting rapid changes in force over very short time intervals, particularly during high-impact activities like jumping. This volatility makes accurate prediction extremely sensitive to the exact timing of ground contact and peak force, a challenge noted in several validation studies [19–21,32]. Wearable accelerometers, typically sampling at 100 Hz, may not capture the precise moment of force application, leading to a smoothing of the data that significantly distorts pLR estimates. This challenge is compounded by inter-individual variability in biomechanics; different subjects exhibit varied landing mechanics, joint stiffness, and movement strategies, all of which can drastically affect loading rates but are not easily captured by accelerometers alone.

Moreover, even slight differences in accelerometer positioning can lead to substantial differences in the data collected. During high-impact activities like jumping, imperceptible shifts in sensor position can result in markedly different acceleration profiles, leading to large discrepancies in pLR predictions [33,34]. While researchers can ensure correct device positioning in laboratory conditions, this is not guaranteed in real-life settings. Subjects may be unaware of errors in accelerometer positioning, and the device's position could shift during extended data collection protocols, significantly contributing to greater prediction errors, thereby compromising the interpretation of study results. Additionally, the variability in human movement patterns, influenced by factors such as gait, speed, and individual biomechanics [35,36], introduces additional noise into the data, challenging the models' ability to generalize across different populations and conditions. These factors collectively highlight the need for more sophisticated modeling approaches that can compensate for limitations in accelerometer sampling rates, account for inter-individual variability in biomechanics, mitigate the effects of sensor placement inconsistencies, and adapt to the complexity and variability of human movement in real-world settings.

These results have important practical implications for researchers studying physical activity-related mechanical loading and using accelerometer-based prediction equations. Our findings suggest that while these models can provide useful estimates, their accuracy can vary significantly depending on the activity type, sample characteristics, and testing conditions, and that this varying accuracy needs to be considered when interpreting the results of studies that apply these equations. In real-world applications, such as sports training or rehabilitation, accurate predictions of mechanical loading are critical for tailoring exercise programs to prevent osteoarticular injury or to optimize bone health. However, the current prediction inaccuracies may limit the practicality of the models in these settings. If not addressed, these limitations could result in suboptimal recommendations, potentially compromising bone health outcomes. Thus, further refinement is essential to ensure these models can be reliably applied in real-world clinical and sports contexts.

This study has some limitations that should be acknowledged in order to adequately interpret its results. Firstly, the testing conditions, while diverse, may not capture all possible real-world scenarios. Future research should aim to test different activities and environments compared to the previous studies, such as examining the mechanical loading of locomotion on different surfaces, climbing stairs, or including sport-specific move-

ments and other specialized activities. Secondly, the study was conducted in a controlled laboratory environment, which may not fully replicate the complexities and variations encountered in free-living conditions. The controlled setting might have reduced external factors like terrain variability, environmental conditions, and daily life movements, potentially influencing the prediction models' performance when compared to their application in real life settings. Furthermore, as the researchers positioned the accelerometers and ensured that their position remained correct for the duration of the trials, the results cannot account for the effect of increased error due to accelerometer misplacement and shifting that can occur in free-living conditions [37]. Finally, this study's sample is relatively small and homogenous in characteristics such as age and body mass index. Therefore, we may not know if these results hold true for people with diverse characteristics, such as the elderly and people with obesity. Despite these limitations, the study's strengths lie in its rigorous methodological approach and the comprehensive evaluation of multiple prediction models across various activities, providing valuable insights into their external validity.

Future studies aiming to improve the accuracy of mechanical loading prediction equations could explore the use of advanced machine learning techniques, which are better equipped to capture the complexity and variability inherent to biomechanical data. Additionally, employing accelerometers with higher sampling frequencies would provide more detailed data, which is essential for accurately detecting critical events like peak loading rates. Techniques that enable the reconstruction of ground reaction force signals from accelerometer data could further enhance accuracy, particularly in pLR predictions, making these models more reliable for diverse real-world applications. Moreover, prediction accuracy could be potentially improved by using data from sensors in two or more placements simultaneously. Although this strategy would not be feasible when collecting daily living data due to a probable decrease in the participant's adherence to the protocol, in more controlled scenarios, such as gathering mechanical loading data from athletes during their sports practice, this could be a valid strategy. Together, these approaches could not only enhance the accuracy of the models but also improve their consistency by mitigating the systematic biases observed in our analysis, reducing the tendency to either consistently overestimate or underestimate the predicted values, and making the bias values closer to zero. In conclusion, this study demonstrates the necessity and value of external validation for mechanical loading prediction equations. Our findings indicate that while existing models can be useful, their accuracy is context-dependent, and further refinement and validation are needed. This research highlights the importance of continuous evaluation and adaptation of prediction models to enhance their applicability and reliability in diverse real-world settings.

Supplementary Materials: The following supporting information can be downloaded at: https://www.mdpi.com/article/10.3390/app142210292/s1. Table S1: Accuracy indices for pGRF and pLR prediction for different walking and running speeds based on the Veras et al. (2022) [20] equations; Table S2: Accuracy indices for pGRF and pLR prediction for different walking and running speeds based on the Neugebauer et al. (2014) [17] equation; Table S3: Accuracy indices for pGRF and pLR prediction for different types of jumping based on the Veras et al. (2023) [21] equations; Video S1: Example of the activities included in the protocol.

Author Contributions: Conceptualization, L.V., F.D.-S., G.B., J.O. and H.F.; formal analysis, L.V. and D.O.; investigation, L.V., D.O., F.D.-S., G.B., A.R.-C., J.O. and H.F.; methodology, L.V., F.D.-S., G.B., J.O. and H.F.; software, L.V. and D.O.; writing—original draft, L.V., D.O. and H.F.; writing—review and editing, L.V., D.O., F.D.-S., G.B., A.R.-C., J.O. and H.F. All authors have read and agreed to the published version of the manuscript.

Funding: This work was performed at the Research Center in Physical Activity, Health, and Leisure (CIAFEL), Faculty of Sport, University of Porto (FADEUP), funded by Fundação Para a Ciência e Tecnologia (FCT grants UIDB/00617/2020, doi: 10.54499/UIDB/00617/2020 and UIDP/00617/2020, doi: 10.54499/UIDP/00617/2020) and the Laboratory for Integrative and Translational Research in Population Health (ITR; FCT grant LA/P/0064/2020). L.V., D.O., F.D.-S., and G.B. were supported

by the FCT (grant numbers UI/BD/150673/2020, 2024.04905.BD, SFRH/BD/117622/2016, and SFRH/BD/146976/2019).

Institutional Review Board Statement: The study was conducted in accordance with the Declaration of Helsinki, and approved by the Ethics Committee of the Faculty of Sport, University of Porto (protocol code CEFADE 15-21, approved on 11 May 2021).

Informed Consent Statement: Informed consent was obtained from all subjects involved in the study.

Data Availability Statement: The data presented in this study are available on request from the corresponding author.

Acknowledgments: The authors thank the participants who took part in this research and all who have collaborated in the research project.

Conflicts of Interest: The authors declare no conflicts of interest.

References

1. Brooke-Wavell, K.; A Skelton, D.; Barker, K.L.; Clark, E.M.; De Biase, S.; Arnold, S.; Paskins, Z.; Robinson, K.R.; Lewis, R.M.; Tobias, J.H.; et al. Strong, steady and straight: UK consensus statement on physical activity and exercise for osteoporosis. *Br. J. Sports Med.* **2022**, *56*, 837–846. [CrossRef] [PubMed]
2. Santos, L.; Elliott-Sale, K.J.; Sale, C. Exercise and bone health across the lifespan. *Biogerontology* **2017**, *18*, 931–946. [CrossRef] [PubMed]
3. Beck, B.R.; Daly, R.M.; Singh, M.A.F.; Taaffe, D.R. Exercise and Sports Science Australia (ESSA) position statement on exercise prescription for the prevention and management of osteoporosis. *J. Sci. Med. Sport.* **2017**, *20*, 438–445. [CrossRef] [PubMed]
4. Fonseca, H.; Moreira-Gonçalves, D.; Coriolano, H.-J.A.; Duarte, J.A. Bone quality: The determinants of bone strength and fragility. *Sports Med.* **2014**, *44*, 37–53. [CrossRef] [PubMed]
5. Harding, A.T.; Beck, B.R. Exercise, Osteoporosis, and Bone Geometry. *Sports* **2017**, *5*, 29. [CrossRef]
6. NIH Consensus Development Panel on Osteoporosis Prevention, Diagnosis and T. Osteoporosis Prevention, Diagnosis, and Therapy. *J. Am. Med. Assoc.* **2001**, *285*, 785–795. [CrossRef]
7. Turner, C.H.; Robling, A.G. Mechanisms by which exercise improves bone strength. *J. Bone Miner. Metab.* **2005**, *23*, 16–22. [CrossRef]
8. Robling, A.G.; Turner, C.H. Mechanical signaling for bone modeling and remodeling. *Crit. Rev. Eukaryot. Gene Expr.* **2009**, *19*, 319–338. [CrossRef]
9. Yuan, Y.; Chen, X.; Zhang, L.; Wu, J.; Guo, J.; Zou, D.; Chen, B.; Sun, Z.; Shen, C.; Zou, J. The roles of exercise in bone remodeling and in prevention and treatment of osteoporosis. *Prog. Biophys. Mol. Biol.* **2016**, *122*, 122–130. [CrossRef]
10. Ren, S.; Chen, Z.; Qin, X.; Zhao, X.; Yang, T.D.; Zhu, W. Measurement and Evaluation of Bone Loading in Physical Activity: A Systematic Review. *Meas. Phys. Educ. Exerc. Sci.* **2020**, *25*, 149–162. [CrossRef]
11. Medved, V. *Measurement of Human Locomotion*; CRC Press: London, UK, 2000.
12. Weeks, B.K.; Beck, B.R. The BPAQ: A bone-specific physical activity assessment instrument. *Osteoporos. Int.* **2008**, *19*, 1567–1577. [CrossRef] [PubMed]
13. Farr, J.N.; Lee, V.R.; Blew, R.M.; Lohman, T.G.; Going, S.B. Quantifying bone-relevant activity and its relation to bone strength in girls. *Med. Sci. Sports Exerc.* **2011**, *43*, 476–483. [CrossRef] [PubMed]
14. Kim, S.; So, W.-Y.; Kim, J.; Sung, D.J. Relationship between bone-specific physical activity scores and measures for body composition and bone mineral density in healthy young college women. *PLoS ONE* **2016**, *11*, e0162127. [CrossRef] [PubMed]
15. Kim, S.; Baker, B.S.; Sharma-Ghimire, P.; Bemben, D.A.; Bemben, M.G. Association between bone-specific physical activity scores and pQCT-derived measures of bone strength and geometry in healthy young and middle-aged premenopausal women. *Arch. Osteoporos.* **2018**, *13*, 83. [CrossRef]
16. Neugebauer, J.M.; Hawkins, D.A.; Beckett, L. Estimating youth locomotion ground reaction forces using an accelerometer-based activity monitor. *PLoS ONE* **2012**, *7*, e48182. [CrossRef]
17. Neugebauer, J.M.; Collins, K.H.; Hawkins, D.A. Ground reaction force estimates from ActiGraph GT3X+ hip accelerations. *PLoS ONE* **2014**, *9*, e99023. [CrossRef]
18. Neugebauer, J.M.; Lafiandra, M. Predicting ground reaction force from a hip-borne accelerometer during load carriage. *Med. Sci. Sports Exerc.* **2018**, *50*, 2369–2374. [CrossRef]
19. Veras, L.; Diniz-Sousa, F.; Boppre, G.; Devezas, V.; Santos-Sousa, H.; Preto, J.; Vilas-Boas, J.P.; Machado, L.; Oliveira, J.; Fonseca, H. Accelerometer-based prediction of skeletal mechanical loading during walking in normal weight to severely obese subjects. *Osteoporos. Int.* **2020**, *31*, 1239–1250. [CrossRef]
20. Veras, L.; Diniz-Sousa, F.; Boppre, G.; Resende-Coelho, A.; Moutinho-Ribeiro, E.; Devezas, V.; Santos-Sousa, H.; Preto, J.; Vilas-Boas, J.P.; Machado, L.; et al. Mechanical loading prediction through accelerometry data during walking and running. *Eur. J. Sport Sci.* **2022**, *23*, 1518–1527. [CrossRef]

21. Veras, L.; Diniz-Sousa, F.; Boppre, G.; Devezas, V.; Santos-Sousa, H.; Preto, J.; Vilas-Boas, J.P.; Machado, L.; Oliveira, J.; Fonseca, H. Using Raw Accelerometer Data to Predict High-Impact Mechanical Loading. *Sensors* **2023**, *23*, 2246. [CrossRef]
22. Migueles, J.H.; Cadenas-Sanchez, C.; Ekelund, U.; Delisle Nyström, C.; Mora-Gonzalez, J.; Löf, M.; Labayen, I.; Ruiz, J.R.; Ortega, F.B. Accelerometer data collection and processing criteria to assess physical activity and other outcomes: A systematic review and practical considerations. *Sports Med.* **2017**, *47*, 1821–1845. [CrossRef] [PubMed]
23. Troiano, R.P.; McClain, J.J.; Brychta, R.J.; Chen, K.Y. Evolution of accelerometer methods for physical activity research. *Br. J. Sports Med.* **2014**, *48*, 1019–1023. [CrossRef] [PubMed]
24. Welk, G.J. Principles of design and analyses for the calibration of accelerometry-based activity monitors. *Med. Sci. Sports Exerc.* **2005**, *37* (Suppl. S11), S501–S511. [CrossRef] [PubMed]
25. Toda, H.; Nagano, A.; Luo, Z. Age and gender differences in the control of vertical ground reaction force by the hip, knee and ankle joints. *J. Phys. Ther. Sci.* **2015**, *27*, 1833–1838. [CrossRef]
26. Patoz, A.; Menéndez, A.F.; Malatesta, D. The effect of severe obesity on three-dimensional ground reaction force signals during walking. *Clin. Biomech.* **2023**, *107*, 106042. [CrossRef]
27. Staudenmayer, J.; Zhu, W.; Catellier, D.J. Statistical considerations in the analysis of accelerometry-based activity monitor data. *Med. Sci. Sports Exerc.* **2012**, *44* (Suppl. S1), S61–S67. [CrossRef]
28. Zhang, Y.; Weijer, R.H.; van Schooten, K.S.; Bruijn, S.M.; Pijnappels, M. External Validation and Further Exploration of Fall Prediction Models Based on Questionnaires and Daily-Life Trunk Accelerometry. *J. Am. Med. Dir. Assoc.* **2024**, *25*, 105107. [CrossRef]
29. Lyden, K.; Kozey, S.L.; Staudenmeyer, J.W.; Freedson, P.S. A comprehensive evaluation of commonly used accelerometer energy expenditure and MET prediction equations. *Eur. J. Appl. Physiol.* **2011**, *111*, 187. [CrossRef]
30. Chastin, S.; Mandrichenko, O.; Helbostadt, J.; Skelton, D. Associations between objectively-measured sedentary behaviour and physical activity with bone mineral density in adults and older adults, the NHANES study. *Bone* **2014**, *64*, 254–262. [CrossRef]
31. Stiles, V.H.; Metcalf, B.S.; Knapp, K.M.; Rowlands, A. A small amount of precisely measured high-intensity habitual physical activity predicts bone heath in pre- and post-menopausal women in UK Biobank. *Int. J. Epidemiol.* **2017**, *46*, 1847–1856. [CrossRef]
32. Fortune, E.; Morrow, M.M.B.; Kaufman, K.R. Assessment of gait kinetics using tri-axial accelerometers. *J. Appl. Biomech.* **2014**, *30*, 668–674. [CrossRef] [PubMed]
33. Tan, T.; Chiasson, D.P.; Hu, H.; Shull, P.B. Influence of IMU position and orientation placement errors on ground reaction force estimation. *J. Biomech.* **2019**, *97*, 109416. [CrossRef] [PubMed]
34. Chen, S.; Brantley, J.S.; Kim, T.; Ridenour, S.A.; Lach, J. Characterising and minimising sources of error in inertial body sensor networks. *Int. J. Auton. Adapt. Commun. Syst.* **2013**, *6*, 253–271. [CrossRef]
35. Jiang, X.; Bíró, I.; Sárosi, J.; Fang, Y.; Gu, Y. Comparison of ground reaction forces as running speed increases between male and female runners. *Front. Bioeng. Biotechnol.* **2024**, *12*, 1378284. [CrossRef]
36. Park, J.; Kim, C. Ground-reaction-force-based gait analysis and its application to gait disorder assessment: New indices for quantifying walking behavior. *Sensors* **2022**, *22*, 7558. [CrossRef]
37. Sara, L.K.; Outerleys, J.; Johnson, C.D. The effect of sensor placement on measured distal tibial accelerations during running. *J. Appl. Biomech.* **2023**, *39*, 199–203. [CrossRef]

Disclaimer/Publisher's Note: The statements, opinions and data contained in all publications are solely those of the individual author(s) and contributor(s) and not of MDPI and/or the editor(s). MDPI and/or the editor(s) disclaim responsibility for any injury to people or property resulting from any ideas, methods, instructions or products referred to in the content.

Supplemental Material

Supplemental Table 1. Accuracy indices for pGRF and pLR prediction for different walking and running speeds based on Veras et al (2022) equations

Vector	Accelerometer placement	Speeds	MAE	MAPE	RMSE
pGRF prediction					
Resultant	Ankle	Slow walking	692.3	99.5%	695.0
		Normal walking	626.6	82.9%	631.5
		Fast walking	500.7	57.6%	510.8
	Lower back	Slow walking	682.5	97.7%	686.4
		Normal walking	616.2	81.4%	621.7
		Fast walking	493.1	56.8%	503.4
	Hip	Slow walking	652.8	93.4%	656.5
		Normal walking	595.0	78.6%	600.5
		Fast walking	482.8	55.4%	493.1
	Ankle	Slow running	184.0	11.8%	231.4
		Fast running	313.4	16.9%	382.7
	Lower back	Slow running	165.6	11.0%	201.7
		Fast running	270.7	14.9%	326.2
	Hip	Slow running	162.9	10.8%	204.3
		Fast running	218.1	12.5%	273.9
Vertical	Ankle	Slow walking	709.0	103.3%	712.4
		Normal walking	640.9	86.1%	645.8
		Fast walking	515.0	60.3%	524.8
	Lower back	Slow walking	676.1	97.4%	679.9
		Normal walking	613.7	82.1%	619.1
		Fast walking	495.8	58.3%	505.6
	Hip	Slow walking	626.6	90.3%	630.6
		Normal walking	574.7	76.9%	580.4
		Fast walking	467.8	54.6%	478.1
	Ankle	Slow running	180.1	11.5%	224.7
		Fast running	310.9	17.6%	366.8
	Lower back	Slow running	177.6	11.6%	216.1
		Fast running	302.4	16.6%	358.6
	Hip	Slow running	167.3	11.0%	211.3
		Fast running	233.9	13.4%	282.6
pLR prediction					
Resultant	Ankle	Slow walking	12 174.1	198.3%	12 332.1
		Normal walking	9 332.8	108.8%	9 702.4
		Fast walking	5 025.6	41.0%	6 034.5

	Lower back	Slow walking	13 033.0	240.3%	13 196.4
		Normal walking	9 921.6	114.8%	10 276.4
		Fast walking	5 254.9	43.3%	6 347.9
	Hip	Slow walking	12 243.7	201.3%	12 420.5
		Normal walking	8 843.5	103.5%	9 313.7
		Fast walking	5 000.1	38.6%	6 153.7
	Ankle	Slow running	10 465.2	31.3%	12 966.4
		Fast running	23 049.4	50.3%	26 051.1
	Lower back	Slow running	10 872.1	32.9%	13 164.0
		Fast running	24 254.7	53.4%	27 111.9
	Hip	Slow running	14 159.5	43.8%	16 636.4
		Fast running	30 861.9	69.9%	33 636.2
Vertical	Ankle	Slow walking	11 081.9	182.1%	11 237.1
		Normal walking	8 405.7	99.4%	8 763.9
		Fast walking	4 635.7	38.1%	5 535.2
	Lower back	Slow walking	14 005.9	260.6%	14 153.0
		Normal walking	10 988.2	128.2%	11 289.2
		Fast walking	5 773.5	49.3%	6 929.4
	Hip	Slow walking	11 634.0	193.7%	11 785.0
		Normal walking	9 026.1	106.1%	9 366.9
		Fast walking	4 797.8	39.6%	5 802.2
	Ankle	Slow running	10 239.2	30.6%	12 659.0
		Fast running	21 574.7	47.6%	24 484.8
	Lower back	Slow running	10 257.3	30.7%	12 656.5
		Fast running	23 006.9	50.8%	25 834.2
	Hip	Slow running	9 264.6	27.8%	11 491.6
		Fast running	19 420.8	43.2%	22 001.5

Abbreviations: MAE, mean absolute error; MAPE, mean absolute percent error; pGRF, peak ground reaction force; pLR, peak loading rate; RMSE, root mean square error

Supplemental Table 2. Accuracy indices for pGRF and pLR prediction for different walking and running speeds based on Neugebauer et al (2014) equations

Vector	Accelerometer placement	Speeds	MAE	MAPE	RMSE
pGRF prediction					
Vertical	Hip	Slow walking	59.6	8.8%	79.9
		Normal walking	69.7	9.7%	104.4
		Fast walking	96.1	10.8%	125.9
		Slow running	150.6	10.8%	188.3
		Fast running	187.9	11.5%	237.2

Abbreviations: MAE, mean absolute error; MAPE, mean absolute percent error; pGRF, peak ground reaction force; pLR, peak loading rate; RMSE, root mean square error

Supplemental Table 3. Accuracy indices for pGRF and pLR prediction for different types of jumping based on Veras et al (2023) equations

Vector	Accelerometer placement	Jumping type	MAE	MAPE	RMSE
pGRF prediction					
Resultant	Ankle	Box jumps	325.4	17.3%	376.3
		Drop jumps	573.9	18.5%	741.5
		Counter-movement jumps - with arms	688.7	22.9%	893.6
		Counter-movement jumps - no arms	713.5	22.3%	914.7
		Continuous jumps - 5cm	803.9	24.6%	956.2
		Continuous jumps - 15cm	565.1	26.9%	698.5
		Forward jumps - landing	531.6	18.8%	688.2
		Forward jumps - take off	675.2	45.0%	709.1
		Side hops - legs apart	627.4	45.9%	694.1
		Side hops - legs together	636.9	21.9%	762.4
	Lower back	Box jumps	198.3	8.6%	270.9
		Drop jumps	409.6	13.4%	524.2
		Counter-movement jumps - with arms	442.9	15.4%	574.8
		Counter-movement jumps - no arms	471.9	16.4%	580.7
		Continuous jumps - 5cm	516.9	16.3%	633.0
		Continuous jumps - 15cm	404.9	16.5%	542.0
		Forward jumps - landing	515.0	18.1%	655.0
		Forward jumps - take off	280.5	18.0%	338.2
		Side hops - legs apart	322.7	22.7%	396.7
		Side hops - legs together	396.1	14.1%	488.9
	Hip	Box jumps	325.2	14.8%	380.0
		Drop jumps	354.0	12.0%	462.5
		Counter-movement jumps - with arms	263.0	10.2%	389.6
		Counter-movement jumps - no arms	468.6	17.5%	601.3
		Continuous jumps - 5cm	487.3	15.3%	609.1

		Continuous jumps - 15cm	376.6	15.4%	512.5
		Forward jumps - landing	374.1	13.4%	476.9
		Forward jumps - take off	267.3	16.9%	348.4
		Side hops - legs apart	241.2	15.7%	331.8
		Side hops - legs together	435.9	15.5%	541.0
Vertical	Ankle	Box jumps	359.3	19.4%	412.5
		Drop jumps	566.0	18.3%	730.6
		Counter-movement jumps - with arms	666.1	22.1%	861.3
		Counter-movement jumps - no arms	679.5	21.7%	869.9
		Continuous jumps - 5cm	726.4	22.6%	874.2
		Continuous jumps - 15cm	593.8	29.0%	720.2
		Forward jumps - landing	492.3	18.7%	637.8
		Forward jumps - take off	833.2	56.9%	859.7
		Side hops - legs apart	758.1	55.3%	806.3
		Side hops - legs together	533.0	19.8%	645.3
	Lower back	Box jumps	160.1	7.1%	225.5
		Drop jumps	441.5	14.6%	566.3
		Counter-movement jumps - with arms	444.0	15.7%	577.0
		Counter-movement jumps - no arms	473.7	16.9%	574.9
		Continuous jumps - 5cm	545.6	17.2%	659.0
		Continuous jumps - 15cm	415.8	16.9%	556.7
		Forward jumps - landing	542.5	20.4%	686.6
		Forward jumps - take off	371.7	25.0%	417.6
		Side hops - legs apart	441.2	31.2%	492.7
		Side hops - legs together	354.0	13.3%	443.0
	Hip	Box jumps	257.1	12.1%	308.5
		Drop jumps	397.7	13.7%	523.3
		Counter-movement jumps - with arms	272.6	10.4%	399.0
		Counter-movement jumps - no arms	534.6	20.3%	655.5
		Continuous jumps - 5cm	450.8	14.3%	568.3

		Continuous jumps - 15cm	363.5	14.2%	497.6
		Forward jumps - landing	601.0	21.3%	771.8
		Forward jumps - take off	268.4	17.8%	330.6
		Side hops - legs apart	267.2	18.4%	366.4
		Side hops - legs together	388.7	14.5%	489.1
pLR prediction					
Resultant	Ankle	Box jumps	63 913.1	495.9%	64 240.5
		Drop jumps	27 739.3	55.6%	31 469.4
		Counter-movement jumps - with arms	31 418.9	94.6%	35 950.4
		Counter-movement jumps - no arms	24 269.6	49.1%	29 095.8
		Continuous jumps - 5cm	35 895.2	101.2%	38 052.7
		Continuous jumps - 15cm	46 132.6	371.8%	50 198.5
		Forward jumps - landing	28 320.3	29.5%	34 921.7
		Forward jumps - take off	72 791.4	1398.2%	73 017.0
		Side hops - legs apart	59 528.2	430.1%	60 021.2
		Side hops - legs together	37 723.5	126.7%%	40 198.1
	Lower back	Box jumps	34 605.6	260.7%	35 495.1
		Drop jumps	19 472.6	37.6%	23 258.1
		Counter-movement jumps - with arms	14 672.9	30.5%	17 480.9
		Counter-movement jumps - no arms	14 420.1	27.6%	17 933.4
		Continuous jumps - 5cm	29 372.4	77.8%	32 600.8
		Continuous jumps - 15cm	27 544.5	262.6%	31 844.0
		Forward jumps - landing	28 387.9	27.4%	34 591.7
		Forward jumps - take off	44 789.3	778.0%	46 006.1
		Side hops - legs apart	36 393.4	249.1%	37 739.2
		Side hops - legs together	29 191.1	89.4%	33 191.5
	Hip	Box jumps	23 401.3	179.3%	23 911.3
		Drop jumps	14 560.6	26.9%	17 067.5
		Counter-movement jumps - with arms	12 587.2	24.1%	16 706.0
		Counter-movement jumps - no arms	12 555.6	24.8%	16 428.8

		Continuous jumps - 5cm	26 036.5	68.1%	29 493.1
		Continuous jumps - 15cm	23 017.0	283.9%	27 685.4
		Forward jumps - landing	32 189.6	31.3%	37 132.2
		Forward jumps - take off	36 804.5	715.7%	39 015.6
		Side hops - legs apart	25 584.9	179.3%	27 267.6
		Side hops - legs together	26 357.9	76.9%	30 234.0
Vertical	Ankle	Box jumps	59 281.3	457.1%	59 649.2
		Drop jumps	27 312.7	54.6%	30 901.3
		Counter-movement jumps - with arms	30 942.8	67.8%	35 649.2
		Counter-movement jumps - no arms	25 899.5	52.4%	30 677.0
		Continuous jumps - 5cm	31 058.3	91.5%	33 287.0
		Continuous jumps - 15cm	45 469.9	412.3%	49 169.7
		Forward jumps - landing	22 588.6	29.6%	29 939.0
		Forward jumps - take off	69 027.4	1542.7%	69 494.7
		Side hops - legs apart	53 589.0	392.4%	54 024.4
		Side hops - legs together	35 121.5	125.0%	37 542.8
	Lower back	Box jumps	45 844.7	347.4%	46 582.6
		Drop jumps	23 374.4	46.0%	26 526.0
		Counter-movement jumps - with arms	18 814.3	41.4%	21 632.4
		Counter-movement jumps - no arms	16 583.3	35.9%	20 231.9
		Continuous jumps - 5cm	32 428.2	89.5%	34 613.2
		Continuous jumps - 15cm	34 133.2	284.1%	38 290.8
		Forward jumps - landing	31 199.3	52.5%	38 839.0
		Forward jumps - take off	54 424.9	1173.6%	55 100.3
		Side hops - legs apart	46 398.1	303.9%	47 396.5
		Side hops - legs together	35 456.0	113.9%	38 224.2
	Hip	Box jumps	29 439.0	222.0%	30 490.5
		Drop jumps	18 768.7	35.0%	22 060.4
		Counter-movement jumps - with arms	13 715.5	28.3%	16 480.7
		Counter-movement jumps - no arms	12 560.1	24.7%	15 953.6

	Continuous jumps - 5cm	28 608.9	74.9%	31 686.9
	Continuous jumps - 15cm	24 555.1	186.2%	28 554.8
	Forward jumps - landing	34 177.2	179.5%	41 055.5
	Forward jumps - take off	38 996.2	862.2%	40 316.0
	Side hops - legs apart	32 493.2	215.5%	34 364.2
	Side hops - legs together	30 085.5	86.8%	33 986.6

Abbreviations: MAE, mean absolute error; MAPE, mean absolute percent error; pGRF, peak ground reaction force; pLR, peak loading rate; RMSE, root mean square error

3.5. Study 4

Veras L, Diniz-Sousa F, Boppre G, Resende-Coelho A, Oliveira J, Fonseca H. Accelerometer-Based Classification of Walking, Running, and Jumping: A Machine Learning Approach for Mechanical Loading Assessment. *Submitted to: Sensors*

sensors

MDPI

Article

Accelerometer-Based Classification of Walking, Running, and Jumping: A Machine Learning Approach for Mechanical Loading Assessment

Lucas Veras [1,2,*], Florêncio Diniz-Sousa [1,2], Giorjines Boppre [1,2], Ana Resende-Coelho [1,2], José Oliveira [1,2] and Hélder Fonseca [1,2]

[1] Research Center in Physical Activity, Health and Leisure (CIAFEL), Faculty of Sport, University of Porto, 4200-450 Porto, Portugal
[2] Laboratory for Integrative and Translational Research in Population Health (ITR), University of Porto, 4200-450 Porto, Portugal
* Correspondence: lucasdsveras@gmail.com

Abstract: Accurate measurement of mechanical loading during physical activities is crucial for developing effective bone health interventions. While accelerometers offer promise for measuring these loads in free-living conditions, current prediction models typically require prior activity identification. This study aimed to develop and validate classification models for differentiating between walking, running, and jumping activities using accelerometer data. Forty-eight healthy adults performed a series of walking, running, and jumping tasks while wearing ActiGraph GT9X Link accelerometers on the ankle, lower back, and hip. Three machine learning algorithms (Random Forest, Support Vector Machine, and K-Nearest Neighbors) were developed and validated using multiple performance metrics. All algorithms demonstrated excellent classification performance across accelerometer placements, with percent agreement ranging between 93.8% and 97.7%, ROC-AUC values consistently above 0.97, and Kappa coefficients exceeding 0.89. These findings indicate that accelerometer-based activity classification is a reliable approach for distinguishing between walking, running, and jumping activities, providing a foundation for the accurate application of activity-specific mechanical loading prediction equations in free-living conditions.

Keywords: accelerometer; activity recognition; mechanical loading; validation; machine learning

Academic Editor: Firstname Lastname

Received: date
Revised: date
Accepted: date
Published: date

Citation: To be added by editorial staff during production.

Copyright: © 2025 by the authors. Submitted for possible open access publication under the terms and conditions of the Creative Commons Attribution (CC BY) license (https://creativecommons.org/licenses/by/4.0/).

1. Introduction

Bone tissue adapts to mechanical loading by modifying its mass, geometry, and microarchitecture to optimize its strength and resistance to fracture [1–3]. Weight-bearing physical activities that generate ground reaction forces through impact with the ground, particularly walking, running, and jumping, have been consistently shown to promote positive skeletal adaptations and are widely prescribed to enhance bone health [4,5]. The osteogenic effects of these impact-generating activities are primarily mediated by specific mechanical loading characteristics, especially the magnitude and rate of the applied forces, which trigger bone's adaptive response [3,6,7].

Accurately measuring these forces during daily activities and exercise is crucial for developing and monitoring effective bone health interventions [8]. While force plates remain the gold standard for measuring ground reaction forces [9], accelerometers have emerged as a promising alternative for measuring mechanical loading in free-living conditions [10–13]. However, current accelerometer-based prediction models typically require prior identification of the type of activity being performed, as different movement patterns produce distinct force profiles that necessitate specific prediction models [14]. This activity-dependent approach limits the practical application of these models in real-world settings, where individuals perform various activities throughout the day without systematic classification.

A potential solution to overcome this limitation is the use of models to automatically identify and classify activities from accelerometer data [15,16]. While various activity recognition approaches have been developed and validated in the literature, they typically focus on distinguishing between broad categories of movement (e.g., sitting, standing, walking) or common activities of daily living (e.g., household chores, stair climbing) [17,18]. Currently, there is a lack of classification models specifically designed to differentiate between the types of movements most relevant for mechanical loading and bone adaptation, such as walking, running and jumping. Such a targeted classification model would enable the appropriate application of activity-specific prediction equations, thereby improving the accuracy of mechanical loading assessment in free-living conditions. Therefore, this study aimed to develop and validate classification models capable of accurately differentiating between walking, running, and jumping activities using only accelerometer data, to enable the appropriate application of activity-specific mechanical loading prediction equations.

2. Materials and Methods

2.1. Participants

A total of 48 participants (26 males, 22 females) were recruited via convenience sampling for this study. Sample characteristics were ($\bar{X}$ ± SD): age (29.0 ± 8.3 years), height (169.3 ± 8.7 cm), body mass (69.7 ± 11.6 kg), and body mass index (24.2 ± 3.0 kg·m^{-2}). Study recruitment was conducted through email distribution within the University of Porto's academic network, detailing study aims, experimental procedures, and participation requirements. Physical measurements were obtained using standardized equipment: height was measured with a Seca stadiometer (model 213, Hamburg, Germany), while body mass was determined using a Seca digital weighing scale (model 899, Hamburg, Germany). To be eligible for participation, individuals needed to be between 18 and 65 years old and physically capable of completing the experimental protocol, which encompassed walking, running, and jumping tasks. Individuals were excluded if they reported any musculoskeletal disorders, cardiovascular conditions, or other health issues that could compromise their ability to safely perform the required activities. Prior to participation, all volunteers received detailed information about the study procedures and provided their written informed consent. The research protocol received approval from the local Ethics Committee (reference: CEFADE 15-21).

2.2. Protocol

The experimental procedures were performed at LABIOMEP-UP (Porto Biomechanics Laboratory). Participants were equipped with three ActiGraph GT9X Link accelerometers (ActiGraph, Pensacola, FL, USA), configured at 100 Hz sampling frequency with a ±16 g range. Each of the devices was placed on a different body position: one on the

anterior axillary line at iliac crest height (right hip), another at the midpoint between the posterior superior iliac spines (lower back), and a third just above the lateral malleolus (right ankle). The selection of waist-level positions (hip and lower back) was based on their proximity to the body's center of mass, enabling comprehensive movement assessment. To ensure proper device fixation, the waist-mounted accelerometers were attached using clips on an elastic belt, while the ankle unit was secured using a combination of adhesive tape and an elastic strap. Research staff personally supervised and verified the correct positioning and orientation of all devices on each participant.

The GT9X Link devices contain two triaxial accelerometers: a primary sensor with ±8 g range and proprietary filtering, and a secondary sensor with ±16 g range providing unfiltered data. For this study, we exclusively utilized data from the secondary accelerometer to maximize measurement precision and study reproducibility by avoiding potential filtering effects. Raw acceleration data along the x, y, and z axes were processed and extracted using ActiLife software (version 6.13.3; ActiGraph, Pensacola, USA). All acceleration measurements were expressed in gravitational units, where 1g equals 9.807 $m \cdot s^{-2}$.

To facilitate activity labeling during data processing, a video camera was positioned perpendicular to the movement path, at the midpoint of the laboratory's main corridor at about 100cm from the floor. This fixed camera position provided a sagittal plane view of the main laboratory path, allowing clear identification and verification of activity types and transitions during the data processing. Views from this camera can be seen in the Video S1.

2.3. Data processing

The activity data labeling process was performed using custom MATLAB scripts (version 2024b; MathWorks, Natick, MA, USA). This procedure involved visual inspection of the acceleration signals alongside video recordings. The video footage, captured from the fixed camera position in the laboratory's main corridor, served as a reference to accurately identify and verify each activity bout, as mentioned previously. Researchers manually identified the beginning and end of each activity segment using an interactive graphical interface that displayed the resultant acceleration signal, with the video timestamps helping to ensure precise temporal segmentation of the activities. The segmented data were then exported as separate files containing the raw triaxial acceleration values (x, y, and z axes) for each activity trial.

Feature extraction from the accelerometer signals was performed using the R software (version 4.3.2; R Foundation for Statistical Computing, Vienna, Austria). For each activity trial, both time- and frequency-domain features were computed using a 1-second sliding window of the triaxial acceleration data. For each acceleration axis (x, y, z), time-domain features included basic statistical measures (mean, standard deviation, coefficient of variation), distribution characteristics (skewness, kurtosis), percentile values (minimum, 25th percentile, median, 75th percentile, maximum), and amplitude-related metrics (mean and standard deviation of the signal magnitude). Similarly, frequency-domain features were calculated independently for each axis using Fast Fourier Transform (FFT), comprising dominant frequency, dominant magnitude, total power, and median frequency. Additionally, cross-axis correlations were computed between all pairs of axes (xy, xz, yz). Lastly, for the orientation features (roll, pitch, yaw), the acceleration signals were first preprocessed using a 2nd-order Butterworth low-pass filter with a 1 Hz cutoff frequency, implemented using zero-phase digital filtering to prevent phase distortion. This process resulted in a comprehensive set of 54 features per activity segment that captured both the temporal and spectral characteristics of the movements.

2.4. Statistical analyses

Three supervised machine learning algorithms were implemented to classify the activities: Random Forest (RF), Support Vector Machine (SVM) with radial basis function kernel, and K-Nearest Neighbors (KNN). The RF algorithm is an ensemble learning method that combines multiple decision trees to handle complex movement patterns [20]. SVM with radial basis function kernel creates optimal boundaries to separate different activity classes [21]. KNN classifies activities based on their similarity to known samples [22]. These algorithms were selected for their strengths in handling non-linear relationships, creating clear activity distinctions, and recognizing movement patterns in accelerometer data [23]. The dataset was split into training (80%) and testing (20%) sets using stratified sampling to maintain class proportions. Prior to model training, features were preprocessed through standardization (centering and scaling of all predictors) and removal of predictors with near-zero variance (variables that showed minimal variation across observations and thus provided little discriminative value). Model hyperparameters were optimized using a grid search approach with 5-fold cross-validation on the training set. For the RF model, we tuned the number of randomly selected predictors, and the minimum number of data points required for a node split, while fixing the number of trees at 500. The SVM model's cost parameter and kernel bandwidth were tuned, while for the KNN model, the number of neighbors was optimized. For each model, 10 different hyperparameter combinations were evaluated.

Model performance was assessed using multiple metrics: accuracy, area under the receiver operating characteristic curve (ROC-AUC), percent agreement, and Cohen's Kappa coefficient. These metrics were calculated both for overall classification performance and for each activity individually using a one-versus-all approach. All analyses were performed separately for each accelerometer placement (ankle, lower back and hip) using R (version 4.3.2) with the tidymodels framework for machine learning (version 1.2.0).

3. Results

All three machine learning algorithms demonstrated excellent classification performance across all accelerometer placements (ankle, lower back, and hip) and activities (walking, running, and jumping). Classification accuracy metrics for each model across all accelerometer placements can be found on Table 1. The overall percent agreement ranged from 93.8% to 97.7%, with ROC-AUC values consistently above 0.97 and Kappa coefficients exceeding 0.89, indicating robust classification capability regardless of the specific algorithm or sensor placement chosen.

The ankle-mounted accelerometer demonstrated marginally superior overall performance, with KNN achieving the highest accuracy (97.7% agreement, ROC-AUC = 0.991, κ = 0.961), followed by RF (96.8% agreement, ROC-AUC = 0.996, κ = 0.945), and SVM (95.9% agreement, ROC-AUC = 0.996, κ = 0.930). For the lower back placement, RF showed the best performance (95.9% agreement, ROC-AUC = 0.994, κ = 0.930), followed closely by SVM (95.7% agreement, ROC-AUC = 0.993, κ = 0.926), and KNN (93.8% agreement, ROC-AUC = 0.971, κ = 0.895). Hip-mounted accelerometers maintained similar high-performance levels, with SVM achieving the highest accuracy (95.3% agreement, ROC-AUC = 0.993, κ = 0.920), followed by RF (94.7% agreement, ROC-AUC = 0.989, κ = 0.909), and KNN (94.0% agreement, ROC-AUC = 0.981, κ = 0.899).

Table 1. Accuracy indices of machine learning algorithms for walking, running and jumping activities classification across different accelerometer placements. Cell's background is colored in grayscale, where darker cells represent higher accuracy values.

Machine Learning Algorithm	Accelerometer Placement	Percent Agreement	ROC-AUC	Kappa
Random Forest	Ankle	96.80%	0.996	0.945
	Lower Back	95.90%	0.994	0.93
	Hip	94.70%	0.989	0.909
Support Vector Machine	Ankle	95.90%	0.996	0.93
	Lower Back	95.70%	0.993	0.926
	Hip	95.30%	0.993	0.92
K-Nearest Neighbors	Ankle	97.70%	0.991	0.961
	Lower Back	93.80%	0.971	0.895
	Hip	94.00%	0.981	0.899

Abbreviation: ROC-AUC, receiver operating characteristic area under the curve.

Table 2 contains the same classification performance metrics for each model across all accelerometer placements, but specifically for each activity. When examining specific activities, all three algorithms demonstrated great performance in classifying walking activities. Very high and similar accuracy was achieved by KNN with ankle placement (98.2% agreement, ROC AUC = 0.995, $\kappa = 0.960$) and RF with lower back placement (98.4% agreement, ROC AUC = 0.999, $\kappa = 0.965$). SVM showed consistent performance across all placements, with agreement rates around 97%.

Running activities were also classified with high accuracy across all algorithms and placements with KNN with ankle placement showing the best performance (98.7% agreement, ROC AUC = 0.985, $\kappa = 0.943$). Random Forest and SVM demonstrated similar performance levels, with agreement rates ranging from 96.0% to 97.7%. The hip placement showed slightly lower but still acceptable performance compared to ankle and lower back placements.

Jumping activities were also classified with high accuracy, particularly by the ankle-mounted accelerometer. KNN achieved the highest accuracy with ankle placement (98.6% agreement, ROC AUC = 0.996, $\kappa = 0.972$). Random Forest and SVM showed strong performance as well, with agreement rates consistently above 95%. The hip placement demonstrated slightly lower accuracy compared to ankle and lower back placements, but still maintained agreement rates above 94%. These consistently high accuracy levels across all activities and placements suggest that these models could be reliably implemented in real-world applications for activity recognition and monitoring.

Analysis of the confusion matrices revealed that each algorithm demonstrated identical classification patterns across all three accelerometer placements, as can be seen in Table 3. The RF models showed exactly the same performance for all placements, correctly classifying 480 walking instances (96.8% of the cases), 163 (91.1%) running instances, and 799 (94.3%) jumping instances, with identical misclassification patterns (39 jumping instances misclassified as running, 14 running instances as jumping). Similarly, SVM maintained consistent performance across all placements, with 480 (94.5%) correct walking classifications, 185 (91.1%) correct running classifications, and 786 (96.9%) correct jumping classifications in each case. The KNN algorithm, which also showed identical results regardless of placement, correctly identified 482 (91.6%) walking instances, 185 (88.5%) running instances, and 764 (97.1%) jumping instances at all locations. Across all algorithms and placements, walking activities showed the highest classification stability with

minimal misclassifications, while the majority of classification errors occurred in distinguishing between running and jumping activities. This identical performance across placements suggests that the classification challenges were inherent to the movement patterns rather than sensor location-dependent.

Table 2. Accuracy indices of machine learning algorithms for walking, running and jumping activities classification across different accelerometer placements and activities. Cell's background is colored in grayscale, where darker cells represent higher accuracy values.

Machine Learning Algorithm	Accelerometer Placement	Activity	Percent Agreement	ROC-AUC	Kappa
Random Forest	Ankle	Walking	98.00%	0.998	0.955
		Running	97.70%	0.995	0.902
		Jumping	97.80%	0.999	0.957
	Lower Back	Walking	98.40%	0.999	0.965
		Running	96.70%	0.989	0.855
		Jumping	96.70%	0.995	0.934
	Hip	Walking	98.20%	0.998	0.96
		Running	96.00%	0.983	0.82
		Jumping	95.30%	0.991	0.905
Support Vector Machine	Ankle	Walking	97.80%	0.998	0.95
		Running	97.30%	0.994	0.882
		Jumping	96.70%	0.998	0.934
	Lower Back	Walking	97.60%	0.996	0.946
		Running	97.20%	0.992	0.878
		Jumping	96.60%	0.993	0.931
	Hip	Walking	97.40%	0.997	0.942
		Running	97.30%	0.992	0.885
		Jumping	95.90%	0.992	0.918
K-Nearest Neighbors	Ankle	Walking	98.20%	0.995	0.96
		Running	98.70%	0.985	0.943
		Jumping	98.60%	0.996	0.972
	Lower Back	Walking	95.70%	0.978	0.904
		Running	97.20%	0.965	0.883
		Jumping	94.70%	0.969	0.894
	Hip	Walking	96.50%	0.992	0.922
		Running	96.90%	0.971	0.869
		Jumping	94.60%	0.982	0.892

Abbreviation: ROC-AUC, receiver operating characteristic area under the curve.

To ensure reproducibility and facilitate implementation of our findings, both the feature extraction code and the trained classification models have been made publicly available at https://github.com/verasls/activity_recognition. The repository includes detailed documentation for implementing the processing pipeline and using the pre-trained models for activity classification.

Table 3. Confusion matrix for activity classification for each machine learning algorithm. Diagonals represent the correct classification and are highlighted in bold. All classification scores are equal across all accelerometer placements within the same algorithm.

Machine Learning Algorithm	Predicted	Observed		
		Walking	Running	Jumping
Random Forest	Walking	**480 (96.8%)**	6 (1.2%)	10 (2.0%)
	Running	2 (1.1%)	**163 (91.1%)**	14 (7.8%)
	Jumping	9 (1.1%)	39 (4.6%)	**799 (94.3%)**
Support Vector Machine	Walking	**480 (94.5%)**	8 (1.3%)	20 (3.9%)
	Running	1 (0.5%)	**185 (91.1%)**	17 (8.4%)
	Jumping	10 (1.2%)	15 (1.8%)	**786 (96.9%)**
K-Nearest Neighbors	Walking	**482 (91.6%)**	9 (1.7%)	35 (6.7%)
	Running	0 (0.0%)	**185 (88.5%)**	24 (11.5%)
	Jumping	9 (1.1%)	14 (1.8%)	**764 (97.1%)**

Data shown as n (%). Percentage values were calculated per row.

4. Discussion

This study aimed to develop and validate classification models capable of accurately differentiating between walking, running, and jumping activities using accelerometer data, to enable the appropriate application of activity-specific mechanical loading prediction equations. Three supervised machine learning algorithms (RF, SVM, and KNN) were implemented and validated using multiple performance metrics. Our results demonstrated that all three algorithms achieved excellent classification accuracy across all accelerometer placements and activities, with percent agreement ranging from 93.8% to 97.7%, ROC-AUC values consistently above 0.97, and Kappa coefficients exceeding 0.89. The ankle-mounted accelerometer showed marginally superior overall performance, with KNN achieving the highest accuracy, though all placements and algorithms demonstrated robust classification capability. These findings indicate that accelerometer-based activity classification is a reliable approach for distinguishing between walking, running, and jumping activities, providing a foundation for the accurate application of activity-specific mechanical loading prediction equations.

Our classification models demonstrated remarkably high accuracy across different accelerometer placements and activities, with only marginal differences between algorithms. The RF, SVM, and KNN algorithms all achieved overall agreement rates above 93%, with minimal variations in performance that are not practically meaningful. All machine learning models achieved slightly superior results using ankle-worn accelerometers, with a 97.7% percent agreement for KNN, 96.8% for RF and 95.9% for SVM. These minimal differences suggest that any combination of algorithm and placement could be effectively implemented.

When analyzing specific activities, walking classifications showed the highest stability across all algorithms and placements, with agreement rates consistently above 95%. Running activities were classified with similarly high accuracy, particularly by KNN with ankle placement (98.7% agreement), though the hip placement showed marginally lower performance compared to ankle and lower back placements. For jumping activities, while maintaining high accuracy levels above 94% across all conditions, the ankle-mounted accelerometer demonstrated particularly strong performance, with KNN achieving 98.6% agreement. The consistency in performance across different placements suggests that the classification challenges were inherent to the movement patterns rather than being sensor location-dependent [18,24]. This was expected, as different movement patterns produce distinct force and acceleration profiles, which is why mechanical loading prediction models are typically activity-specific [14,25]. While the ankle placement showed a slight advantage in overall accuracy, these differences were not substantial enough to preclude the use of any placement location.

Examining the performance by activity type, our models showed consistently high accuracy across all activities, with only minor variations between them. Walking was very accurately classified across all models and placements, with percent agreement ranging from 95.7% to 98.4% and ROC-AUC values above 0.992. This high accuracy for walking can be attributed to its distinctive rhythmic pattern and acceleration magnitude that clearly differentiates it from both static activities and higher-intensity movements [26,27]. Running classification showed similarly high accuracy, with percent agreement ranging from 96.0% to 98.7% across placements and models. The main challenge in running classification appeared in its occasional misclassification as jumping, particularly when using the hip placement (14 to 24 misclassified instances). This confusion likely occurs due to the similar impact characteristics of these activities, such as their high magnitude and frequency [28,29]. Jumping activities also showed high classification accuracy (94.6% to 98.6% agreement). The confusion matrices reveal that jumping was most commonly misclassified as running, with 39 instances in the RF model and 14-15 instances in the SVM and KNN models. This misclassification pattern was consistent across all accelerometer placements, suggesting that the challenge lies in the inherent similarity of the movement patterns rather than sensor location [30]. The ankle placement showed marginally better discrimination between jumping and running activities, likely due to an ability to better capture the distinct landing mechanics of jumps versus running strides [31].

Our results can be compared with several previous studies that used similar methodologies for activity classification. Bach et al. (2022) [17] used a dual accelerometer setup (lower back and thigh) with an extreme gradient boosting classifier to detect sitting, standing, lying, walking, running, and cycling during free-living conditions. Their dual-accelerometer setup achieved up to 96% accuracy, while their single thigh and back accelerometer setups achieved up to 93% and 84% accuracy, respectively. In comparison, our models achieved similar accuracies (93.8-97.7%) but with single accelerometer placements, suggesting that our approach might be more efficient as it eliminates the need for multiple sensors. Chong et al. (2021) [15] used a single hip-worn accelerometer to classify activities including lying, standing, walking, jogging, cycling, and various daily activities, testing artificial neural networks, SVM, and RF algorithms. For the hip placement, which allows direct comparison with our study, their models achieved accuracies between 86.9% and 88.0%, while our hip-placed models achieved 94.0-95.3% accuracy across all three algorithms, representing a consistent improvement. Nunavath et al. (2021) [32] employed deep learning approaches (deep feed-forward neural network and deep recurrent neural network) with both wrist-worn and hip-worn accelerometers to classify various activities including lying, sitting, standing, walking, running, and other daily activities. For the hip-worn setup classifying walking and running activities, they achieved accuracies between

84.89% and 89.31%, while our machine learning approaches achieved 94.0-95.3% accuracy for the same placement, suggesting that simpler algorithms might be more effective for this specific classification task.

The current study presents several key methodological strengths. First, while each model requires only a single accelerometer to function, we validated our approach across three different placements (ankle, lower back, and hip), achieving consistently high accuracy across all locations. This multi-placement validation is particularly valuable as it allows researchers to select the most appropriate placement for their specific needs [33], making our models compatible with existing datasets and studies that may have used different sensor locations. Second, our focus on walking, running, and jumping activities was specifically designed to address the needs of bone health research, as these activities are consistently shown to promote positive skeletal adaptations and are widely prescribed in bone health interventions [4,34]. The high classification accuracy achieved for these particular activities (>94% agreement across all activities) enhances the models' utility for monitoring and prescribing bone-targeted exercise interventions. Third, the robust performance across different machine learning algorithms (RF, SVM, and KNN) and accelerometer placements demonstrates the reliability and stability of our approach, with all combinations achieving above 93% agreement. Finally, to ensure practical implementation of our findings, we have made available both the feature extraction code and the trained classification models. This open availability of the complete analysis pipeline significantly facilitates the direct application of our methods in future research and clinical practice, addressing a common limitation in machine learning studies in which methods are often not readily implementable by other researchers.

The activity classification models developed in this study open important practical applications, particularly when integrated with previously developed mechanical loading prediction equations [10,11,13,28,29]. By accurately identifying specific activities, these models address a critical limitation in mechanical loading assessment, as applying equations without distinguishing between activity types can lead to significant prediction errors – for instance, using walking-based equations for running or jumping activities could substantially underestimate peak forces and loading rates due to the distinct biomechanical characteristics of each movement [35,36]. Our models enable the appropriate application of activity-specific equations to free-living data through automated activity classification, allowing accurate prediction of mechanical loading variables such as ground reaction forces and loading rates, which are key determinants of bone adaptation [37,38].

This integration provides a comprehensive method to monitor both the type and mechanical load characteristics of physical activities in free-living conditions. Such capability has significant implications for bone health monitoring, as it allows researchers and clinicians to precisely quantify the osteogenic potential of daily activities by combining information about movement patterns and their associated mechanical loads [39], for which there is currently no available tool. In exercise prescription and rehabilitation, this method could also help ensure that patients receive adequate bone-stimulating forces while avoiding excessive loads that might increase injury risk [40,41]. For instance, clinicians could monitor not only if a patient is performing the prescribed activities (e.g., walking versus running), but also track the cumulative mechanical loading throughout the day [42]. However, considerations for real-world implementation include the need of strategies for managing data collection and processing in large-scale studies, and the development of user-friendly interfaces for clinicians and researchers who may not have programming expertise.

Some limitations should also be acknowledged. First, while our sample size of 48 participants was adequate for model development and validation, it may not fully capture the variability in movement patterns across different populations. Future studies should

validate these models in larger and more diverse cohorts, particularly including participants with greater variability in age, body mass, and pathologies, as these factors are known to influence model performance [43]. Second, although our protocol included various activities performed in a semi-controlled environment, it may not completely represent the complexity and variability of movements in free-living conditions. Despite instructing participants to perform activities naturally, the laboratory setting might have influenced their movement patterns. Therefore, future research should validate these models during extended periods of free-living activities to ensure their reliability in real-world conditions.

In conclusion, this study successfully developed and validated machine learning models capable of accurately classifying walking, running, and jumping activities using accelerometer data from a single sensor. The high classification accuracy achieved across different algorithms (RF, SVM, and KNN), accelerometer placements (ankle, lower back, and hip), and activities (walking, running and jumping) demonstrates the robustness and reliability of our approach. The consistent performance across different sensor locations provides researchers flexibility in choosing the most appropriate placement for their specific needs. When combined with previously developed mechanical loading prediction equations, these models enable the comprehensive assessment of both activity types and their associated mechanical loads during free-living conditions. This integration represents a significant advancement in the objective monitoring of bone-targeted exercise interventions, offering researchers and clinicians a practical tool for quantifying the osteogenic potential of daily activities.

Supplementary Materials: The following supporting information can be downloaded at: www.mdpi.com/xxx/s1, Video S1: View from the camera used in the protocol.

Author Contributions: Conceptualization, Lucas Veras, Florêncio Diniz-Sousa, Giorjines Boppre, José Oliveira and Hélder Fonseca; Formal analysis, Lucas Veras; Investigation, Lucas Veras, Florêncio Diniz-Sousa, Giorjines Boppre, Ana Resende-Coelho, José Oliveira and Hélder Fonseca; Methodology, Lucas Veras, Florêncio Diniz-Sousa, Giorjines Boppre, José Oliveira and Hélder Fonseca; Software, Lucas Veras; Writing – original draft, Lucas Veras and Hélder Fonseca; Writing – review & editing, Lucas Veras, Florêncio Diniz-Sousa, Giorjines Boppre, Ana Resende-Coelho, José Oliveira and Hélder Fonseca.

Funding: This work was performed at the Research Centre in Physical Activity, Health and Leisure (CIAFEL), Faculty of Sport, University of Porto (FADEUP), funded by Fundação Para a Ciência e Tecnologia (FCT grants UIDB/00617/2020, doi: 10.54499/UIDB/00617/2020 and UIDP/00617/2020, doi: 10.54499/UIDP/00617/2020) and the Laboratory for Integrative and Translational Research in Population Health (ITR; FCT grant LA/P/0064/2020). L.V., F.D.-S., and G.B. were supported by the FCT (grant numbers UI/BD/150673/2020, SFRH/BD/117622/2016, and SFRH/BD/146976/2019).

Institutional Review Board Statement: The study was conducted in accordance with the Declaration of Helsinki, and approved by the Ethics Committee of the Faculty of Sport, University of Porto (protocol code CEFADE 15-21, approved on 11 May 2021).

Informed Consent Statement: Informed consent was obtained from all subjects involved in the study.

Data Availability Statement: The data presented in this study are available on request from the corresponding author.

Acknowledgments: The authors thank the participants who took part in this research and all who have collaborated in the research project.

Conflicts of Interest: The authors declare no conflict of interest.

Abbreviations

The following abbreviations are used in this manuscript:

KNN	K-nearest neighbors
RF	Random forest
ROC-AUC	Area under the receiver operating characteristic curve
SVM	Support vector machine

References

1. Fonseca, H.; Moreira-Gonçalves, D.; Coriolano, H.-J.A.; Duarte, J.A. Bone Quality: The Determinants of Bone Strength and Fragility. *Sports Med.* **2014**, *44*, 37–53, doi:10.1007/s40279-013-0100-7.
2. Rosa, N.; Simoes, R.; Magalhães, F.D.; Marques, A.T. From Mechanical Stimulus to Bone Formation: A Review. *Med. Eng. Phys.* **2015**, *37*, 719–728, doi:10.1016/j.medengphy.2015.05.015.
3. Turner, C.H.; Robling, A.G. Designing Exercise Regimens to Increase Bone Strength. *Exerc. Sport Sci. Rev.* **2003**, *31*, 45–50, doi:10.1097/00003677-200301000-00009.
4. Beck, B.R.; Daly, R.M.; Singh, M.A.F.; Taaffe, D.R. Exercise and Sports Science Australia (ESSA) Position Statement on Exercise Prescription for the Prevention and Management of Osteoporosis. *J. Sci. Med. Sport* **2017**, *20*, 438–445, doi:10.1016/j.jsams.2016.10.001.
5. Kemmler, W.; Häberle, L.; von Stengel, S. Effects of Exercise on Fracture Reduction in Older Adults: A Systematic Review and Meta-Analysis. *Osteoporos. Int.* **2013**, *24*, 1937–1950, doi:10.1007/s00198-012-2248-7.
6. Turner, C.H.; Owan, I.; Takano, Y. Mechanotransduction in Bone: Role of Strain Rate. *Am. J. Physiol.-Endocrinol. Metab.* **1995**, *269*, E438–E442, doi:10.1152/ajpendo.1995.269.3.E438.
7. Rubin, C.T.; Lanyon, L.E. Regulation of Bone Formation by Applied Dynamic Loads. *J. Bone Jt. Surg.* **1984**, *66*, 397.
8. Ren, S.; Chen, Z.; Qin, X.; Zhao, X.; Yang, T.D.; Zhu, W. Measurement and Evaluation of Bone Loading in Physical Activity: A Systematic Review. *Meas. Phys. Educ. Exerc. Sci.* **2021**, *25*, 149–162, doi:10.1080/1091367X.2020.1855590.
9. Medved, V. *Measurement of Human Locomotion*; CRC Press: Boca Raton, 2000; ISBN 978-0-429-11775-6.
10. Fortune, E.; Morrow, M.M.; Kaufman, K.R. Assessment of Gait Kinetics Using Triaxial Accelerometers. *J. Appl. Biomech.* **2014**, *30*, 668–674, doi:10.1123/jab.2014-0037.
11. Neugebauer, J.M.; Collins, K.H.; Hawkins, D.A. Ground Reaction Force Estimates from ActiGraph GT3X+ Hip Accelerations. *PLOS ONE* **2014**, *9*, e99023, doi:10.1371/journal.pone.0099023.
12. Neugebauer, J.M.; Hawkins, D.A.; Beckett, L. Estimating Youth Locomotion Ground Reaction Forces Using an Accelerometer-Based Activity Monitor. *PLOS ONE* **2012**, *7*, e48182, doi:10.1371/journal.pone.0048182.
13. Veras, L.; Diniz-Sousa, F.; Boppre, G.; Devezas, V.; Santos-Sousa, H.; Preto, J.; Vilas-Boas, J.P.; Machado, L.; Oliveira, J.; Fonseca, H. Accelerometer-Based Prediction of Skeletal Mechanical Loading during Walking in Normal Weight to Severely Obese Subjects. *Osteoporos. Int.* **2020**, *31*, 1239–1250, doi:10.1007/s00198-020-05295-2.
14. Ancillao, A.; Tedesco, S.; Barton, J.; O'Flynn, B. Indirect Measurement of Ground Reaction Forces and Moments by Means of Wearable Inertial Sensors: A Systematic Review. *Sensors* **2018**, *18*, 2564, doi:10.3390/s18082564.
15. Chong, J.; Tjurin, P.; Niemelä, M.; Jämsä, T.; Farrahi, V. Machine-Learning Models for Activity Class Prediction: A Comparative Study of Feature Selection and Classification Algorithms. *Gait Posture* **2021**, *89*, 45–53, doi:10.1016/j.gaitpost.2021.06.017.
16. Preece, S.J.; Goulermas, J.Y.; Kenney, L.P.J.; Howard, D. A Comparison of Feature Extraction Methods for the Classification of Dynamic Activities From Accelerometer Data. *IEEE Trans. Biomed. Eng.* **2009**, *56*, 871–879, doi:10.1109/TBME.2008.2006190.
17. Bach, K.; Kongsvold, A.; Bårdstu, H.; Bardal, E.M.; Kjærnli, H.S.; Herland, S.; Logacjov, A.; Mork, P.J. A Machine Learning Classifier for Detection of Physical Activity Types and Postures During Free-Living. *J. Meas. Phys. Behav.* **2022**, *5*, 24–31, doi:10.1123/jmpb.2021-0015.
18. Attal, F.; Mohammed, S.; Dedabrishvili, M.; Chamroukhi, F.; Oukhellou, L.; Amirat, Y. Physical Human Activity Recognition Using Wearable Sensors. *Sensors* **2015**, *15*, 31314–31338, doi:10.3390/s151229858.
19. Veras, L.; Oliveira, D.; Diniz-Sousa, F.; Boppre, G.; Resende-Coelho, A.; Oliveira, J.; Fonseca, H. External Validation of Accelerometry-Based Mechanical Loading Prediction Equations. *Appl. Sci.* **2024**, *14*, 10292, doi:10.3390/app142210292.
20. Breiman, L. Random Forests. *Mach. Learn.* **2001**, *45*, 5–32, doi:10.1023/A:1010933404324.
21. Burges, C.J.C. A Tutorial on Support Vector Machines for Pattern Recognition. *Data Min. Knowl. Discov.* **1998**, *2*, 121–167, doi:10.1023/A:1009715923555.
22. Cunningham, P.; Delany, S.J. K-Nearest Neighbour Classifiers - A Tutorial. *ACM Comput Surv* **2021**, *54*, 128:1-128:25, doi:10.1145/3459665.
23. James, G.; Witten, D.; Hastie, T.; Tibshirani, R. *An Introduction to Statistical Learning with Applications in R*; Springer: New York, 2022; ISBN 978-1-0716-1420-4.
24. Cleland, I.; Kikhia, B.; Nugent, C.; Boytsov, A.; Hallberg, J.; Synnes, K.; McClean, S.; Finlay, D. Optimal Placement of Accelerometers for the Detection of Everyday Activities. *Sensors* **2013**, *13*, 9183–9200, doi:10.3390/s130709183.

25. Verheul, J.; Warmenhoven, J.; Lisboa, P.; Gregson, W.; Vanrenterghem, J.; Robinson, M.A. Identifying Generalised Segmental Acceleration Patterns That Contribute to Ground Reaction Force Features across Different Running Tasks. *J. Sci. Med. Sport* **2019**, *22*, 1355–1360, doi:10.1016/j.jsams.2019.07.006.
26. Zheng, X.; Otten, E.; Reneman, M.F.; Lamoth, C.J. Explaining Deep Learning Models for Age-Related Gait Classification Based on Acceleration Time Series. *Comput. Biol. Med.* **2025**, *184*, 109338, doi:10.1016/j.compbiomed.2024.109338.
27. Mannini, A.; Sabatini, A.M. Machine Learning Methods for Classifying Human Physical Activity from On-Body Accelerometers. *Sensors* **2010**, *10*, 1154–1175, doi:10.3390/s100201154.
28. Veras, L.; Diniz-Sousa, F.; Boppre, G.; Resende-Coelho, A.; Moutinho-Ribeiro, E.; Devezas, V.; Santos-Sousa, H.; Preto, J.; Vilas-Boas, J.P.; Machado, L.; et al. Mechanical Loading Prediction through Accelerometry Data during Walking and Running. *Eur. J. Sport Sci.* **2023**, *23*, 1518–1527, doi:10.1080/17461391.2022.2102437.
29. Veras, L.; Diniz-Sousa, F.; Boppre, G.; Devezas, V.; Santos-Sousa, H.; Preto, J.; Vilas-Boas, J.P.; Machado, L.; Oliveira, J.; Fonseca, H. Using Raw Accelerometer Data to Predict High-Impact Mechanical Loading. *Sensors* **2023**, *23*, 2246, doi:10.3390/s23042246.
30. Liu, S.; Gao, R.X.; John, D.; Staudenmayer, J.W.; Freedson, P.S. Multisensor Data Fusion for Physical Activity Assessment. *IEEE Trans. Biomed. Eng.* **2012**, *59*, 687–696, doi:10.1109/TBME.2011.2178070.
31. Bezuidenhout, L.; Thurston, C.; Hagströmer, M.; Moulaee Conradsson, D. Validity of Hip and Ankle Worn Actigraph Accelerometers for Measuring Steps as a Function of Gait Speed during Steady State Walking and Continuous Turning. *Sensors* **2021**, *21*, 3154, doi:10.3390/s21093154.
32. Nunavath, V.; Johansen, S.; Johannessen, T.S.; Jiao, L.; Hansen, B.H.; Berntsen, S.; Goodwin, M. Deep Learning for Classifying Physical Activities from Accelerometer Data. *Sensors* **2021**, *21*, 5564, doi:10.3390/s21165564.
33. Migueles, J.H.; Cadenas-Sanchez, C.; Ekelund, U.; Delisle Nyström, C.; Mora-Gonzalez, J.; Löf, M.; Labayen, I.; Ruiz, J.R.; Ortega, F.B. Accelerometer Data Collection and Processing Criteria to Assess Physical Activity and Other Outcomes: A Systematic Review and Practical Considerations. *Sports Med.* **2017**, *47*, 1821–1845, doi:10.1007/s40279-017-0716-0.
34. Kohrt, W.M.; Bloomfield, S.A.; Little, K.D.; Nelson, M.E.; Yingling, V.R.; American College of Sports Medicine American College of Sports Medicine Position Stand: Physical Activity and Bone Health. *Med. Sci. Sports Exerc.* **2004**, *36*, 1985–1996, doi:10.1249/01.mss.0000142662.21767.58.
35. Rowlands, A.V.; Stiles, V.H. Accelerometer Counts and Raw Acceleration Output in Relation to Mechanical Loading. *J. Biomech.* **2012**, *45*, 448–454, doi:10.1016/j.jbiomech.2011.12.006.
36. Ahola, R.; Korpelainen, R.; Vainionpää, A.; Jämsä, T. Daily Impact Score in Long-Term Acceleration Measurements of Exercise. *J. Biomech.* **2010**, *43*, 1960–1964, doi:10.1016/j.jbiomech.2010.03.021.
37. Yuan, Y.; Chen, X.; Zhang, L.; Wu, J.; Guo, J.; Zou, D.; Chen, B.; Sun, Z.; Shen, C.; Zou, J. The Roles of Exercise in Bone Remodeling and in Prevention and Treatment of Osteoporosis. *Prog. Biophys. Mol. Biol.* **2016**, *122*, 122–130, doi:10.1016/j.pbiomolbio.2015.11.005.
38. Robling, A.G.; Turner, C.H. Mechanical Signaling for Bone Modeling and Remodeling. *Crit. Rev. Eukaryot. Gene Expr.* **2009**, *19*, 319–338.
39. Tobias, J.H.; Gould, V.; Brunton, L.; Deere, K.; Rittweger, J.; Lipperts, M.; Grimm, B. Physical Activity and Bone: May the Force Be with You. *Front. Endocrinol.* **2014**, *5*, 20, doi:10.3389/fendo.2014.00020.
40. Warden, S.J.; Davis, I.S.; Fredericson, M. Management and Prevention of Bone Stress Injuries in Long-Distance Runners. *J. Orthop. Sports Phys. Ther.* **2014**, *44*, 749–765, doi:10.2519/jospt.2014.5334.
41. Warden, S.J.; Edwards, W.B.; Willy, R.W. Preventing Bone Stress Injuries in Runners with Optimal Workload. *Curr. Osteoporos. Rep.* **2021**, *19*, 298–307, doi:10.1007/s11914-021-00666-y.
42. Diniz-Sousa, F.; Veras, L.; Boppre, G.; Devezas, V.; Santos-Sousa, H.; Preto, J.; Machado, L.; Vilas-Boas, J.P.; Oliveira, J.; Fonseca, H. The Effect of Bariatric Surgery on Gravitational Loading and Its Impact on Bone Mass. *Bone* **2021**, *153*, 116153, doi:10.1016/j.bone.2021.116153.
43. Welk, G.J. Principles of Design and Analyses for the Calibration of Accelerometry-Based Activity Monitors. *Med. Sci. Sports Exerc.* **2005**, *37*, S501, doi:10.1249/01.mss.0000185660.38335.de.

Disclaimer/Publisher's Note: The statements, opinions and data contained in all publications are solely those of the individual author(s) and contributor(s) and not of MDPI and/or the editor(s). MDPI and/or the editor(s) disclaim responsibility for any injury to people or property resulting from any ideas, methods, instructions or products referred to in the content.

Chapter 4: General discussion

4.1. General discussion

This thesis was structured to achieve two main objectives. The first was to develop and validate accelerometer-based mechanical loading prediction equations for walking, running, and jumping activities and to test the external validation of existing mechanical loading prediction equations. The second objective was to develop and validate activity classification algorithms capable of accurately differentiating these activities using only accelerometer data. By addressing these two key aims, this thesis sought to advance the field of accelerometer-based mechanical loading assessment, enhancing the accuracy and practical applicability of these methods for monitoring mechanical loading in free-living conditions.

The first two studies focused on developing and validating accelerometer-based prediction equations for estimating peak ground reaction forces and peak loading rates during walking, running, and jumping activities. These studies demonstrated that peak ground reaction forces could be accurately predicted using accelerometer data from the ankle, lower back, and hip. However, the peak loading rate prediction equations yielded much lower accuracies, highlighting the challenge of capturing the rapid changes in force that occur during high-impact activities using accelerometers with relatively low sampling frequencies [41]. Despite this limitation, the development of these prediction equations represents a significant step forward in the field of accelerometer-based mechanical loading assessment, as they enable the estimation of key loading parameters during a wide range of activities known to stimulate bone adaptation [9].

The third study provided the external validation of existing prediction equations by applying them to a new sample and testing conditions, revealing substantial variability in prediction accuracy across different equations and activities. This study emphasized the importance of considering population-specific factors, such as age, sex, and body composition, and movement-specific tasks, such as freely walking and running at different speeds and jumps at various heights and directions, when applying prediction equations developed in other cohorts [47,48].

These findings have important implications for using accelerometer-based methods in research and clinical settings, as they underscore the need for careful selection and validation of prediction equations based on the characteristics of the target population and the activities of interest [35,47].

The fourth study developed and validated activity classification models for differentiating between walking, running, and jumping activities using accelerometer data, achieving high classification accuracy across all accelerometer placements. This study addressed a critical gap in the field, as previous research has primarily focused on developing accelerometer-based mechanical loading prediction equations tailored to specific activities [29–32,38,39,147]. This was essential to achieve acceptable levels of accuracy, as the relationship between acceleration and ground reaction force varies with the movement being performed [35]. However, the practical application of these prediction equations in free-living conditions has been limited due to the lack of a reliable method to classify these activities outside laboratory settings accurately [41,132]. By demonstrating the feasibility of accurately classifying bone-loading activities using accelerometer data, this study lays the foundation for applying activity-specific prediction equations in real-world settings, where individuals engage in various activities throughout the day. Integrating activity classification models with mechanical loading prediction equations represents a powerful approach for assessing the mechanical loading experienced by the skeleton, which is a key determinant of bone health [9,69].

The first and second studies recruited more diverse samples than previous research [29–31,38], which aimed to develop more robust and generalizable prediction equations. However, as demonstrated by the third study, the external validation of these equations revealed substantial variability in prediction accuracy across different populations and activities, emphasizing the need for further refinement of these methods. Additionally, these studies included a wide range of activities, such as walking, running, and jumping, among the most commonly prescribed exercises for improving bone health [16,17,54].

Study 1 yielded excellent results for ground reaction force prediction during walking and running, with errors of less than 7%, while loading rate prediction was noticeably worse, with prediction errors of around 19%. These models generally performed well when compared to previous literature [30,31]. The ground reaction force prediction models for walking and running showed similar accuracy to the best results from Fortune et al. (2014) [31], which had errors of around 6.5% for walking only and outperformed the accuracy achieved by Neugebauer et al. (2014) [30] of approximately 8%. Moreover, the loading rate prediction models from Study 1 were better than those obtained by Fortune et al. [31], whose best results had errors of approximately 25% for walking only.

The superior results compared to previous literature can be attributed to our substantially larger sample of 131 subjects in Study 1, in contrast to the 10 subjects in Fortune et al. (2014) [31] and 39 in Neugebauer et al. (2014) [30]. Furthermore, Study 1 tested 13 speeds between walking and running and utilized data from multiple strides at each speed. Fortune et al. (2014) [31] used data from 1 to 5 steps per trial and measured 8 to 10 trials of walking at varying speeds. Although Neugebauer et al. (2014) [30] used more trials than our study (8-10 walking and 8-10 running trials), they only used data from a single step per trial. As the models from our Study 1 were trained with a considerably larger number of data points, they could more comprehensively capture the relationship between acceleration and ground reaction forces during walking and running, resulting in better estimates.

Study 2 achieved lower accuracy for ground reaction force and loading rate prediction during jumping compared to the prediction models for walking and running. The overall results for jumping ground reaction force prediction produced around 14% error, while jumping loading rate prediction showed lower accuracy, with prediction errors of around 22%. We hypothesize that this is due to the more variable movement patterns in jumping and the inclusion of several different types and heights of jumps in a diverse sample in terms of body composition and motor skills.

When testing the accuracy of the mechanical loading prediction models in a different sample for external validation in Study 3, the prediction equations from Study 1 for walking showed unacceptable errors, reaching 80% for ground reaction force prediction and 120% for loading rate prediction. In contrast, when tested in this external sample, equations from Neugebauer et al. (2014) [30] had walking ground reaction force prediction errors of just around 10%. For running prediction, models from Study 1 presented errors of around 12%, while Neugebauer et al. (2014) [30] prediction errors were around 11%, showing very similar results. A possible explanation for the inflated errors in mechanical loading prediction during walking with the equations from Study 1 is that a large portion of this study's walking sample comprised patients with class II-III obesity, which may not have generalized well to the external validation sample from Study 3, mainly consisting of individuals with body mass index classified as normal. This issue did not affect the mechanical loading prediction equations during running, as most patients with obesity did not perform the running trials due to physical limitations, resulting in a running sample more similar to the characteristics of the external validation sample from Study 3. This confirms previous reports in the literature that accelerometer-based prediction equations must be applied to samples with characteristics similar to those of their original study to achieve better prediction accuracy [47,48].

The jumping mechanical loading prediction equations from Study 2 showed lower accuracy in the external validation sample of Study 3, which was expected [47,48]. However, the difference in prediction accuracy was minimal, particularly for predictions based on data from lower back- or hip-worn accelerometers, where the prediction errors increased from around 13% in the original study (Study 2) to around 16% in the external validation study (Study 3). This is remarkable, as Study 3 included types of jumps that were not included in the original validation study, demonstrating the generalizability of the findings from Study 2, especially for the lower back and hip accelerometer placements.

The machine learning algorithms for activity classification developed in Study 4 showed very high classification accuracy across all accelerometer placements and machine learning algorithms, with all results above 90% accuracy [133,134,143,144]. These results are comparable to the highest classification accuracy found in the literature but are tailored to classify the most commonly recommended activities for bone health improvement. These models are particularly useful in this context, especially when combined with the mechanical loading prediction models.

One of the key strengths of the studies that form this thesis is the inclusion of multiple accelerometer placements, namely at the ankle, lower back, and hip, and the validation of prediction equations and classification models across these different sensor locations. This comprehensive approach allows for the comparison of model performance across different body sites. It allows researchers to choose the most appropriate placement for their specific research questions or practical constraints [142]. For example, hip-worn accelerometers have been widely used in large-scale epidemiological studies and are often preferred for long-term monitoring due to their comfort and unobtrusiveness [37,125].

Another strength of this thesis is the use of advanced statistical methods and machine learning techniques for developing and validating prediction equations and classification models, reflecting an advance regarding regression methods frequently used in the literature. The first two studies employed linear mixed models, which account for the hierarchical structure of the data (i.e., multiple observations per participant) and allow for the inclusion of both fixed and random effects [160]. This approach has been shown to provide more accurate and precise estimates compared to traditional regression models, particularly when dealing with repeated measures data [161]. The fourth study utilized a range of machine learning algorithms, including random forests, support vector machines, and k-nearest neighbors, which have demonstrated high performance in classification tasks [162–164].

Despite the contributions of this thesis to the field of accelerometer-based mechanical loading assessment, it is important to acknowledge certain limitations. One of the main limitations is the low accuracy of the peak loading rate prediction equations, which may not be sufficiently reliable for use in clinical or research settings. This is particularly concerning, given the importance of loading rates in determining the osteogenic potential of mechanical stimuli [13,45,46]. High loading rates have been shown to elicit greater bone adaptation compared to low loading rates, even when the peak forces are similar [68]. Therefore, the ability to accurately predict loading rates is crucial for understanding the mechanisms underlying the relationship between physical activity and bone health and designing effective interventions to optimize bone loading [165]. Future research should prioritize the development of more accurate loading rate prediction equations by exploring new signal processing techniques, which could be better suited to capturing the rapid changes in force that occur during high-impact activities. Additionally, the use of machine learning algorithms, such as neural networks or support vector regression, may provide a more flexible and adaptive approach to modeling the complex relationship between accelerometer output and loading rates [163,166]. Finally, using accelerometers with higher sampling frequencies (e.g., 200 Hz or above) may be necessary to fully capture the high-frequency components of the loading signal [41].

Another limitation of the studies presented in this thesis is focusing on a relatively narrow range of activities, primarily walking, running, and jumping. While these activities are important for bone health and are commonly prescribed in exercise interventions [16,17,54], they do not represent the full spectrum of mechanical loading experienced by the skeleton during daily life [21]. Many occupational, recreational, and household activities, such as lifting, carrying, and stair climbing, also impose significant mechanical loads on the bones and may contribute to the osteogenic stimulus [25,109]. Moreover, the prediction equations developed in this thesis have not been validated for sport-specific movements, such as side-cutting maneuvers in soccer or vertical jumps in volleyball, which are known

to impose high mechanical loads on the skeleton [167]. To fully capture the mechanical loading profile of an individual, it is necessary to develop and validate prediction equations and classification models for a broader range of activities, including both everyday daily tasks and sport-specific movements.

Despite the study's limitations, the accelerometer-based methods developed and validated in this thesis have numerous practical applications and clinical implications for bone health assessment, monitoring, and management. These methods offer a continuous and objective measure of physical activity, enabling more accurate quantification of the mechanical loading experienced by the skeleton compared to traditional subjective methods, such as questionnaires [26,122]. By providing detailed insights into the magnitude, frequency, and duration of mechanical loading during various activities, the prediction equations developed in the first and second studies can be applied to accelerometer data collected in free-living conditions to assess an individual's daily mechanical loading profile. This information can help researchers and clinicians better understand the relationship between physical activity and bone health, identify individuals who may not be engaging in sufficient bone-stimulating activities, and guide the prescription of targeted interventions and personalized exercise recommendations to improve bone health.

For example, the equations could be used to monitor the mechanical loading experienced by older adults at risk of osteoporosis. By tracking daily activities and estimating the associated ground reaction forces and loading rates, clinicians could calculate the total mechanical loading experienced over a given period and compare it to established thresholds for maintaining bone mass [168]. If an individual is found to have inadequate mechanical stimulation, personalized exercise recommendations could be provided, such as increasing the duration or intensity of weight-bearing activities or incorporating additional high-impact exercises into their daily routine [102,169]. This approach could help optimize exercise interventions for bone health by ensuring that individuals receive sufficient mechanical stimulation to

maintain or improve bone strength while minimizing the risk of overloading or injury [18,169].

Similarly, the equations could be used to assess the mechanical loading experienced by athletes and to optimize their training programs for bone health. This application is particularly important, as athletes engaged in high-impact sports, such as gymnastics, basketball, and volleyball, have been shown to have higher bone mineral density compared to those involved in low-impact sports, such as swimming and cycling [170,171]. By quantifying the mechanical loading experienced during different training activities, coaches and exercise physiologists could design programs to maximize the osteogenic potential while minimizing the risk of overuse injuries [12,172]. However, it is essential to note that the current prediction equations have been primarily validated for activities such as walking, running, and jumping. Their applicability to sport-specific movements may be limited. Future research should thereby focus on developing and validating prediction equations for a broader range of sport-specific activities, such as cutting maneuvers and landing tasks, to enable the effective use of these methods in athletic populations.

The activity classification models developed in the fourth study also have important practical applications for bone health assessment. These models can automatically identify the type of activity being performed based on accelerometer data, allowing for the application of activity-specific prediction equations in free-living conditions, where individuals engage in various activities throughout the day [51]. By integrating these classification models into wearable devices or smartphone applications, users could receive real-time feedback and personalized recommendations based on their daily activity profile, such ting them to increase their step count or engage in high-impact activities. This type of personalized custom has been shown to be effective in promoting behavior change and improving health outcomes. It could be particularly useful for individuals at risk of bone disorders who may benefit from targeted interventions to increase their mechanical loading [173,174].

In research settings, the accelerometer-based methods developed in this thesis have significant potential for investigating the effectiveness of interventions for improving bone health and for better understanding the dose-response relationship between mechanical loading and bone health outcomes. Researchers can objectively assess the patient's response and optimize treatment outcomes by quantifying mechanical loading before and after an intervention, such as a new exercise program or medication. Furthermore, these methods can be applied in large-scale studies to investigate the associations between different loading profiles and bone health outcomes, such as changes in bone mineral density, microarchitecture, and strength [10,18,28,92,109]. This type of research could help to identify the specific loading characteristics that are most effective for promoting bone health, such as the optimal magnitude, frequency, and duration of loading, as well as the relative importance of different loading parameters, such as peak forces versus loading rates [9]. Ultimately, this knowledge could inform the development of evidence-based physical activity and exercise guidelines specifically tailored to optimize bone health outcomes in different populations.

There are several key areas for future research and development in the accelerometer-based mechanical loading assessment field. Firstly, there is a need to test the existing prediction equations and classification models in diverse populations and settings to assess their generalizability and identify potential limitations. When existing methods do not perform adequately, new prediction equations and classification models should be developed and validated to ensure their applicability to the target population. This may require collecting new accelerometer datasets designed to capture the unique loading patterns and movement characteristics of these populations.

Secondly, future research should focus on extending the prediction equations and classification models to a wider range of activities and loading conditions, beyond just walking, running, and jumping. This should include the development of equations and models for sport-specific activities, such as cutting maneuvers,

landing tasks, and resistance exercises, which are known to impose high mechanical loads on the skeleton [80,167]. Additionally, there is a need for prediction equations and classification models that can accurately assess mechanical loading during activities of daily living, such as stair climbing, lifting, and carrying. By capturing a more comprehensive range of activities, these methods could provide a more complete picture of an individual's mechanical loading profile and enable more targeted interventions to optimize bone health [175].

Furthermore, future research should explore integrating accelerometer-based methods with other technologies and data sources to provide a more comprehensive assessment of bone health. For example, combining accelerometer data with imaging techniques, such as dual-energy X-ray absorptiometry or high-resolution peripheral quantitative computed tomography, could provide a more detailed understanding of the relationship between mechanical loading and bone structure and strength [176–178]. By combining information on the magnitude and distribution of mechanical loading with data on bone density, geometry, and microarchitecture, researchers could gain new insights into the mechanisms underlying bone adaptation and identify potential targets for intervention [178]. Similarly, integrating accelerometer data with bone metabolism biomarkers, such as bone formation and resorption markers, could provide a more dynamic and sensitive assessment of the bone response to mechanical loading [179].

Additionally, user-friendly tools and interfaces need to be developed to facilitate the implementation of accelerometer-based methods in research and clinical settings. Currently, these methods requires knowledge and expertise in data processing, statistical analysis, and machine learning, which may limit their adoption by researchers and clinicians who are not experts in these fields. To overcome this barrier, future work should focus on developing automated data processing pipelines, standardized protocols, and intuitive visualization tools to make these methods more accessible and user-friendly. This could include the development of software packages or web-based platforms that guide users through data collection,

processing, and interpretation, and providing clear recommendations for action based on the results. By making these methods more accessible and easier to use, researchers and clinicians will be better equipped to incorporate them into their work and to translate the findings into practical applications for bone health.

Finally, future research should investigate the potential of machine learning and artificial intelligence techniques to improve the accuracy and efficiency of accelerometer-based mechanical loading assessment. Machine learning algorithms, such as deep learning neural networks and support vector machines, have shown promising results in activity recognition and load prediction tasks using accelerometer data [41,148,180]. These techniques can handle large and complex datasets, learn from patterns in the data, and adapt to new situations without being explicitly programmed [162–164,181]. By leveraging these capabilities, researchers could develop more sophisticated prediction equations and classification models that can accurately assess mechanical loading across a wide range of activities and populations, without the need for extensive manual feature engineering or model tuning. Additionally, machine learning techniques could be used to identify novel loading parameters or patterns that are most predictive of bone health outcomes, beyond the isolated use of peak forces and loading rates. This type of data-driven discovery could lead to new insights into the mechanisms of bone adaptation and inform the development of more effective interventions for improving bone health.

Chapter 5: Conclusion

5.1. General conclusions and future perspectives

The findings from the original studies included in this thesis lead to the following main conclusions:

1. Accelerometry-based equations can accurately predict peak ground reaction forces during walking, running, and various jumping activities. However, peak loading rate predictions show lower accuracy than peak ground reaction force predictions for all activities.
2. External validation of mechanical loading prediction equations revealed varying accuracy and high errors, particularly for peak loading rate, emphasizing the need to refine models by accounting for individual biomechanical differences, accelerometer placement, and high-impact activities to ensure reliability in real-world applications.
3. Using accelerometer data, machine learning models can accurately classify walking, running, and jumping activities, enabling a comprehensive assessment of activity types and associated mechanical loads in free-living conditions.

The results of this thesis highlight the potential of accelerometer-based methods for assessing mechanical loading during various physical activities. However, they also underscore the need for further refinement and validation of these methods, particularly in estimating peak loading rates. Future research should focus on developing more advanced signal processing techniques and machine learning algorithms to improve the accuracy of loading rate predictions. Additionally, the development of user-friendly tools and platforms is essential to facilitate the translation of these methods into clinical and research settings, ultimately contributing to the prevention and management of bone disorders on a global scale.

Chapter 6: References

6.1. References

1. Robling, A.G.; Castillo, A.B.; Turner, C.H. Biomechanical and Molecular Regulation of Bone Remodeling. *Annu. Rev. Biomed. Eng.* 2006, *8*, 455–498, doi:10.1146/annurev.bioeng.8.061505.095721.
2. Robling, A.G.; Turner, C.H. Mechanical Signaling for Bone Modeling and Remodeling. *Crit. Rev. Eukaryot. Gene Expr.* 2009, *19*, 319–338, doi:10.1615/critreveukargeneexpr.v19.i4.50.
3. Alenghat, F.J.; Ingber, D.E. Mechanotransduction: All Signals Point to Cytoskeleton, Matrix, and Integrins. *Sci. STKE* 2002, *2002*, pe6–pe6, doi:10.1126/stke.2002.119.pe6.
4. Papachroni, K.K.; Karatzas, D.N.; Papavassiliou, K.A.; Basdra, E.K.; Papavassiliou, A.G. Mechanotransduction in Osteoblast Regulation and Bone Disease. *Trends Mol. Med.* 2009, *15*, 208–216, doi:10.1016/j.molmed.2009.03.001.
5. Ni, Z.; Zhou, S.; Li, S.; Kuang, L.; Chen, H.; Luo, X.; Ouyang, J.; He, M.; Du, X.; Chen, L. Exosomes: Roles and Therapeutic Potential in Osteoarthritis. *Bone Res.* 2020, *8*, 25, doi:10.1038/s41413-020-0100-9.
6. Jaasma, M.J.; Jackson, W.M.; Tang, R.Y.; Keaveny, T.M. Adaptation of Cellular Mechanical Behavior to Mechanical Loading for Osteoblastic Cells. *J. Biomech.* 2007, *40*, 1938–1945, doi:10.1016/j.jbiomech.2006.09.010.
7. Bonewald, L.F.; Johnson, M.L. Osteocytes, Mechanosensing and Wnt Signaling. *Bone* 2008, *42*, 606–615, doi:10.1016/j.bone.2007.12.224.
8. Klein-Nulend, J.; Bakker, A.D.; Bacabac, R.G.; Vatsa, A.; Weinbaum, S. Mechanosensation and Transduction in Osteocytes. *Bone* 2013, *54*, 182–190, doi:10.1016/j.bone.2012.10.013.
9. Turner, C.H. Three Rules for Bone Adaptation to Mechanical Stimuli. *Bone* 1998, *23*, 399–407, doi:10.1016/S8756-3282(98)00118-5.
10. Hart, N.H.; Nimphius, S.; Rantalainen, T.; Ireland, A.; Siafarikas, A.; Newton, R.U. Mechanical Basis of Bone Strength: Influence of Bone Material, Bone Structure and Muscle Action. *J. Musculoskelet. Neuronal Interact.* 2017, *17*, 114–139.
11. Fonseca, H.; Moreira-Gonçalves, D.; Coriolano, H.-J.A.; Duarte, J.A. Bone Quality: The Determinants of Bone Strength and Fragility. *Sports Med.* 2014, *44*, 37–53, doi:10.1007/s40279-013-0100-7.
12. Dolan, E.; Varley, I.; Ackerman, K.E.; Pereira, R.M.R.; Elliott-Sale, K.J.; Sale, C. The Bone Metabolic Response to Exercise and Nutrition. *Exerc. Sport Sci. Rev.* 2020, *48*, 49, doi:10.1249/JES.0000000000000215.

13. Turner, C.H.; Owan, I.; Takano, Y. Mechanotransduction in Bone: Role of Strain Rate. *Am. J. Physiol.-Endocrinol. Metab.* 1995, *269*, E438–E442, doi:10.1152/ajpendo.1995.269.3.E438.

14. Turner, C.H.; Robling, A.G. Designing Exercise Regimens to Increase Bone Strength. *Exerc. Sport Sci. Rev.* 2003, *31*, 45–50, doi:10.1097/00003677-200301000-00009.

15. Turner, C.H.; Robling, A.G. Mechanisms by Which Exercise Improves Bone Strength. *J. Bone Miner. Metab.* 2005, *23 Suppl*, 16–22, doi:10.1007/BF03026318.

16. Kohrt, W.M.; Bloomfield, S.A.; Little, K.D.; Nelson, M.E.; Yingling, V.R.; American College of Sports Medicine American College of Sports Medicine Position Stand: Physical Activity and Bone Health. *Med. Sci. Sports Exerc.* 2004, *36*, 1985–1996, doi:10.1249/01.mss.0000142662.21767.58.

17. Beck, B.R.; Daly, R.M.; Singh, M.A.F.; Taaffe, D.R. Exercise and Sports Science Australia (ESSA) Position Statement on Exercise Prescription for the Prevention and Management of Osteoporosis. *J. Sci. Med. Sport* 2017, *20*, 438–445, doi:10.1016/j.jsams.2016.10.001.

18. Allison, S.J.; Folland, J.P.; Rennie, W.J.; Summers, G.D.; Brooke-Wavell, K. High Impact Exercise Increased Femoral Neck Bone Mineral Density in Older Men: A Randomised Unilateral Intervention. *Bone* 2013, *53*, 321–328, doi:10.1016/j.bone.2012.12.045.

19. Hinton, P.S.; Nigh, P.; Thyfault, J. Effectiveness of Resistance Training or Jumping-Exercise to Increase Bone Mineral Density in Men with Low Bone Mass: A 12-Month Randomized, Clinical Trial. *Bone* 2015, *79*, 203–212, doi:10.1016/j.bone.2015.06.008.

20. Nilsson, M.; Ohlsson, C.; Odén, A.; Mellström, D.; Lorentzon, M. Increased Physical Activity Is Associated with Enhanced Development of Peak Bone Mass in Men: A Five-Year Longitudinal Study. *J. Bone Miner. Res.* 2012, *27*, 1206–1214, doi:10.1002/jbmr.1549.

21. Vainionpää, A.; Korpelainen, R.; Vihriälä, E.; Rinta–Paavola, A.; Leppäluoto, J.; Jämsä, T. Intensity of Exercise Is Associated with Bone Density Change in Premenopausal Women. *Osteoporos. Int.* 2006, *17*, 455–463, doi:10.1007/s00198-005-0005-x.

22. Stiles, V.H.; Metcalf, B.S.; Knapp, K.M.; Rowlands, A.V. A Small Amount of Precisely Measured High-Intensity Habitual Physical Activity Predicts Bone Health in Pre- and Post-Menopausal Women in UK Biobank. *Int. J. Epidemiol.* 2017, *46*, 1847–1856, doi:10.1093/ije/dyx080.

23. Medved, V. *Measurement of Human Locomotion*; CRC Press: Boca Raton, 2000; ISBN 978-0-429-11775-6.

24. Dolan, S.H.; Williams, D.P.; Ainsworth, B.E.; Shaw, J.M. Development and Reproducibility of the Bone Loading History Questionnaire. *Med. Sci. Sports Exerc.* 2006, *38*, 1121, doi:10.1249/01.mss.0000222841.96885.a8.

25. Weeks, B.K.; Beck, B.R. The BPAQ: A Bone-Specific Physical Activity Assessment Instrument. *Osteoporos. Int.* 2008, *19*, 1567–1577, doi:10.1007/s00198-008-0606-2.

26. Prince, S.A.; Adamo, K.B.; Hamel, M.E.; Hardt, J.; Connor Gorber, S.; Tremblay, M. A Comparison of Direct versus Self-Report Measures for Assessing Physical Activity in Adults: A Systematic Review. *Int. J. Behav. Nutr. Phys. Act.* 2008, *5*, 56, doi:10.1186/1479-5868-5-56.

27. Kim, S.; Baker, B.S.; Sharma-Ghimire, P.; Bemben, D.A.; Bemben, M.G. Association between Bone-Specific Physical Activity Scores and pQCT-Derived Measures of Bone Strength and Geometry in Healthy Young and Middle-Aged Premenopausal Women. *Arch. Osteoporos.* 2018, *13*, 83, doi:10.1007/s11657-018-0495-8.

28. Farr, J.N.; Lee, V.R.; Blew, R.M.; Lohman, T.G.; Going, S.B. Quantifying Bone-Relevant Activity and Its Relation to Bone Strength in Girls. *Med. Sci. Sports Exerc.* 2011, *43*, 476–483, doi:10.1249/MSS.0b013e3181eeb2f2.

29. Neugebauer, J.M.; Hawkins, D.A.; Beckett, L. Estimating Youth Locomotion Ground Reaction Forces Using an Accelerometer-Based Activity Monitor. *PLOS One* 2012, *7*, e48182, doi:10.1371/journal.pone.0048182.

30. Neugebauer, J.M.; Collins, K.H.; Hawkins, D.A. Ground Reaction Force Estimates from ActiGraph GT3X+ Hip Accelerations. *PLOS One* 2014, *9*, e99023, doi:10.1371/journal.pone.0099023.

31. Fortune, E.; Morrow, M.M.; Kaufman, K.R. Assessment of Gait Kinetics Using Triaxial Accelerometers. *J. Appl. Biomech.* 2014, *30*, 668–674, doi:10.1123/jab.2014-0037.

32. Veras, L.; Diniz-Sousa, F.; Boppre, G.; Devezas, V.; Santos-Sousa, H.; Preto, J.; Vilas-Boas, J.P.; Machado, L.; Oliveira, J.; Fonseca, H. Accelerometer-Based Prediction of Skeletal Mechanical Loading during Walking in Normal Weight to Severely Obese Subjects. *Osteoporos. Int.* 2020, *31*, 1239–1250, doi:10.1007/s00198-020-05295-2.

33. Janz, K.F.; Rao, S.; Baumann, H.J.; Schultz, J.L. Measuring Children's Vertical Ground Reaction Forces with Accelerometry during Walking, Running, and Jumping: The Iowa Bone Development Study. *Pediatr. Exerc. Sci.* 2003, *15*, 34–43, doi:10.1123/pes.15.1.34.

34. Liikavainio, T.; Bragge, T.; Hakkarainen, M.; Jurvelin, J.S.; Karjalainen, P.A.; Arokoski, J.P. Reproducibility of Loading Measurements With Skin-Mounted Accelerometers During Walking. *Arch. Phys. Med. Rehabil.* 2007, *88*, 907–915, doi:10.1016/j.apmr.2007.03.031.

35. Rowlands, A.V.; Stiles, V.H. Accelerometer Counts and Raw Acceleration Output in Relation to Mechanical Loading. *J. Biomech.* 2012, *45*, 448–454, doi:10.1016/j.jbiomech.2011.12.006.

36. Troiano, R.P.; McClain, J.J.; Brychta, R.J.; Chen, K.Y. Evolution of Accelerometer Methods for Physical Activity Research. *Br. J. Sports Med.* 2014, *48*, 1019–1023, doi:10.1136/bjsports-2014-093546.

37. Migueles, J.H.; Cadenas-Sanchez, C.; Ekelund, U.; Delisle Nyström, C.; Mora-Gonzalez, J.; Löf, M.; Labayen, I.; Ruiz, J.R.; Ortega, F.B. Accelerometer Data Collection and Processing Criteria to Assess Physical Activity and Other Outcomes: A Systematic Review and Practical Considerations. *Sports Med.* 2017, *47*, 1821–1845, doi:10.1007/s40279-017-0716-0.

38. Wundersitz, D.W.T.; Netto, K.J.; Aisbett, B.; Gastin, P.B. Validity of an Upper-Body-Mounted Accelerometer to Measure Peak Vertical and Resultant Force during Running and Change-of-Direction Tasks. *Sports Biomech.* 2013, *12*, 403–412, doi:10.1080/14763141.2013.811284.

39. Meyer, U.; Ernst, D.; Schott, S.; Riera, C.; Hattendorf, J.; Romkes, J.; Granacher, U.; Göpfert, B.; Kriemler, S. Validation of Two Accelerometers to Determine Mechanical Loading of Physical Activities in Children. *J. Sports Sci.* 2015, *33*, 1702–1709, doi:10.1080/02640414.2015.1004638.

40. Chastin, S.F.M.; Mandrichenko, O.; Helbostadt, J.L.; Skelton, D.A. Associations between Objectively-Measured Sedentary Behaviour and Physical Activity with Bone Mineral Density in Adults and Older Adults, the NHANES Study. *Bone* 2014, *64*, 254–262, doi:10.1016/j.bone.2014.04.009.

41. Ancillao, A.; Tedesco, S.; Barton, J.; O'Flynn, B. Indirect Measurement of Ground Reaction Forces and Moments by Means of Wearable Inertial Sensors: A Systematic Review. *Sensors* 2018, *18*, 2564, doi:10.3390/s18082564.

42. Deere, K.; Sayers, A.; Rittweger, J.; Tobias, J.H. Habitual Levels of High, but Not Moderate or Low, Impact Activity Are Positively Related to Hip BMD and Geometry: Results from a Population-Based Study of Adolescents. *J. Bone Miner. Res.* 2012, *27*, 1887–1895, doi:10.1002/jbmr.1631.

43. Stiles, V.H.; Griew, P.J.; Rowlands, A.V. Use of Accelerometry to Classify Activity Beneficial to Bone in Premenopausal Women. *Med. Sci. Sports Exerc.* 2013, *45*, 2353–2361, doi:10.1249/MSS.0b013e31829ba765.

44. Ahola, R.; Korpelainen, R.; Vainionpää, A.; Jämsä, T. Daily Impact Score in Long-Term Acceleration Measurements of Exercise. *J. Biomech.* 2010, *43*, 1960–1964, doi:10.1016/j.jbiomech.2010.03.021.

45. Judex, S.; Zernicke, R.F. High-Impact Exercise and Growing Bone: Relation between High Strain Rates and Enhanced Bone Formation. *J. Appl. Physiol.* 2000, *88*, 2183–2191, doi:10.1152/jappl.2000.88.6.2183.

46. Mosley, J.R.; Lanyon, L.E. Strain Rate as a Controlling Influence on Adaptive Modeling in Response to Dynamic Loading of the Ulna in Growing Male Rats. *Bone* 1998, *23*, 313–318, doi:10.1016/S8756-3282(98)00113-6.

47. Welk, G.J. Principles of Design and Analyses for the Calibration of Accelerometry-Based Activity Monitors. *Med. Sci. Sports Exerc.* 2005, *37*, S501, doi:10.1249/01.mss.0000185660.38335.de.

48. Staudenmayer, J.; Zhu, W.; Catellier, D.J. Statistical Considerations in the Analysis of Accelerometry-Based Activity Monitor Data. *Med. Sci. Sports Exerc.* 2012, *44*, S61, doi:10.1249/MSS.0b013e3182399e0f.

49. Steyerberg, E.W.; Vergouwe, Y. Towards Better Clinical Prediction Models: Seven Steps for Development and an ABCD for Validation. *Eur. Heart J.* 2014, *35*, 1925–1931, doi:10.1093/eurheartj/ehu207.

50. Justice, A.C.; Covinsky, K.E.; Berlin, J.A. Assessing the Generalizability of Prognostic Information. *Ann. Intern. Med.* 1999, *130*, 515–524, doi:10.7326/0003-4819-130-6-199903160-00016.

51. Attal, F.; Mohammed, S.; Dedabrishvili, M.; Chamroukhi, F.; Oukhellou, L.; Amirat, Y. Physical Human Activity Recognition Using Wearable Sensors. *Sensors* 2015, *15*, 31314–31338, doi:10.3390/s151229858.

52. Mannini, A.; Sabatini, A.M. Machine Learning Methods for Classifying Human Physical Activity from On-Body Accelerometers. *Sensors* 2010, *10*, 1154–1175, doi:10.3390/s100201154.

53. Skotte, J.; Korshøj, M.; Kristiansen, J.; Hanisch, C.; Holtermann, A. Detection of Physical Activity Types Using Triaxial Accelerometers. *J. Phys. Act. Health* 2014, *11*, 76–84, doi:10.1123/jpah.2011-0347.

54. Cosman, F.; de Beur, S.J.; LeBoff, M.S.; Lewiecki, E.M.; Tanner, B.; Randall, S.; Lindsay, R. Clinician's Guide to Prevention and Treatment of Osteoporosis. *Osteoporos. Int.* 2014, *25*, 2359–2381, doi:10.1007/s00198-014-2794-2.

55. Brooke-Wavell, K.; Skelton, D.A.; Barker, K.L.; Clark, E.M.; Biase, S.D.; Arnold, S.; Paskins, Z.; Robinson, K.R.; Lewis, R.M.; Tobias, J.H.; et al. Strong, Steady and Straight: UK Consensus Statement on Physical Activity and Exercise for Osteoporosis. *Br. J. Sports Med.* 2022, *56*, 837–846, doi:10.1136/bjsports-2021-104634.

56. Diniz-Sousa, F.; Veras, L.; Boppre, G.; Devezas, V.; Santos-Sousa, H.; Preto, J.; Machado, L.; Vilas-Boas, J.P.; Oliveira, J.; Fonseca, H. The Effect of Bariatric Surgery on Gravitational Loading and Its Impact on Bone Mass. *Bone* 2021, *153*, 116153, doi:10.1016/j.bone.2021.116153.

57. Warden, S.J.; Davis, I.S.; Fredericson, M. Management and Prevention of Bone Stress Injuries in Long-Distance Runners. *J. Orthop. Sports Phys. Ther.* 2014, *44*, 749–765, doi:10.2519/jospt.2014.5334.

58. Warden, S.J.; Edwards, W.B.; Willy, R.W. Preventing Bone Stress Injuries in Runners with Optimal Workload. *Curr. Osteoporos. Rep.* 2021, *19*, 298–307, doi:10.1007/s11914-021-00666-y.

59. Turner, C.H.; Forwood, M.R.; Otter, M.W. Mechanotransduction in Bone: Do Bone Cells Act as Sensors of Fluid Flow? *FASEB J.* 1994, *8*, 875–878, doi:10.1096/fasebj.8.11.8070637.

60. Wolff, J. *The Law of Bone Remodelling*; Springer: Berlin, Heidelberg, 1986; ISBN 978-3-642-71033-9.

61. Lee, T.; Staines, A.; Taylor, D. Bone Adaptation to Load: Microdamage as a Stimulus for Bone Remodelling. *J. Anat.* 2002, *201*, 437–446, doi:10.1046/j.1469-7580.2002.00123.x.

62. Frost, H.M. Bone “Mass” and the “Mechanostat”: A Proposal. *Anat. Rec.* 1987, *219*, 1–9, doi:10.1002/ar.1092190104.

63. Frost, H.M. Bone’s Mechanostat: A 2003 Update. *Anat. Rec.* 2003, *275*, 1081–1101, doi:10.1002/ar.a.10119.

64. Bonewald, L.F. The Amazing Osteocyte. *J. Bone Miner. Res.* 2011, *26*, 229–238, doi:10.1002/jbmr.320.

65. Yuan, Y.; Chen, X.; Zhang, L.; Wu, J.; Guo, J.; Zou, D.; Chen, B.; Sun, Z.; Shen, C.; Zou, J. The Roles of Exercise in Bone Remodeling and in Prevention and Treatment of Osteoporosis. *Prog. Biophys. Mol. Biol.* 2016, *122*, 122–130, doi:10.1016/j.pbiomolbio.2015.11.005.

66. Seeman, E. Bone Modeling and Remodeling. *Crit. Rev. Eukaryot. Gene Expr.* 2009, *19*, 219–233, doi:10.1615/critreveukargeneexpr.v19.i3.40.

67. Turner, C.H.; Robling, A.G. Designing Exercise Regimens to Increase Bone Strength. *Exerc. Sport Sci. Rev.* 2003, *31*, 45–50, doi:10.1097/00003677-200301000-00009.

68. Rubin, C.T.; Lanyon, L.E. Regulation of Bone Formation by Applied Dynamic Loads. *J. Bone Jt. Surg.* 1984, *66*, 397.

69. Burr, D.B.; Robling, A.G.; Turner, C.H. Effects of Biomechanical Stress on Bones in Animals. *Bone* 2002, *30*, 781–786, doi:10.1016/S8756-3282(02)00707-X.

70. Burr, D.B.; Turner, C.H.; Naick, P.; Forwood, M.R.; Ambrosius, W.; Sayeed Hasan, M.; Pidaparti, R. Does Microdamage Accumulation Affect the Mechanical Properties of Bone? *J. Biomech.* 1998, *31*, 337–345, doi:10.1016/S0021-9290(98)00016-5.

71. Jacobs, C.R.; Yellowley, C.E.; Davis, B.R.; Zhou, Z.; Cimbala, J.M.; Donahue, H.J. Differential Effect of Steady versus Oscillating Flow on Bone Cells. *J. Biomech.* 1998, *31*, 969–976, doi:10.1016/s0021-9290(98)00114-6.

72. Qin, Y.X.; Kaplan, T.; Saldanha, A.; Rubin, C. Fluid Pressure Gradients, Arising from Oscillations in Intramedullary Pressure, Is Correlated with the Formation of Bone and Inhibition of Intracortical Porosity. *J. Biomech.* 2003, *36*, 1427–1437, doi:10.1016/s0021-9290(03)00127-1.

73. Hsieh, Y.; Turner, C.H. Effects of Loading Frequency on Mechanically Induced Bone Formation. *J. Bone Miner. Res.* 2001, *16*, 918–924, doi:10.1359/jbmr.2001.16.5.918.

74. Robling, A.G.; Burr, D.B.; Turner, C.H. Recovery Periods Restore Mechanosensitivity to Dynamically Loaded Bone. *J. Exp. Biol.* 2001, *204*, 3389–3399, doi:10.1242/jeb.204.19.3389.

75. Srinivasan, S.; Weimer, D.A.; Agans, S.C.; Bain, S.D.; Gross, T.S. Low-Magnitude Mechanical Loading Becomes Osteogenic When Rest Is Inserted Between Each Load Cycle. *J. Bone Miner. Res.* 2002, *17*, 1613–1620.

76. Srinivasan, S.; Ausk, B.J.; Poliachik, S.L.; Warner, S.E.; Richardson, T.S.; Gross, T.S. Rest-Inserted Loading Rapidly Amplifies the Response of Bone to Small Increases in Strain and Load Cycles. *J. Appl. Physiol.* 2007, *102*, 1945–1952, doi:10.1152/japplphysiol.00507.2006.

77. Robling, A.G.; Hinant, F.M.; Burr, D.B.; Turner, C.H. Improved Bone Structure and Strength after Long-Term Mechanical Loading Is Greatest If Loading Is Separated into Short Bouts. *J. Bone Miner. Res.* 2002, *17*, 1545–1554, doi:10.1359/jbmr.2002.17.8.1545.

78. Rubin, C.; Turner, A.S.; Bain, S.; Mallinckrodt, C.; McLeod, K. Low Mechanical Signals Strengthen Long Bones. *Nature* 2001, *412*, 603–604, doi:10.1038/35088122.

79. Kiel, D.P.; Hannan, M.T.; Barton, B.A.; Bouxsein, M.L.; Sisson, E.; Lang, T.; Allaire, B.; Dewkett, D.; Carroll, D.; Magaziner, J.; et al. Low-Magnitude Mechanical Stimulation to Improve Bone Density in Persons of Advanced Age: A Randomized, Placebo-Controlled Trial. *J. Bone Miner. Res.* 2015, *30*, 1319–1328, doi:10.1002/jbmr.2448.

80. Martyn-St James, M.; Carroll, S. Effects of Different Impact Exercise Modalities on Bone Mineral Density in Premenopausal Women: A Meta-Analysis. *J. Bone Miner. Metab.* 2010, *28*, 251–267, doi:10.1007/s00774-009-0139-6.

81. Zhao, R.; Zhao, M.; Zhang, L. Efficiency of Jumping Exercise in Improving Bone Mineral Density among Premenopausal Women: A Meta-Analysis. *Sports Med.* 2014, *44*, 1393–1402, doi:10.1007/s40279-014-0220-8.

82. Mackelvie, K.J.; McKay, H.A.; Khan, K.M.; Crocker, P.R. A School-Based Exercise Intervention Augments Bone Mineral Accrual in Early Pubertal Girls. *J. Pediatr.* 2001, *139*, 501–508, doi:10.1067/mpd.2001.118190.

83. Gunter, K.; Baxter-Jones, A.D.; Mirwald, R.L.; Almstedt, H.; Fuchs, R.K.; Durski, S.; Snow, C. Impact Exercise Increases BMC during Growth: An 8-Year

Longitudinal Study. *J. Bone Miner. Res.* 2008, *23*, 986–993, doi:10.1359/jbmr.071201.

84. Watson, S.L.; Weeks, B.K.; Weis, L.J.; Harding, A.T.; Horan, S.A.; Beck, B.R. High-Intensity Resistance and Impact Training Improves Bone Mineral Density and Physical Function in Postmenopausal Women With Osteopenia and Osteoporosis: The LIFTMOR Randomized Controlled Trial. *J. Bone Miner. Res.* 2018, *33*, 211–220, doi:10.1002/jbmr.3284.

85. Guadalupe-Grau, A.; Fuentes, T.; Guerra, B.; Calbet, J.A.L. Exercise and Bone Mass in Adults. *Sports Med.* 2009, *39*, 439–468, doi:10.2165/00007256-200939060-00002.

86. Harding, A.T.; Beck, B.R. Exercise, Osteoporosis, and Bone Geometry. *Sports* 2017, *5*, 29, doi:10.3390/sports5020029.

87. Martyn-St James, M.; Carroll, S. High-Intensity Resistance Training and Postmenopausal Bone Loss: A Meta-Analysis. *Osteoporos. Int.* 2006, *17*, 1225–1240, doi:10.1007/s00198-006-0083-4.

88. Tan, V.P.S.; Macdonald, H.M.; Kim, S.; Nettlefold, L.; Gabel, L.; Ashe, M.C.; McKay, H.A. Influence of Physical Activity on Bone Strength in Children and Adolescents: A Systematic Review and Narrative Synthesis. *J. Bone Miner. Res.* 2014, *29*, 2161–2181, doi:10.1002/jbmr.2254.

89. Tenforde, A.S.; Fredericson, M. Influence of Sports Participation on Bone Health in the Young Athlete: A Review of the Literature. *PM R* 2011, *3*, 861–867, doi:10.1016/j.pmrj.2011.05.019.

90. Behringer, M.; Gruetzner, S.; McCourt, M.; Mester, J. Effects of Weight-Bearing Activities on Bone Mineral Content and Density in Children and Adolescents: A Meta-Analysis. *J. Bone Miner. Res.* 2014, *29*, 467–478, doi:10.1002/jbmr.2036.

91. Wilks, D.C.; Winwood, K.; Gilliver, S.F.; Kwiet, A.; Chatfield, M.; Michaelis, I.; Sun, L.W.; Ferretti, J.L.; Sargeant, A.J.; Felsenberg, D.; et al. Bone Mass and Geometry of the Tibia and the Radius of Master Sprinters, Middle and Long Distance Runners, Race-Walkers and Sedentary Control Participants: A pQCT Study. *Bone* 2009, *45*, 91–97, doi:10.1016/j.bone.2009.03.660.

92. Palombaro, K.M. Effects of Walking-Only Interventions on Bone Mineral Density at Various Skeletal Sites: A Meta-Analysis. *J. Geriatr. Phys. Ther.* 2005, *28*, 102–107, doi:10.1519/00139143-200512000-00006.

93. Martyn-St James, M.; Carroll, S. A Meta-Analysis of Impact Exercise on Postmenopausal Bone Loss: The Case for Mixed Loading Exercise Programmes. *Br. J. Sports Med.* 2009, *43*, 898–908, doi:10.1136/bjsm.2008.052704.

94. Gómez-Cabello, A.; Ara, I.; González-Agüero, A.; Casajús, J.A.; Vicente-Rodríguez, G. Effects of Training on Bone Mass in Older Adults: A Systematic

Review. *Sports Med.* 2012, *42*, 301–325, doi:10.2165/11597670-000000000-00000.

95. Ma, D.; Wu, L.; He, Z. Effects of Walking on the Preservation of Bone Mineral Density in Perimenopausal and Postmenopausal Women: A Systematic Review and Meta-Analysis. *Menopause* 2013, *20*, 1216–1226, doi:10.1097/GME.0000000000000100.

96. Feskanich, D.; Willett, W.; Colditz, G. Walking and Leisure-Time Activity and Risk of Hip Fracture in Postmenopausal Women. *JAMA* 2002, *288*, 2300–2306, doi:10.1001/jama.288.18.2300.

97. Sherrington, C.; Tiedemann, A.; Fairhall, N.; Close, J.C.T.; Lord, S.R. Exercise to Prevent Falls in Older Adults: An Updated Meta-Analysis and Best Practice Recommendations. *New South Wales Public Health Bull.* 2011, *22*, 78–83, doi:10.1071/NB10056.

98. Howe, T.E.; Shea, B.; Dawson, L.J.; Downie, F.; Murray, A.; Ross, C.; Harbour, R.T.; Caldwell, L.M.; Creed, G. Exercise for Preventing and Treating Osteoporosis in Postmenopausal Women. *Cochrane Database Syst. Rev.* 2011, CD000333, doi:10.1002/14651858.CD000333.pub2.

99. Kemmler, W.; Bebenek, M.; Kohl, M.; von Stengel, S. Exercise and Fractures in Postmenopausal Women. Final Results of the Controlled Erlangen Fitness and Osteoporosis Prevention Study (EFOPS). *Osteoporos. Int.* 2015, *26*, 2491–2499, doi:10.1007/s00198-015-3165-3.

100. Tenforde, A.S.; Kraus, E.; Fredericson, M. Bone Stress Injuries in Runners. *Phys. Med. Rehabil. Clin. N. Am.* 2016, *27*, 139–149, doi:10.1016/j.pmr.2015.08.008.

101. Heinonen, A.; Sievänen, H.; Kyröläinen, H.; Perttunen, J.; Kannus, P. Mineral Mass, Size, and Estimated Mechanical Strength of Triple Jumpers' Lower Limb. *Bone* 2001, *29*, 279–285, doi:10.1016/s8756-3282(01)00574-9.

102. Lanyon, L.E. Using Functional Loading to Influence Bone Mass and Architecture: Objectives, Mechanisms, and Relationship with Estrogen of the Mechanically Adaptive Process in Bone. *Bone* 1996, *18*, 37S-43S, doi:10.1016/8756-3282(95)00378-9.

103. Heikkinen, R.; Vihriälä, E.; Vainionpää, A.; Korpelainen, R.; Jämsä, T. Acceleration Slope of Exercise-Induced Impacts Is a Determinant of Changes in Bone Density. *J. Biomech.* 2007, *40*, 2967–2974, doi:10.1016/j.jbiomech.2007.02.003.

104. Judex, S.; Gross, T.S.; Zernicke, R.F. Strain Gradients Correlate with Sites of Exercise-Induced Bone-Forming Surfaces in the Adult Skeleton. *J. Bone Miner. Res.* 1997, *12*, 1737–1745.

105. Fuchs, R.K.; Bauer, J.J.; Snow, C.M. Jumping Improves Hip and Lumbar Spine Bone Mass in Prepubescent Children: A Randomized Controlled Trial. *J. Bone Miner. Res.* 2001, *16*, 148–156.

106. Whiteford, J.; Ackland, T.R.; Dhaliwal, S.S.; James, A.P.; Woodhouse, J.J.; Price, R.; Prince, R.L.; Kerr, D.A. Effects of a 1-Year Randomized Controlled Trial of Resistance Training on Lower Limb Bone and Muscle Structure and Function in Older Men. *Osteoporos. Int.* 2010, *21*, 1529–1536, doi:10.1007/s00198-009-1132-6.

107. Kukuljan, S.; Nowson, C.A.; Sanders, K.M.; Nicholson, G.C.; Seibel, M.J.; Salmon, J.; Daly, R.M. Independent and Combined Effects of Calcium-Vitamin D3 and Exercise on Bone Structure and Strength in Older Men: An 18-Month Factorial Design Randomized Controlled Trial. *J. Clin. Endocrinol. Metab.* 2011, *96*, 955–963, doi:10.1210/jc.2010-2284.

108. Sherrington, C.; Michaleff, Z.A.; Fairhall, N.; Paul, S.S.; Tiedemann, A.; Whitney, J.; Cumming, R.G.; Herbert, R.D.; Close, J.C.T.; Lord, S.R. Exercise to Prevent Falls in Older Adults: An Updated Systematic Review and Meta-Analysis. *Br. J. Sports Med.* 2017, *51*, 1750–1758, doi:10.1136/bjsports-2016-096547.

109. Daly, R.M.; Bass, S.L. Lifetime Sport and Leisure Activity Participation Is Associated with Greater Bone Size, Quality and Strength in Older Men. *Osteoporos. Int.* 2006, *17*, 1258–1267, doi:10.1007/s00198-006-0114-1.

110. Meakin, L.B.; Price, J.S.; Lanyon, L.E. The Contribution of Experimental in Vivo Models to Understanding the Mechanisms of Adaptation to Mechanical Loading in Bone. *Front. Endocrinol.* 2014, *5*, doi:10.3389/fendo.2014.00154.

111. Abdul Razak, A.H.; Zayegh, A.; Begg, R.K.; Wahab, Y. Foot Plantar Pressure Measurement System: A Review. *Sensors* 2012, *12*, 9884–9912, doi:10.3390/s120709884.

112. Lanyon, L.E.; Smith, R.N. Measurements of Bone Strain in the Walking Animal. *Res. Vet. Sci.* 1969, *10*, 93–94, doi:10.1016/S0034-5288(18)34492-8.

113. Lanyon, L.E.; Hampson, W.G.; Goodship, A.E.; Shah, J.S. Bone Deformation Recorded in Vivo from Strain Gauges Attached to the Human Tibial Shaft. *Acta Orthop. Scand.* 1975, *46*, 256–268, doi:10.3109/17453677508989216.

114. Shahabpoor, E.; Pavic, A. Measurement of Walking Ground Reactions in Real-Life Environments: A Systematic Review of Techniques and Technologies. *Sensors* 2017, *17*, 2085, doi:10.3390/s17092085.

115. Nigg, B.M.; Herzog, W. *Biomechanics of the Musculo-Skeletal System*; 3rd ed.; Wiley: Hoboken, New Jersey, 2007;

116. Crea, S.; Donati, M.; De Rossi, S.M.M.; Oddo, C.M.; Vitiello, N. A Wireless Flexible Sensorized Insole for Gait Analysis. *Sensors* 2014, *14*, 1073–1093, doi:10.3390/s140101073.

117. Barnett, S.; Cunningham, J.L.; West, S. A Comparison of Vertical Force and Temporal Parameters Produced by an In-Shoe Pressure Measuring System and a Force Platform. *Clin. Biomech.* 2001, *16*, 353–357, doi:10.1016/s0268-0033(01)00026-2.

118. Strath, S.J.; Kaminsky, L.A.; Ainsworth, B.E.; Ekelund, U.; Freedson, P.S.; Gary, R.A.; Richardson, C.R.; Smith, D.T.; Swartz, A.M.; American Heart Association Physical Activity Committee of the Council on Lifestyle and Cardiometabolic Health and Cardiovascular, Exercise, Cardiac Rehabilitation and Prevention Committee of the Council on Clinical Cardiology, and Council Guide to the Assessment of Physical Activity: Clinical and Research Applications: A Scientific Statement from the American Heart Association. *Circulation* 2013, *128*, 2259–2279, doi:10.1161/01.cir.0000435708.67487.da.

119. Ainsworth, B.E.; Haskell, W.L.; Herrmann, S.D.; Meckes, N.; Bassett, D.R.; Tudor-Locke, C.; Greer, J.L.; Vezina, J.; Whitt-Glover, M.C.; Leon, A.S. 2011 Compendium of Physical Activities: A Second Update of Codes and MET Values. *Med. Sci. Sports Exerc.* 2011, *43*, 1575–1581, doi:10.1249/MSS.0b013e31821ece12.

120. Weeks, B.K.; Beck, B.R. Twice-Weekly, in-School Jumping Improves Lean Mass, Particularly in Adolescent Boys. *Pediatr. Obes.* 2012, *7*, 196–204, doi:10.1111/j.2047-6310.2011.00026.x.

121. Kindler, J.M.; Ross, H.L.; Laing, E.M.; Modlesky, C.M.; Pollock, N.K.; Baile, C.A.; Lewis, R.D. Load-Specific Physical Activity Scores Are Related to Tibia Bone Architecture. *Int. J. Sport Nutr. Exerc. Metab.* 2015, *25*, 136–144, doi:10.1123/ijsnem.2013-0258.

122. Shephard, R.J. Limits to the Measurement of Habitual Physical Activity by Questionnaires. *Br. J. Sports Med.* 2003, *37*, 197–206; discussion 206, doi:10.1136/bjsm.37.3.197.

123. Chen, K.Y.; Bassett, D.R. The Technology of Accelerometry-Based Activity Monitors: Current and Future. *Med. Sci. Sports Exerc.* 2005, *37*, S490-500, doi:10.1249/01.mss.0000185571.49104.82.

124. Freedson, P.S.; Melanson, E.; Sirard, J. Calibration of the Computer Science and Applications, Inc. Accelerometer. *Med. Sci. Sports Exerc.* 1998, *30*, 777–781, doi:10.1097/00005768-199805000-00021.

125. Troiano, R.P.; Berrigan, D.; Dodd, K.W.; Mâsse, L.C.; Tilert, T.; McDowell, M. Physical Activity in the United States Measured by Accelerometer. *Med. Sci. Sports Exerc.* 2008, *40*, 181–188, doi:10.1249/mss.0b013e31815a51b3.

126. Kavanagh, J.J.; Menz, H.B. Accelerometry: A Technique for Quantifying Movement Patterns during Walking. *Gait Posture* 2008, *28*, 1–15, doi:10.1016/j.gaitpost.2007.10.010.

127. Scott, R.; James, R.; Barnett, C.T.; Sale, C.; Varley, I. Perspectives from Research and Practice: A Survey on External Load Monitoring and Bone in Sport. *Front. Sports Act. Living* 2023, *5*, doi:10.3389/fspor.2023.1150052.

128. Freedson, P.; Pober, D.; Janz, K.F. Calibration of Accelerometer Output for Children. *Med. Sci. Sports Exerc.* 2005, *37*, S523-530, doi:10.1249/01.mss.0000185658.28284.ba.

129. Yang, C.-C.; Hsu, Y.-L. A Review of Accelerometry-Based Wearable Motion Detectors for Physical Activity Monitoring. *Sensors* 2010, *10*, 7772–7788, doi:10.3390/s100807772.

130. Zeng, H.; Zhao, Y. Sensing Movement: Microsensors for Body Motion Measurement. *Sensors* 2011, *11*, 638–660, doi:10.3390/s110100638.

131. van Hees, V.T.; Gorzelniak, L.; Dean León, E.C.; Eder, M.; Pias, M.; Taherian, S.; Ekelund, U.; Renström, F.; Franks, P.W.; Horsch, A.; et al. Separating Movement and Gravity Components in an Acceleration Signal and Implications for the Assessment of Human Daily Physical Activity. *PLOS One* 2013, *8*, e61691, doi:10.1371/journal.pone.0061691.

132. Mathie, M.J.; Coster, A.C.F.; Lovell, N.H.; Celler, B.G. Accelerometry: Providing an Integrated, Practical Method for Long-Term, Ambulatory Monitoring of Human Movement. *Physiol. Meas.* 2004, *25*, R1-20, doi:10.1088/0967-3334/25/2/r01.

133. Karantonis, D.M.; Narayanan, M.R.; Mathie, M.; Lovell, N.H.; Celler, B.G. Implementation of a Real-Time Human Movement Classifier Using a Triaxial Accelerometer for Ambulatory Monitoring. *IEEE Trans. Inf. Technol. Biomed.* 2006, *10*, 156–167, doi:10.1109/titb.2005.856864.

134. Preece, S.J.; Goulermas, J.Y.; Kenney, L.P.J.; Howard, D.; Meijer, K.; Crompton, R. Activity Identification Using Body-Mounted Sensors-a Review of Classification Techniques. *Physiol. Meas.* 2009, *30*, R1-33, doi:10.1088/0967-3334/30/4/R01.

135. Kamada, M.; Shiroma, E.J.; Harris, T.B.; Lee, I.-M. Comparison of Physical Activity Assessed Using Hip- and Wrist-Worn Accelerometers. *Gait Posture* 2016, *44*, 23–28, doi:10.1016/j.gaitpost.2015.11.005.

136. Cavanagh, P.R.; Lafortune, M.A. Ground Reaction Forces in Distance Running. *J. Biomech.* 1980, *13*, 397–406, doi:10.1016/0021-9290(80)90033-0.

137. Lieberman, D.E.; Venkadesan, M.; Werbel, W.A.; Daoud, A.I.; D'Andrea, S.; Davis, I.S.; Mang'eni, R.O.; Pitsiladis, Y. Foot Strike Patterns and Collision Forces in Habitually Barefoot versus Shod Runners. *Nature* 2010, *463*, 531–535, doi:10.1038/nature08723.

138. Nilsson, J.; Thorstensson, A. Ground Reaction Forces at Different Speeds of Human Walking and Running. *Acta Physiol. Scand.* 1989, *136*, 217–227, doi:10.1111/j.1748-1716.1989.tb08655.x.

139. Zadpoor, A.A.; Nikooyan, A.A. The Relationship between Lower-Extremity Stress Fractures and the Ground Reaction Force: A Systematic Review. *Clin. Biomech.* 2011, *26*, 23–28, doi:10.1016/j.clinbiomech.2010.08.005.

140. Crowell, H.P.; Davis, I.S. Gait Retraining to Reduce Lower Extremity Loading in Runners. *Clin. Biomech.* 2011, *26*, 78–83, doi:10.1016/j.clinbiomech.2010.09.003.

141. Preece, S.J.; Goulermas, J.Y.; Kenney, L.P.J.; Howard, D. A Comparison of Feature Extraction Methods for the Classification of Dynamic Activities From Accelerometer Data. *IEEE Trans. Biomed. Eng.* 2009, *56*, 871–879, doi:10.1109/TBME.2008.2006190.

142. Cleland, I.; Kikhia, B.; Nugent, C.; Boytsov, A.; Hallberg, J.; Synnes, K.; McClean, S.; Finlay, D. Optimal Placement of Accelerometers for the Detection of Everyday Activities. *Sensors* 2013, *13*, 9183–9200, doi:10.3390/s130709183.

143. Sasaki, J.E.; Hickey, A.M.; Staudenmayer, J.W.; John, D.; Kent, J.A.; Freedson, P.S. Performance of Activity Classification Algorithms in Free-Living Older Adults. *Med. Sci. Sports Exerc.* 2016, *48*, 941–950, doi:10.1249/MSS.0000000000000844.

144. Ellis, K.; Kerr, J.; Godbole, S.; Staudenmayer, J.; Lanckriet, G. Hip and Wrist Accelerometer Algorithms for Free-Living Behavior Classification. *Med. Sci. Sports Exerc.* 2016, *48*, 933–940, doi:10.1249/MSS.0000000000000840.

145. Migueles, J.H.; Aadland, E.; Andersen, L.B.; Brønd, J.C.; Chastin, S.F.; Hansen, B.H.; Konstabel, K.; Kvalheim, O.M.; McGregor, D.E.; Rowlands, A.V.; et al. GRANADA Consensus on Analytical Approaches to Assess Associations with Accelerometer-Determined Physical Behaviours (Physical Activity, Sedentary Behaviour and Sleep) in Epidemiological Studies. *Br. J. Sports Med.* 2022, *56*, 376–384, doi:10.1136/bjsports-2020-103604.

146. Veras, L.; Diniz-Sousa, F.; Boppre, G.; Resende-Coelho, A.; Moutinho-Ribeiro, E.; Devezas, V.; Santos-Sousa, H.; Preto, J.; Vilas-Boas, J.P.; Machado, L.; et al. Mechanical Loading Prediction through Accelerometry Data during Walking and Running. *Eur. J. Sport Sci.* 2023, *23*, 1518–1527, doi:10.1080/17461391.2022.2102437.

147. Neugebauer, J.M.; Lafiandra, M. Predicting Ground Reaction Force from a Hip-Borne Accelerometer during Load Carriage. *Med. Sci. Sports Exerc.* 2018, *50*, 2369–2374, doi:10.1249/MSS.0000000000001686.

148. Halilaj, E.; Rajagopal, A.; Fiterau, M.; Hicks, J.L.; Hastie, T.J.; Delp, S.L. Machine Learning in Human Movement Biomechanics: Best Practices,

Common Pitfalls, and New Opportunities. *J. Biomech.* 2018, *81*, 1–11, doi:10.1016/j.jbiomech.2018.09.009.

149. Bassett, D.R.; Rowlands, A.; Trost, S.G. Calibration and Validation of Wearable Monitors. *Med. Sci. Sports Exerc.* 2012, *44*, S32-38, doi:10.1249/MSS.0b013e3182399cf7.

150. Kluitenberg, B.; Bredeweg, S.W.; Zijlstra, S.; Zijlstra, W.; Buist, I. Comparison of Vertical Ground Reaction Forces during Overground and Treadmill Running. A Validation Study. *BMC Musculoskelet. Disord.* 2012, *13*, 235, doi:10.1186/1471-2474-13-235.

151. Cauley, J.A. Public Health Impact of Osteoporosis. *J. Gerontol.* 2013, *68*, 1243–1251, doi:10.1093/gerona/glt093.

152. Johnell, O.; Kanis, J.A. An Estimate of the Worldwide Prevalence and Disability Associated with Osteoporotic Fractures. *Osteoporos. Int.* 2006, *17*, 1726–1733, doi:10.1007/s00198-006-0172-4.

153. Benedetti, M.G.; Furlini, G.; Zati, A.; Letizia Mauro, G. The Effectiveness of Physical Exercise on Bone Density in Osteoporotic Patients. *BioMed Res. Int.* 2018, *2018*, 4840531, doi:10.1155/2018/4840531.

154. Nikander, R.; Sievänen, H.; Heinonen, A.; Daly, R.M.; Uusi-Rasi, K.; Kannus, P. Targeted Exercise against Osteoporosis: A Systematic Review and Meta-Analysis for Optimising Bone Strength throughout Life. *BMC Med.* 2010, *8*, 47, doi:10.1186/1741-7015-8-47.

155. Curtis, E.M.; Moon, R.J.; Harvey, N.C.; Cooper, C. The Impact of Fragility Fracture and Approaches to Osteoporosis Risk Assessment Worldwide. *Bone* 2017, *104*, 29–38, doi:10.1016/j.bone.2017.01.024.

156. Shapses, S.A.; Sukumar, D. Bone Metabolism in Obesity and Weight Loss. *Annu. Rev. Nutr.* 2012, *32*, 287–309, doi:10.1146/annurev.nutr.012809.104655.

157. Arterburn, D.E.; Courcoulas, A.P. Bariatric Surgery for Obesity and Metabolic Conditions in Adults. *BMJ* 2014, *349*, g3961, doi:10.1136/bmj.g3961.

158. Hernández-Martínez, A.; Veras, L.; Boppre, G.; Soriano-Maldonado, A.; Oliveira, J.; Diniz-Sousa, F.; Fonseca, H. Changes in Volumetric Bone Mineral Density and Bone Quality after Roux-En-Y Gastric Bypass: A Meta-Analysis with Meta-Regression. *Obes. Rev.* 2022, *23*, e13479, doi:10.1111/obr.13479.

159. Saad, R.K.; Ghezzawi, M.; Habli, D.; Alami, R.S.; Chakhtoura, M. Fracture Risk Following Bariatric Surgery: A Systematic Review and Meta-Analysis. *Osteoporos. Int.* 2022, *33*, 511–526, doi:10.1007/s00198-021-06206-9.

160. Bates, D.; Mächler, M.; Bolker, B.; Walker, S. Fitting Linear Mixed-Effects Models Using Lme4. *J. Stat. Softw.* 2015, *67*, 1–48, doi:10.18637/jss.v067.i01.

161. Cnaan, A.; Laird, N.M.; Slasor, P. Using the General Linear Mixed Model to Analyse Unbalanced Repeated Measures and Longitudinal Data. *Stat. Med.* 1997, *16*, 2349–2380, doi:10.1002/(sici)1097-0258(19971030)16:20<2349::aid-sim667>3.0.co;2-e.

162. Breiman, L. Random Forests. *Mach. Learn.* 2001, *45*, 5–32, doi:10.1023/A:1010933404324.

163. Cortes, C.; Vapnik, V. Support-Vector Networks. *Mach. Learn.* 1995, *20*, 273–297, doi:10.1007/BF00994018.

164. Cunningham, P.; Delany, S.J. K-Nearest Neighbour Classifiers - A Tutorial. *ACM Comput. Surv.* 2021, *54*, 128:1-128:25, doi:10.1145/3459665.

165. Judex, S.; Carlson, K.J. Is Bone's Response to Mechanical Signals Dominated by Gravitational Loading? *Med. Sci. Sports Exerc.* 2009, *41*, 2037–2043, doi:10.1249/MSS.0b013e3181a8c6e5.

166. Paluzo-Hidalgo, E.; Gonzalez-Diaz, R.; Gutiérrez-Naranjo, M.A. Two-Hidden-Layer Feed-Forward Networks Are Universal Approximators: A Constructive Approach. *Neural Netw.* 2020, *131*, 29–36, doi:10.1016/j.neunet.2020.07.021.

167. Besier, T.F.; Lloyd, D.G.; Cochrane, J.L.; Ackland, T.R. External Loading of the Knee Joint during Running and Cutting Maneuvers. *Med. Sci. Sports Exerc.* 2001, *33*, 1168–1175, doi:10.1097/00005768-200107000-00014.

168. Marques, E.A.; Mota, J.; Carvalho, J. Exercise Effects on Bone Mineral Density in Older Adults: A Meta-Analysis of Randomized Controlled Trials. *Age* 2012, *34*, 1493–1515, doi:10.1007/s11357-011-9311-8.

169. Giangregorio, L.M.; Papaioannou, A.; Macintyre, N.J.; Ashe, M.C.; Heinonen, A.; Shipp, K.; Wark, J.; McGill, S.; Keller, H.; Jain, R.; et al. Too Fit To Fracture: Exercise Recommendations for Individuals with Osteoporosis or Osteoporotic Vertebral Fracture. *Osteoporos. Int.* 2014, *25*, 821–835, doi:10.1007/s00198-013-2523-2.

170. Tenforde, A.S.; Carlson, J.L.; Sainani, K.L.; Chang, A.O.; Kim, J.H.; Golden, N.H.; Fredericson, M. Sport and Triad Risk Factors Influence Bone Mineral Density in Collegiate Athletes. *Med. Sci. Sports Exerc.* 2018, *50*, 2536–2543, doi:10.1249/MSS.0000000000001711.

171. Scofield, K.L.; Hecht, S. Bone Health in Endurance Athletes: Runners, Cyclists, and Swimmers. *Curr. Sports Med. Rep.* 2012, *11*, 328–334, doi:10.1249/JSR.0b013e3182779193.

172. Warden, S.J.; Mantila Roosa, S.M. Physical Activity Completed When Young Has Residual Bone Benefits at 94 Years of Age: A within-Subject Controlled Case Study. *J. Musculoskelet. Neuronal Interact.* 2014, *14*, 239–243.

173. Patel, S.; Park, H.; Bonato, P.; Chan, L.; Rodgers, M. A Review of Wearable Sensors and Systems with Application in Rehabilitation. *J. Neuroengineering Rehabil.* 2012, *9*, 21, doi:10.1186/1743-0003-9-21.

174. Appelboom, G.; Camacho, E.; Abraham, M.E.; Bruce, S.S.; Dumont, E.L.; Zacharia, B.E.; D'Amico, R.; Slomian, J.; Reginster, J.Y.; Bruyère, O.; et al. Smart Wearable Body Sensors for Patient Self-Assessment and Monitoring. *Arch. Public Health* 2014, *72*, 28, doi:10.1186/2049-3258-72-28.

175. Morseth, B.; Emaus, N.; Jørgensen, L. Physical Activity and Bone: The Importance of the Various Mechanical Stimuli for Bone Mineral Density. A Review. *Nor. Epidemiol.* 2011, *20*, doi:10.5324/nje.v20i2.1338.

176. Vainionpää, A.; Korpelainen, R.; Sievänen, H.; Vihriälä, E.; Leppäluoto, J.; Jämsä, T. Effect of Impact Exercise and Its Intensity on Bone Geometry at Weight-Bearing Tibia and Femur. *Bone* 2007, *40*, 604–611, doi:10.1016/j.bone.2006.10.005.

177. Jämsä, T.; Vainionpää, A.; Korpelainen, R.; Vihriälä, E.; Leppäluoto, J. Effect of Daily Physical Activity on Proximal Femur. *Clin. Biomech.* 2006, *21*, 1–7, doi:10.1016/j.clinbiomech.2005.10.003.

178. Allison, S.J.; Poole, K.E.S.; Treece, G.M.; Gee, A.H.; Tonkin, C.; Rennie, W.J.; Folland, J.P.; Summers, G.D.; Brooke-Wavell, K. The Influence of High-Impact Exercise on Cortical and Trabecular Bone Mineral Content and 3D Distribution Across the Proximal Femur in Older Men: A Randomized Controlled Unilateral Intervention. *J. Bone Miner. Res.* 2015, *30*, 1709–1716, doi:10.1002/jbmr.2499.

179. Maïmoun, L.; Sultan, C. Effects of Physical Activity on Bone Remodeling. *Metabolism.* 2011, *60*, 373–388, doi:10.1016/j.metabol.2010.03.001.

180. Bach, K.; Kongsvold, A.; Bårdstu, H.; Bardal, E.M.; Kjærnli, H.S.; Herland, S.; Logacjov, A.; Mork, P.J. A Machine Learning Classifier for Detection of Physical Activity Types and Postures During Free-Living. *J. Meas. Phys. Behav.* 2022, *5*, 24–31, doi:10.1123/jmpb.2021-0015.

181. Burges, C.J.C. A Tutorial on Support Vector Machines for Pattern Recognition. *Data Min. Knowl. Discov.* 1998, *2*, 121–167, doi:10.1023/A:1009715923555.